AD-A086 754 BOEING VERTOL CO PHILADELPHIA PA F/G 1/3
DESIGN, DEVELOPMENT, AND FLIGHT DEMONSTRATION OF THE LOADS AND --ETC(U)
JUN 80 P G DIXON DAAJ02-76-C-0026
UNCLASSIFIED USAAVRADCOM-TR-80-D-3 NL

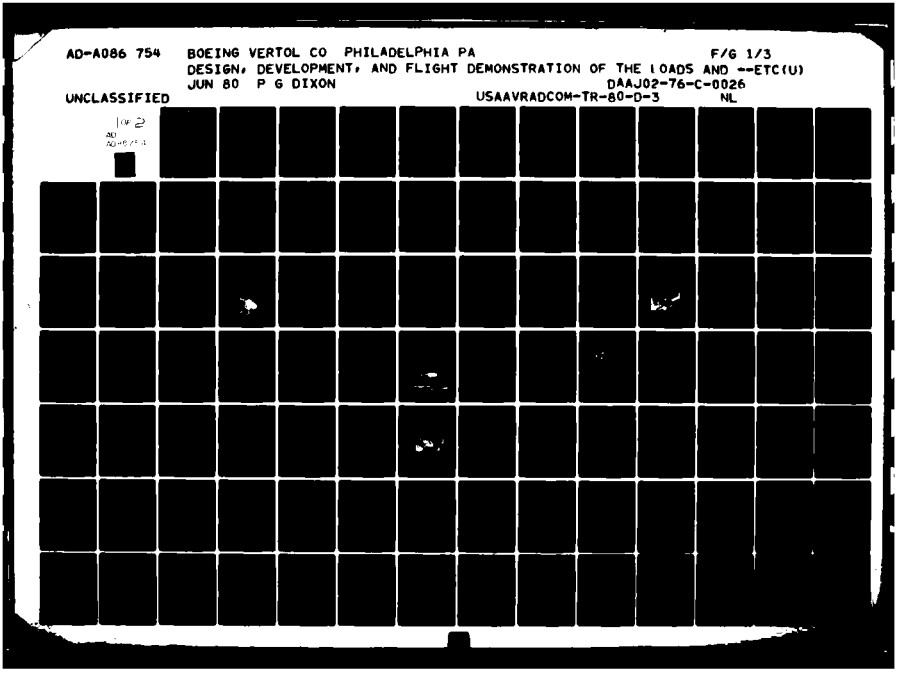

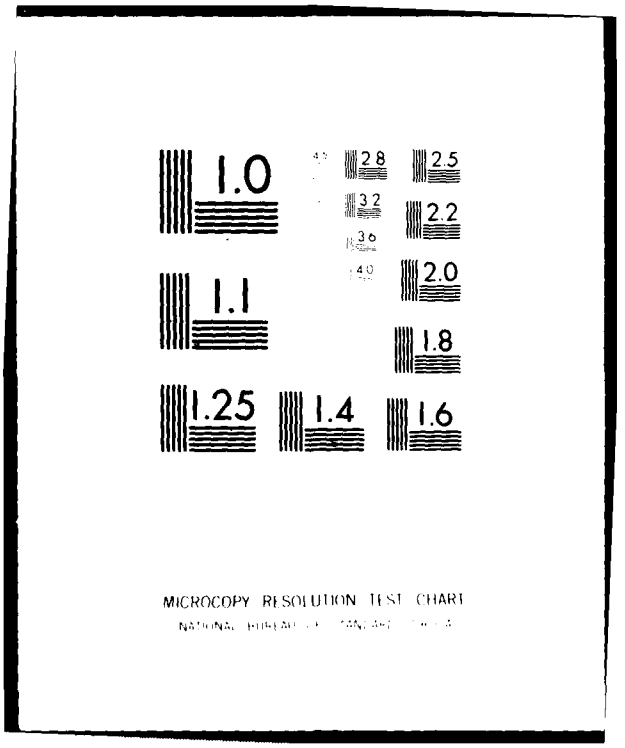
1.0
2.8
2.5
3.2
2.2
3.6
4.0
2.0
1.1
1.8
1.25
1.4
1.6
MICROCOPY RESOLUTION TEST CHART

LEVEL II

USAAVRADCOM-TR-80-D-3

AD A086754

DESIGN, DEVELOPMENT, AND FLIGHT DEMONSTRATION OF THE LOADS AND STABILITY CHARACTERISTICS OF A BEARINGLESS MAIN ROTOR

Peter G. C. Dixon
Boeing Vertol Company
Boeing Center, P. O. Box 16858
Philadelphia, Pennsylvania 19142

June 1980

Final Report for Period June 1976 - October 1979

Prepared for

APPLIED TECHNOLOGY LABORATORY
U. S. ARMY RESEARCH AND TECHNOLOGY LABORATORIES (AVRADCOM)
Fort Eustis, Va. 23604

APPLIED TECHNOLOGY LABORATORY POSITION STATEMENT

This report summarizes the results of a helicopter flight research program to evaluate the capability to describe and predict structural and aeroelastic response characteristics of an existing BO-105 aircraft modified to incorporate a bearingless hub configuration. Included in this summary report are the Bearingless Main Rotor (BMR) loads, stability, handling qualities, aircraft performance data, and the determination of the level of predictability of the technical characteristics of a helicopter using a flexible hub assembly to accommodate control system pitch inputs and normal flap and lag motions.

The technical program direction was provided by Messrs. P. A. Cancro (Contracting Officer's Representative (Technical)), W. E. Nettles, H. R. Reddick, and J. P. Whitman of the Aeronautical Technology Division, Applied Technology Laboratory; and Dr. W. F. White of the Structures Laboratory, USARTL.

UNCLASSIFIED

SECURITY CLASSIFICATION OF THIS PAGE (When Data Entered)

REPORT DOCUMENTATION PAGE	READ INSTRUCTIONS BEFORE COMPLETING FORM
1. REPORT NUMBER: USAAVRADCOM-TR-80-D-3	2. GOVT ACCESSION NO.: AD-A086754
	3. RECIPIENT'S CATALOG NUMBER
4. TITLE (and Subtitle): DESIGN, DEVELOPMENT, AND FLIGHT DEMONSTRATION OF THE LOADS AND STABILITY CHARACTERISTICS OF A BEARINGLESS MAIN ROTOR	5. TYPE OF REPORT & PERIOD COVERED: Final Report, Jun 76 — Oct 79
	6. PERFORMING ORG. REPORT NUMBER
7. AUTHOR(s): Peter G. C. Dixon	8. CONTRACT OR GRANT NUMBER(s): DAAJ02-76-C-0026
9. PERFORMING ORGANIZATION NAME AND ADDRESS: Boeing Vertol Company, Boeing Center, P. O. Box 16858, Philadelphia, PA 19142	10. PROGRAM ELEMENT, PROJECT, TASK AREA & WORK UNIT NUMBERS: 63211A 1F263211D157 11 003 EK
11. CONTROLLING OFFICE NAME AND ADDRESS: Applied Technology Laboratory, U. S. Army Research and Technology Laboratories (AVRADCOM), Fort Eustis, VA 23604	12. REPORT DATE: June 1980
	13. NUMBER OF PAGES: 161
14. MONITORING AGENCY NAME & ADDRESS (if different from Controlling Office)	15. SECURITY CLASS (of this report): Unclassified
	15a. DECLASSIFICATION DOWNGRADING SCHEDULE

16. DISTRIBUTION STATEMENT (of this Report)

Approved for public release; distribution unlimited.

17. DISTRIBUTION STATEMENT (of the abstract entered in Block 20, if different from Report)

18. SUPPLEMENTARY NOTES

19. KEY WORDS (Continue on reverse side if necessary and identify by block number)

BEARINGLESS ROTORS	FLIGHT MANEUVERS	HELICOPTERS
AEROELASTICITY	FLIGHT LOADS	FLEXIBLE STRUCTURES
STABILITY	TORQUE TUBES	HELICOPTER ROTORS
VIBRATION	FLIGHT CHARACTERISTICS	AERODYNAMIC STABILITY
LOADS (FORCES)	TUBULAR STRUCTURES	

20. ABSTRACT (Continue on reverse side if necessary and identify by block number)

The successful design, development, bench and whirl testing, and flight demonstration of the loads and stability characteristics of a bearingless main rotor (BMR) on the BO-105 helicopter were accomplished. A 35-hour flight test program was accomplished. The initial tests indicated that ground resonance damping was inadequate. For this program, a minimal modification, the stiffening of the aircraft skid landing gear, provided adequate damping for continuation of the program. The BMR/BO-105 had similar air resonance to the baseline BO-105, except at low collective

DD FORM 1 JAN 73 1473 EDITION OF 1 NOV 65 IS OBSOLETE

UNCLASSIFIED 403682

SECURITY CLASSIFICATION OF THIS PAGE (When Data Entered)

ITEM 20. (Continued)

pitch settings where the BMR had lower but sufficient damping. Vibration levels were generally similar to the baseline, but in some regimes were higher. Maneuvering stability showed a significant improvement and other flight characteristics were similar to those of the standard BO-105. The level flight speed was limited only by power available and the flight test program was not limited by structural characteristics.

The feasibility of helicopter bearingless main rotors has thus been demonstrated, and further development to improve the aeromechanical stability and vibration characteristics and reduce weight and drag should be undertaken so that the high potential of such systems can be realized.

Understanding of the loads distribution in the two-beam lag/flap/torsion flexure at the blade root of this configuration needs improvement. Use of Froude scaled model wind tunnel testing accurately predicted the flight aeromechanical stability characteristics of the BMR; however, the analytical stability prediction methodology, although sufficiently accurate in hover, requires improvement and expansion into the forward flight modes.

PREFACE

A flight test program for a Bearingless Main Rotor (BMR) was conducted for the Applied Technology Laboratory (ATL), U.S. Army Research and Technology Laboratories (AVRADCOM) under Contract DAAJ02-76-C-0026. Program Direction was under P. A. Cancro, Contracting Officer Representative.

W. W. Walls was Program Manager and P. G. Dixon was Project Engineer for Boeing Vertol. BMR aeroelastic stability and vibration analytical and test support was provided by Boeing Vertol's Dynamics Unit; Boeing Vertol's Flight Test personnel took an active part in developing and executing the BMR flight test plan and in processing flight test data; and Boeing Computer Services installed a Moving Block data analysis computer program on the Boeing Vertol flight test computer facility. This program was used to process aeroelastic stability test data. Technical support of the flight test program was also provided by H. I. MacDonald of ATL and Dr. W. White of the U.S. Army Structures Technology Laboratory at Langley Research Center. Members of the Army Safety of Flight Review Board for the BMR/BO-105 flight test program included C. H. Carper, Jr., D. Good, H. I. MacDonald, J. Macrino, W. F. White and J. P. Whitman, with P. A. Cancro and H. K. Reddick acting as advisers to the board. J. P. Whitman acted as the Army representative at Boeing Vertol during most of the BMR/BO-105 ground and flight testing.

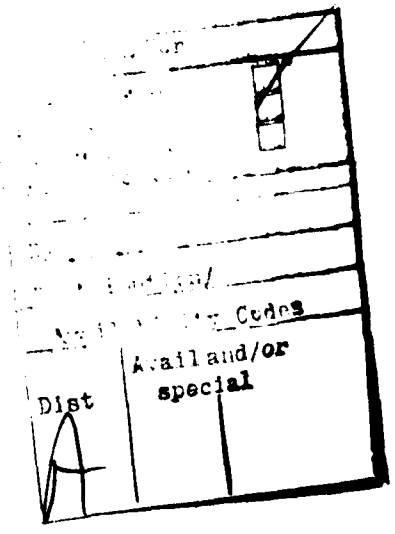

TABLE OF CONTENTS

TABLE OF CONTENTS (Continued)

TABLE OF CONTENTS (Continued)

TABLE OF CONTENTS (Continued)

TABLE OF CONTENTS (Concluded)

LIST OF ILLUSTRATIONS

LIST OF ILLUSTRATIONS
(Continued)

LIST OF ILLUSTRATIONS
(Continued)

LIST OF ILLUSTRATIONS
(Continued)

LIST OF ILLUSTRATIONS
(Continued)

LIST OF ILLUSTRATIONS
(Continued)

LIST OF ILLUSTRATIONS
(Continued)

LIST OF TABLES

INTRODUCTION

The Boeing Vertol/U.S. Army BMR, illustrated in Figure 1, is a four-bladed soft-in-plane rotor with no flap, lag, or pitch bearings. These are replaced by twin, parallel beam fiberglass flexures which have low torsional stiffness. Blade pitch motion is introduced at the flexure to blade junction through a filament-wound graphite torque tube, rigidly attached to the blade attachment hardware and supported at its inboard end by a pivot which reacts the control loads input by a conventional swashplate/pitch link control system.

This BMR is sized to fly on the Messerschmidt Boelkow Bloehm BO-105 helicopter and is designed to replace that rotor system directly without any modifications to the basic aircraft or control system.

PROGRAM OBJECTIVES

The technical objectives of this program: (1) to validate the capability to describe and predict structural and aeroelastic response characteristics of a BMR configuration by flight test of a modified existing aircraft; (2) to conduct exploratory development of a BMR to determine loads, rotor stability, handling qualities, and aircraft performance characteristics; and (3) to define design problems which require further attention before production hardware using the BMR concept can be developed.

Earlier work done in the 1960's indicated that the BMR concept had the potential advantages of reduced weight and complexity, lower costs, and reduced drag; however, the program was terminated at that time because air/ground resonance could not be predicted accurately and the aircraft stability was marginal. With the advent of improved analysis methods, results of experimental investigations, and improved composite materials, the BMR system appeared to be a promising candidate for rotary wing aircraft. This program was designed to investigate an experimental BMR system up to 35 feet in diameter. This report describes the rotor system, flight test vehicle, and flight demonstration, presents the results thereof, and discusses the characteristics of this Bearingless Main Rotor.

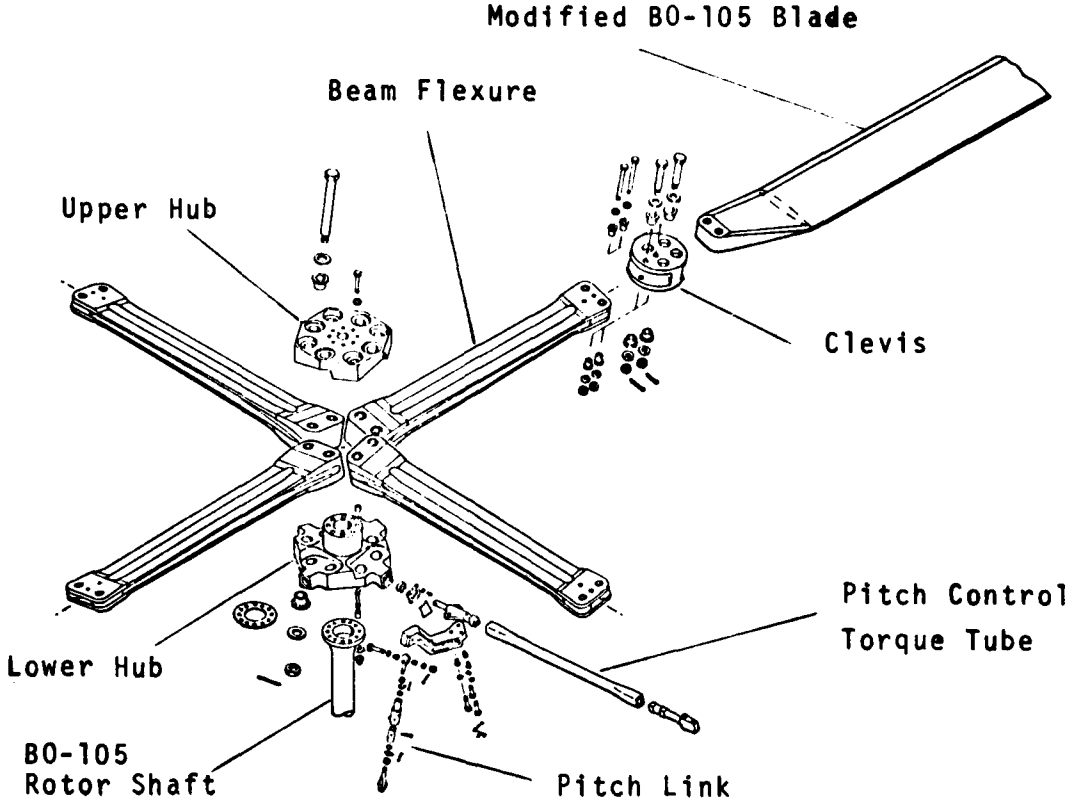

FIGURE 1. THE BEARINGLESS MAIN ROTOR SYSTEM.

PROGRAM HISTORY

During 1974 and 1975, conceptual studies led to an attractive BMR concept and in June 1976, a contract resulting from a competitive procurement was awarded to Boeing Vertol Company. The program passed through the critical phases of preliminary design and development through model and bench testing by September 1977. After fabrication and whirl testing of flight hardware, a successful flight demonstration of the loads, stability, flying qualities, and vibration characteristics of the system was concluded in January 1979.

EVOLUTION OF THE PRELIMINARY DESIGN

Overview

The application of bearingless rotor system technology to the BO-105 was begun in November 1974, following the completion of the proposal for an Improved Rotor Hub Concept (Reference 1; submitted to the Eustis Directorate of USAAMRDL). That document reported previous work which narrowed a field of 10 candidates for soft inplane, main rotor hub designs down to two candidates. As shown in Figure 2, the two candidates were really variations on the one theme of a lag-torsion flexure. Indications were that articulated rotors suitable to the tandem helicopter

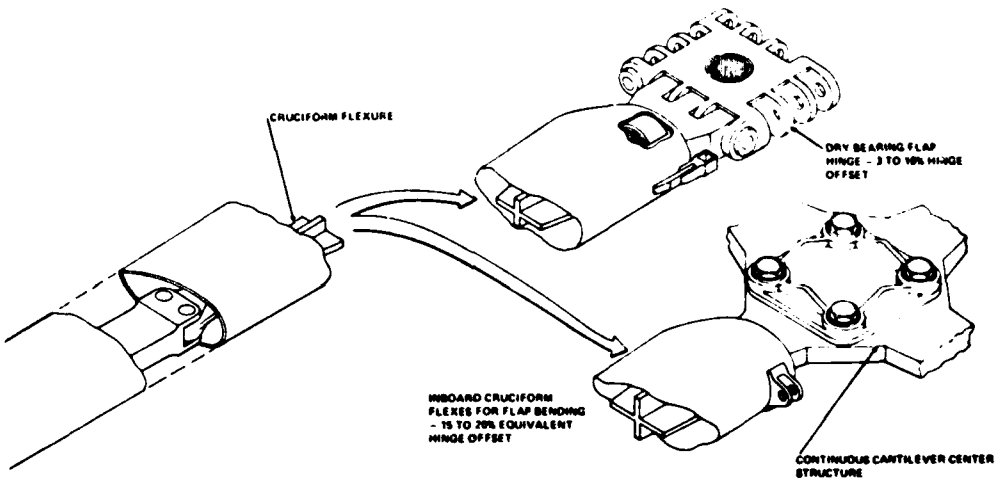

FIGURE 2. LAG TORSION FLEXURE APPLIED TO ARTICULATED AND HINGELESS ROTOR SYSTEMS.

still required the use of flapping bearings to obtain the large tip path plane tilt needed for yaw control in that configuration but lag and pitch motion could be accomplished with the lag-torsion flexure. The benefit to the tandem articulated rotor would be the removal of the lag damper and introduction of elastomeric bearings for flapping motion. The second candidate applied the lag-torsion flexure to the single rotor helicopter, and, drawing upon hingeless rotor technology, Boeing Vertol found that flapping could be accommodated by structural bending.

1. PROPOSAL FOR AN IMPROVED ROTOR HUB CONCEPT, Boeing Vertol Document D210-10860-1, October 1974

Subsequent efforts focused on translating a feasible conceptual design approach into a very promising preliminary design for a soft inplane bearingless main rotor system suitable to the BO-105 helicopter. The research objectives were: (1) To find a direct replacement rotor system that requires no modification to the other major, currently FAA-certified, BO-105 systems such as the control and drive systems. (2) To develop a bearingless rotor hub configuration having the shortest lag-torsion flexure possible. (3) To provide a design that required as little change to the current BO-105 blade as possible.

Key Design Constraints and Criteria

In initiating design of the bearingless main rotor system for the BO-105, aeroelastic stability, structural loads, fatigue stresses, and existing control system actuator power constituted the key criteria from which to evolve a successful trial design. These four major factors are intimately related through the basic geometry of the BMR, particularly over the flap-lag-torsion flexural beam which accommodates the major blade motion. This interrelation becomes apparent by recognizing that for a desired flight condition constraints and criteria must be considered.

Constraints

1. Aeroelastic stability depends on coupled natural frequencies and mode shapes which in turn are dependent on spanwise distributions of mass and stiffness.

2. Structural loads are dependent on spanwise distributions of mass and stiffness.

3. Stresses depend on structural loads, spanwise distribution of stiffness, material, and major dimensions of the cross section.

4. The pitch link load is dependent on the spanwise distribution of torsional rigidity of the flexure beam as well as the rotating inertial and aerodynamic pitching moment of the blade.

Design Criteria

1. Chordwise, flapwise, and torsion stiffness and mass distributions selected to yield aeroelastically stable, coupled mode shapes and current BO-105 frequencies, which are:

1st flap	=	1.12 per rev
1st chord	=	0.70 per rev
1st torsion	=	3.2 per rev

2. No modification to the BO-105 rotor shaft so that hub moments at the shaft centerline are consistent with the current mast moment endurance limit of 60,000 in.-lb. This means assessing fatigue stresses along the blade root for at least four flight conditions based on current BO-105 experience.

From BO-105 flight tests, indications are that banked turn data with forward and aft center of gravity gives representative load data.

The data show that mast bending moments and blade flap bending moments are greatest with forward center of gravity and high load factor, but that aft center of gravity is likely to produce the highest chord bending moments.

3. Selection of materials having excellent allowable stresses at 10^8 cycles with appropriate elastic moduli in bending (E) and torsion (G) which means,

Material	Allowable Tensile Fatigue Stress, Mean - 3σ(psi)	E (psi)	G (psi)
S-Glass	13,000	6.4×10^6	0.64×10^6
Kevlar 49	28,000	12.5×10^6	0.4×10^6

4. No modification to the BO-105 control system which at maximum hydraulic pressure of 1450 psi and 6.50-inch pitch arm can now safely produce:

Control	Blade Angle (deg)	Max Pitch Link Load (lb)
Collective	-0.2 to 15.8	230
Long. Cyclic	-10.5 fwd to 4.7 aft	525
Lat. Cyclic	-5.65 left to 4.23 right	525

5. Blade joint to flap-lag-torsion flexure beam as close to hub centerline as possible to avoid vibration due to the added mass of the joint.

6. Adaptation of current BO-105 cambered airfoil blades with airfoil fairing and appropriate stiffness added to the present swan neck.

7. A torsion axis (shear center) of the inboard flexure beam close to the blade quarter-chord line, placed to help insure individual blade aeroelastic stability and classical flutter stability.

8. For aeroelastic stability, the equivalent feathering axis was to be placed near the plane of rotation to maximize the intermodal coupling between the lag mode and the torsion mode, which is a proven source of rotor aerodynamic damping. (e.g., YUH61A hingeless rotors).

These key design criteria and constraints require the redesign of the most inboard span of the BO-105 blade so that an easily twisted section that still retains the BO-105 hingeless features in the flapwise and chordwise direction could be achieved.

Preliminary Selection of Flexure Cross Sections

Several different beam cross-section shapes are known to be easy to twist, but retain out-of-plane bending stiffness. Cross-section shapes like slit tubes, I-beams, and cruciforms are foremost in having this low torsional rigidity characteristic. But regardless of the cross section under study, the same two fundamental constraints apply. These two constraints, applicable at any inboard span station over the flexing element, are that: (1) the flapwise and chordwise stiffness must be on the same order of magnitude as the BO-105 values at that span station to retain BO-105 dynamic characteristics, and that (2) the flapwise and chordwise bending moments will, therefore, also be on the same order as the BO-105 at the span station. A given shape must change its dimensions to suit a particular stiffness and load condition at that radius station, but the basic shape, once selected, can be expected to be optimum at all stations. Since a reasonable length of inboard blade span is used to achieve a desired twist, an investigation of the torsion moment necessary to twist a constant dimensioned beam having any given cross-sectional shape and fixed at both ends provides a great deal of insight into the problem. By also defining a typical fatigue load and stiffness, the stress situation can be assessed.

Figure 3 summarizes the shapes, and ranges in wall thickness investigated. The same basic approach was followed regardless of the cross section being studied. For a given section (other than the solid ellipse) a wall thickness (t) was selected and the overall width and height were determined to give a flap stiffness (EI_f) of 10 x 10^6 lb -in.^{2} and a chord stiffness (EI_c) of 34 x 10^6 lb -in.^{2}. Then the fatigue stress, assuming a realistic alternating flap moment (M_f) of 4000 in.-lb and an alternating chord moment (M_c) of 7500 in.-lb , was determined (assuming one of the two materials under consideration). Lastly, the torsional moment to twist the 30-inch-long beam 8 degrees was calculated.

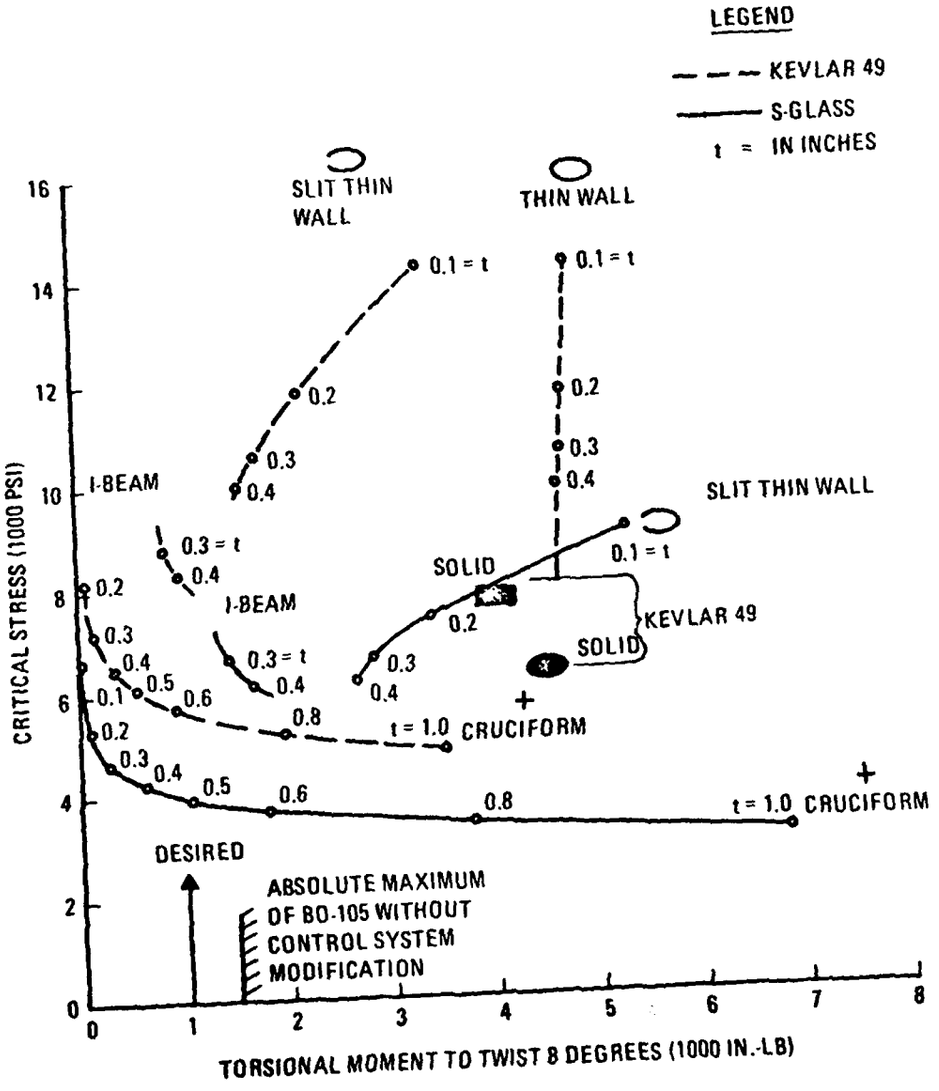

FIGURE 3. SUMMARY RESULTS OF CROSS SECTION SELECTION STUDY.

The typical fatigue stress level in the critical fiber is plotted versus the torsional moment to twist a 30-inch-long beam 8 degrees for the given cross sections, each examined with two materials. The BO-105 control system constraint of roughly 1400 in.-lb provides an absolute maximum limit to allowable torsional moment, and therefore a measure of how low the torsion moment must be for a successful cross section. Since the torsional moment presented in Figure 3 is calculated without including either inertia or aerodynamic contributions, a 1400 in.-lb absolute maximum limit, in fact, required the cross sections to show feasibility at a desired torsional moment more on the order of 1000 in.-lb., which only the I-beam and the cruciform cross sections achieved. Furthermore, the higher elastic modulus material, Kevlar 49, increases the stress (but did make a smaller section) for both I-beam and cruciform configurations.

In conclusion then, there were two feasible cross sections. One was the cruciform, the other was the I-beam. Both configurations could be made from either S-glass having $E=6.4 \times 10^6$ psi or from Kevlar 49 with its $E=12.5 \times 10^6$ psi. Therefore, there were four candidate cross sections from which to choose. These candidates are shown in Figure 4 and are drawn in relative size for the condition of the desired 1000 in.-lb torsional moment.

The selection made at this time was the I-beam cross section fabricated from Kevlar 49. It was concluded that the higher modulus material offered the lower G/E and yielded the smaller cross sections and that the I-beam cross-section approach offered:

1. The greatest potential for a simple hand layup process that could eventually be automated in the production phase.

2. The lowest torsional moment.

3. The greatest margins in fatigue stress due to bending and torsion.

4. The simplest pin wrap and carrythrough for blade retention.

5. The most efficient use of material using the flanges to produce both flap and chord stiffness.

6. The easiest configuration to modify, given exact E and G properties.

7. The best height to fair an airfoil shape around.

NOTES

1. ALL SECTIONS ARE DESIGNED FOR THE SAME MOMENTS AND STIFFNESS AND HAVE APPROXIMATELY 1000 IN.-LB TORSION MOMENT TO TWIST A 30 INCH LONG BEAM 8 DEGREES.
2. ALL DIMENSIONS ARE IN INCHES.

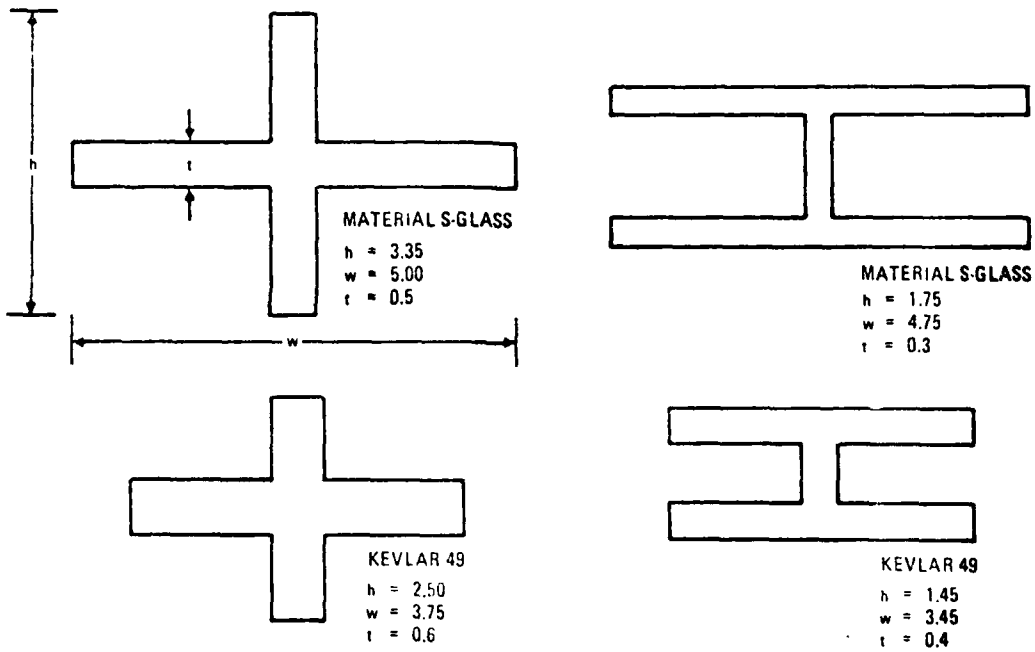

FIGURE 4. FOUR CANDIDATE CROSS SECTIONS FEASIBLE FOR BO-105 BEARINGLESS MAIN ROTOR.

The layout drawing of the selected I-beam trial design BMR system for the BO-105 is shown in Figure 5.

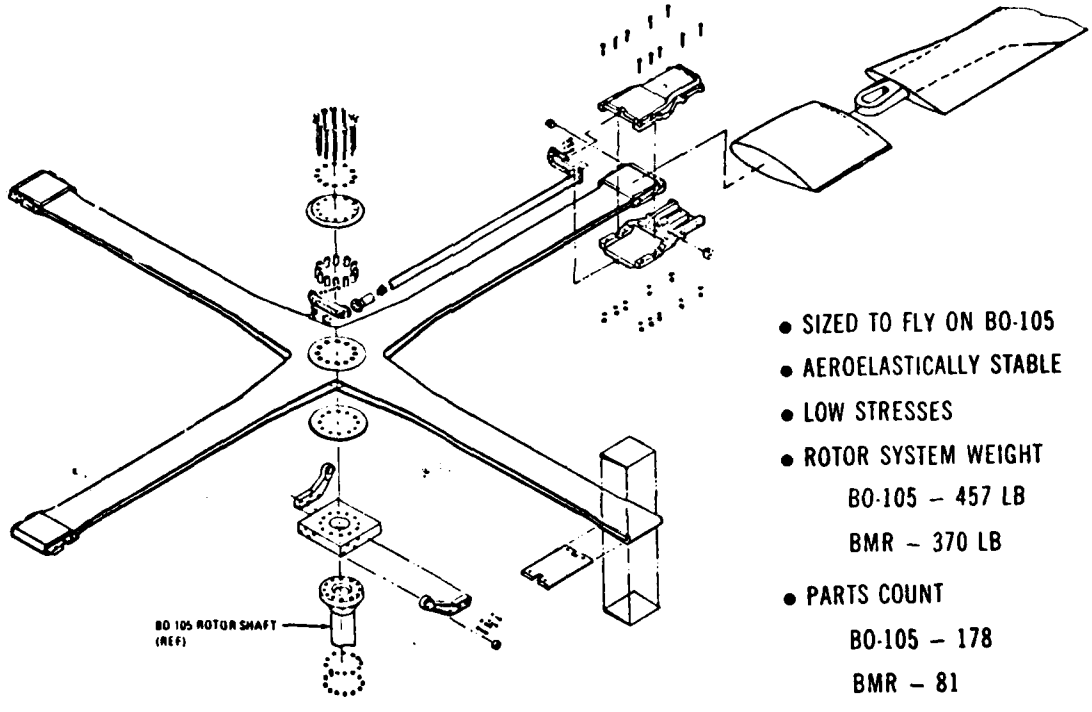

FIGURE 5. FIRST CONFIGURATION DECISION - KEVLAR 49 I-BEAMS WITH LEADING EDGE TORQUE TUBE.

Selection of Blade Pitch Control Mechanism

The search for a satisfactory way to control blade collective and cyclic pitch was begun by starting with twelve variations on three fundamental approaches. The three practical approaches considered were:

1. A torque sleeve that had served as the baseline during more than 2 years of work and needed study as to where the pitch-arm/pitch-link joint should be placed.

2. A torque tube variation of that successfully flown by Lockheed on their XH-51 helicopter in the research program reported in USAAMRDL Technical Report 68-72 (Reference 2).

3. A cantilevered pitch arm, either long or short, as developed and successfully flown on the Boeing Vertol UTTAS stiff in-plane bearingless tail rotor.

The 12 variations considered location and physical positioning of the pitch-arm/pitch-link joints. Nine variations are shown in Figure 6.

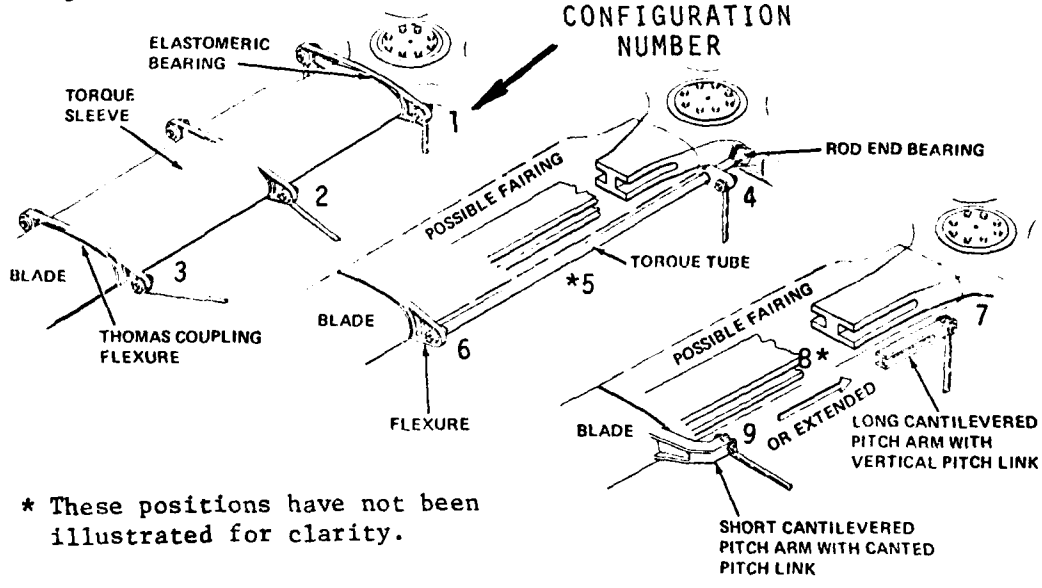

FIGURE 6. BLADE PITCH CONTROL STUDY SHOWED THE TORQUE TUBE OR TORQUE SLEEVE FEASIBLE.

2. Cardinale, S. V., SOFT IN-PLANE MATCHED-STIFFNESS/FLEXURE-ROOT-BLADE ROTOR SYSTEM SUMMARY REPORT, Lockheed-California Co.; USAAVLABS Technical Report 68-72, U. S. Army Aviation Materiel Laboratories, Fort Eustis, Virginia, August 1979, AD 863063.

Aeroelastic stability of the several configurations was the primary consideration as the study group set out to narrow the field of candidates. Theoretical studies showed that the level of aeroelastic stability could be significantly altered or even made unstable by selecting, what is in essence, an incorrect mechanical flap-pitch coupling. Favorable mechanical flap-pitch coupling of flap-up/pitch-down can be used to stabilize even an elastically unstable combination of flap-pitch and lag-pitch coupling. Theoretical studies showed that the baseline configuration of torque sleeve with a leading pitch-arm/pitch-link pivot joint located near the hub would provide a BO-105 level of aeroelastic stability. Experimental investigation, used so extensively and successfully in developing the main and tail rotors for the UTTAS, was initiated.

The objective of the experimental investigation was to evaluate the relative aeroelastic stability of the several blade pitch control candidates displayed in Figure 6. The experiments were conducted with the 28-inch rotor diameter, Froude scaled model shown in Figure 7.

The hub and flap-lag-torsion flexural beam was machined from nylon and sized to produce representative first mode rotating frequencies of 1.1 flapwise and 0.72 chordwise at the nominal model rotor speed of 1400 rpm. With the torque sleeve in place, the measured nonrotating flap frequency was 8.2 cycles per second and the chord frequency was 15.6 cycles per second, which was quite satisfactory for the proposed configuration study.

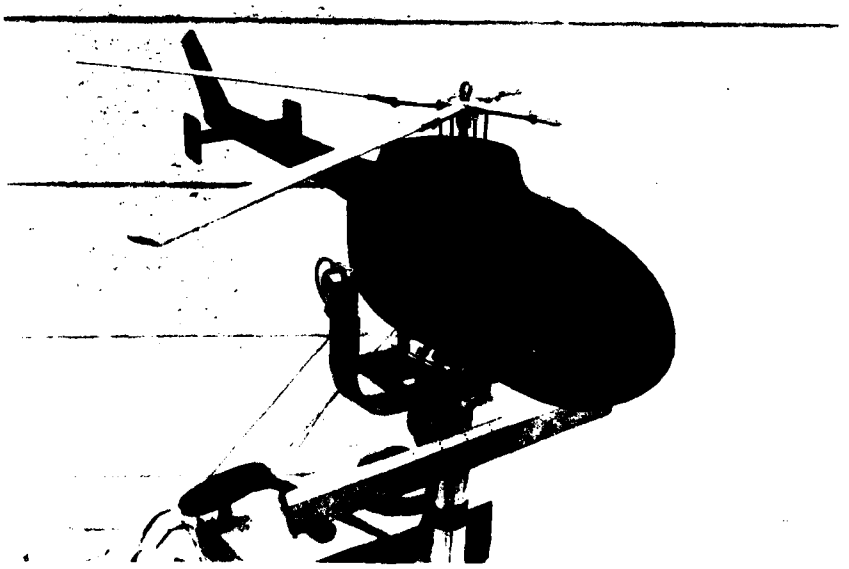

FIGURE 7. 1/13.8 FROUDE SCALED BO-105 MODEL USED IN PRELIMINARY AEROELASTIC STABILITY INVESTIGATION.

Bang tests of the assembled configuration showed a non-rotating inplane critical damping ratio of 2 percent.

In summary, the theoretical and experimental aeroelastic stability studies, plus design layouts, showed that:

1. The torque tube along the leading edge was an excellent way of controlling blade collective and cyclic pitch.

2. The torque sleeve was just as feasible as way of controlling pitch, but provided an aerodynamic fairing.

3. Aeroelastic stability could be improved by moving the pitch arm out along the span in either the torque tube or torque sleeve approach.

4. Cantilevered pitch arms for bearingless soft inplane main rotors would require more investigation than either a torque tube or torque sleeve approach.

A full-scale layout drawing of the torque tube blade pitch control approach was completed, as shown in Figure 5. This illustration reflects the selection of the I-beam cross-section for the flap-lag-torsion flexural beam.

The final selection for the control of blade collective and cyclic pitch was the torque tube. It was concluded that in the torque tube approach we could:

1. Use a conventional rod-end type bearing to react the pitch-link load and tube centrifugal force rather than having to develop an elastomeric bearing and attach it to the I-beam.

2. Evaluate the I-beam during flight research without a fairing, thus giving complete accessibility for inspection and instrumentation maintenance.

3. Study the influence of aerodynamic fairing over the I-beam and torque tube separately, after demonstrating in flight an aeroelastically stable and structurally sound configuration.

4. Draw heavily upon the growing high-modulus graphite experience with drive shafts to get the lightest and smallest torque tube possible in the future.

Critique of the System Concept

In arriving at this bearingless main rotor configuration for the BO-105, the contractor investigated:

1. Ten main rotor system concepts, and selected a cantilevered lag-torsion flexural beam as the best approach to improving the hingeless rotor by removing the pitch bearings.

2. Fourteen combinations of flexural beam cross sections and materials, and selected an I-beam made with Kevlar 49 because it was the easiest to twist, had the greatest margin in stress, and would be the easiest to fabricate.

3. Twelve ways to control blade pitch (nine in detail and six experimentally) and selected the torque tube approach with leading pitch arm for the flight research phase because it required no elastomeric bearing development and kept the I-beam open for inspection and instrumentation maintenance.

The trial design bearingless main rotor hub required some gentle tailoring in the spanwise stiffness distributions to insure a better starting point for preliminary design.

The design at this point had a first flap frequency of 1.105 versus the desired 1.125 per rev and a first chord frequency of 0.747 per rev versus the desired 0.70 per rev of the BO-105. The design incorporates the "mismatched" stiffness distribution of the BO-105 to insure aeroelastically stable coupling even beyond the BO-105 normal rpm range of 85 to 110 percent. Work into the first iteration of preliminary design continued with the commencement of the contract effort. Through normal evolution, further design decisions were made.

It was decided that due to the comparative lack of fatigue data at that time and the questionable compressive strength of Kevlar 49 it would be prudent to change to the other proven alternate material, S-glass. Furthermore, the necessity for an outboard flexure to accommodate the discontinuity in slope between the torque tube and the pitched blade detracted from the intended simplicity of the BMR objectives. A parallel effort had concluded that if the I-beam was split into two (].[) channels and separated, the torque tube could be placed at the center of twist and thus eliminate the requirement for the outboard flexure. The design was reiterated with the result as shown in Figure 8.

The mainstream effort was then applied to the dual beam concept. New tools for structural and dynamic analysis had to be evolved since the dual beam under torsional bending and CF loading was not a classical textbook

problem. Reference 3 discusses, in depth, details in the concept evolution to this time; however, improvements to the configuration were not yet complete.

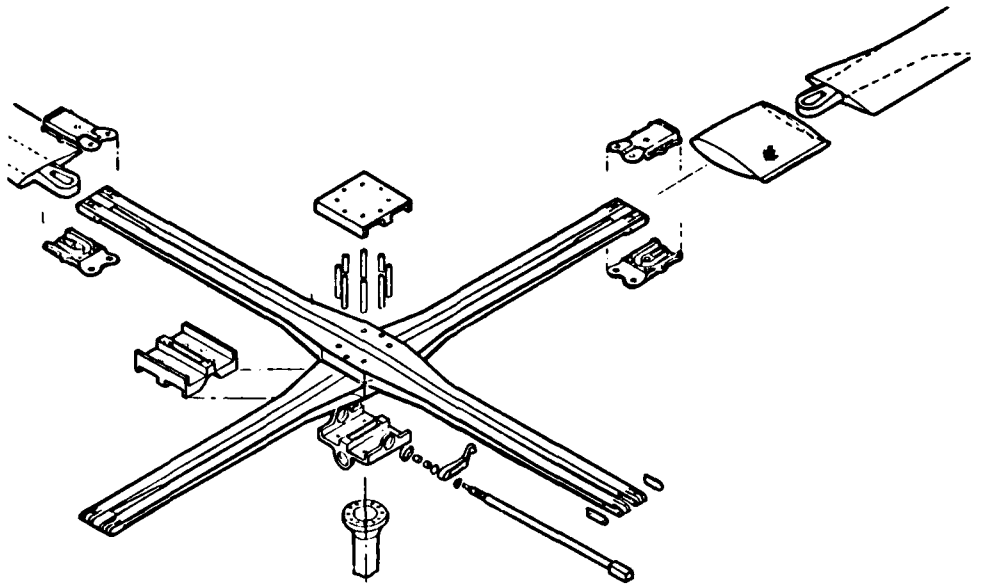

FIGURE 8. SECOND CONFIGURATION. S-GLASS, SPLIT I-BEAM, STACKED, WITH CENTERED TORQUE TUBE.

Analytical Evaluation of the Preliminary Design

The second configuration concept was then evaluated regarding (1) structural integrity, (2) aeroelastic stability, (3) impact on cost and reliability, and (4) the capability to change those geometric parameters which were known to affect stability with comparative ease (if required during full-scale testing). The following conclusions resulted:

1. A fatigue life of 4900 hrs, assuming the flight operation was flown all at the heaviest gross weight and most severe possible CG location, was calculated. Thus, this BMR configuration was structurally sound.

2. The system was predicted to have an adequate stability envelope with the upper rotor limit imposed by ground resonance stability at 550 rpm and the lower rotor limit

3. INTERIM TECHNICAL REPORT FOR TASK I, PRELIMINARY DESIGN, Volumes A, B, and C, Boeing Vertol Document D210-11129-1, September 1976.

by the air resonance mode at 335 rpm. Lag natural frequency for this configuration was 0.71 per rev (425 rpm = normal) and it was concluded that the stability range could be widened by the judicious choice of lag frequency and flap-lag coupling.

3. An evaluation of the design and cost risk areas concluded that if the existing BO-105 blade root end were used, the requirement of $\theta_{.7R} = 10°$ at the untwisted hub (cruise) condition necessitated a twist of 12-1/2° incorporated in the attachment hardware between the flexure end and the blade root. Furthermore, the single pin blade attachment required additional socketing with resulting cost and excessive weight. It was then recommended that since new modified blades had to be manufactured anyway and that an aerodynamic cuff would be required and the major component of blade cost would be the fittings, the correct configuration should include a blade root with 12-1/2° of twist and an integral fairing together with a two-pin wraparound concept to preclude the socket requirement and to provide a variable sweep if required.

Furthermore, the original attachment contained cavities for the horizontal beam wraps which require expensive numerical control methods in the fabrication of the part. Conventional machining methods could be used if the flexure wraps were vertical and a two-vertical-pin attachment used, and the discontinuous web plies could be made continuous and so preclude peeling and delamination. An additional advantage of vertical wraps was their similarity with those at the recommended blade root end.

The metal torque tube had a horizontal pivot at the blade attachment to relieve the tube of excessive bending moments due to its own flap stiffness resisting changes in blade displacements. This complexity, together with the excessive weight of metal components, could be relieved if a graphite composite fiber structure was used.

Since the prime objective of the program was to demonstrate the stability of the system, and precone of the blade relative to the torsion flexure was known to have a stabilizing influence on the rotor system, it was recommended that the capability to vary precone be included. Since the configuration of precone at the shaft and blade root must total 2-1/2° (for steady flap bending relief) this capacity had to be included at both the beam-to-blade junction and the beam-to-shaft junction, which precluded the straight-through-hub concept.

Modification to the Preliminary Design

After careful evaluation of the above recommendations, they were adopted in their entirety resulting in the R&D configuration shown in Figure 9.

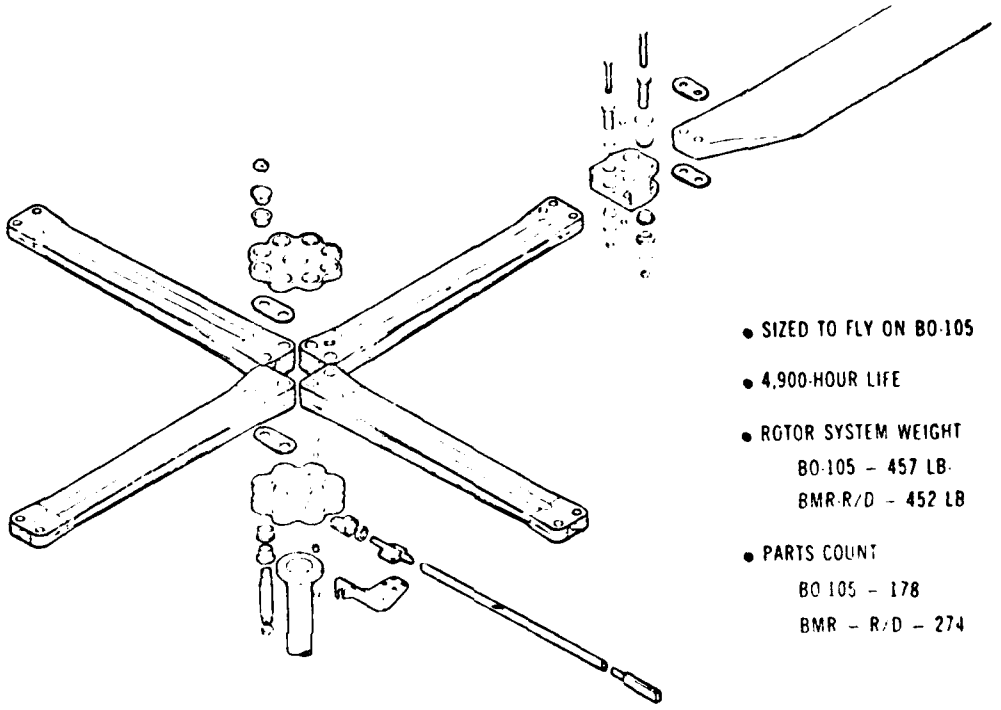

FIGURE 9. R&D CONFIGURATION INCLUDING GEOMETRY VARIABLES REQUIRED TO CHANGE AEROELASTIC STABILITY VARIABLES DURING FLIGHT RESEARCH PROGRAM.

For this concept, the design was reiterated because of the change in the beam-to-shaft attachment of the second configuration (Figure 8).

Variation in blade/flexure precone was included through the use of numerous but simple bushings at each attachment. Each set of bushings had its bore located eccentrically in axis location and orientation relative to its outside cylindrical surface. Wedges provided the parallelism between the blade and beam preconed upper and lower surface with its mate in the attachment hardware. The additional features of beam spacing and hence 1st chord modal frequency variation and/or blade sweep were then provided.

Final Preliminary Design

The configuration to which testing and development effort was directed was now fixed. A profound structural and life analysis was made and analyses were conducted to predict the overall hover and ground resonance stability and the effects of geometric variations thereon.

The results of the analyses indicated that the objectives of the program would be met in all respects.

The detail design, fabrication of test hardware, and wind tunnel model and bench test evaluation were initiated.

The first of three full-scale beam assembly test specimens was manufactured. However, a series of loading tests revealed that the beam assembly was too stiff in both the flapwise and chordwise direction as well as torsionally. This was due to the manufacturing procedure of partially curing the flanges separately and then final curing the whole assembly, which resulted in a high degree of compaction. That meant the material had a lower than nominal resin content. This gave a value of Young's modulus (E) and torsion modulus (G) higher than the published values for the 1002SF1 unidirectional fiberglass at 0° fiber orientation.

The decision was made to revise the configuration and make the necessary tooling changes to bring the physical properties of the remaining beam assemblies into line with those desired. With the knowledge of the material properties gained from the test results and with a greater degree of sophistication through developing a digital computer program that could rapidly predict stresses and fatigue life for any cross section, the dual beam assembly was revised. There were three basic changes to the flexure configuration. First, the overall spanwise height distribution of the beam was reduced along the span except at both inboard and outboard pin locations. This height reduction was dictated by the requirement to maintain a 3600-hour fatigue life at every location while trying to achieve a close match to the BO-105 flap frequencies at nominal rpm. The second change was a retailoring and reduction by one-half of the amount of fiberglass crossply wrap in each flange while maintaining crossply at the corner of the web and flange. This yielded a reduction in the overall torsional rigidity of the beam assembly while retaining shear strength integrity. Finally, the measured flange thickness was incorporated in the analysis.

To complement the air and ground resonance theories, a Froude-scaled air resonance model as shown in Figure 10 was developed. This 5.5-foot-diameter model has a scale

factor of 1/5.86. The model is free to pitch and roll about a two-axis gimbal system. A pilot "flies" the model with a complete fly-by-wire control system. Testing as reported in Reference 4 was conducted in both hover and forward flight and covered the complete FAA-approved envelope of the BO-105. Parametric studies were conducted to investigate the effects of geometric variations upon stability and these indicated that additional stability margin could be achieved by pretwisting the beam flexure at the beam/shaft attachment (L.E. up) and thus provide additional lag/flap coupling. Careful consideration was given to incorporating this change in the final preliminary design. Advantages were that the margin of stability in the reduced rpm ranges would be substantially increased and that the 12-1/2° of twist required to maintain a near cruise collective with an untwisted beam (or control system failure) could be at the beam-shaft attachment instead of in a short length of the blade root.

Disadvantages were that the hub plates with built-in pretwist became more complex and expensive and due to the compound angles thus introduced, easy variation in beam to hub precone was negated. In spite of these factors this final change to the configuration was adopted.

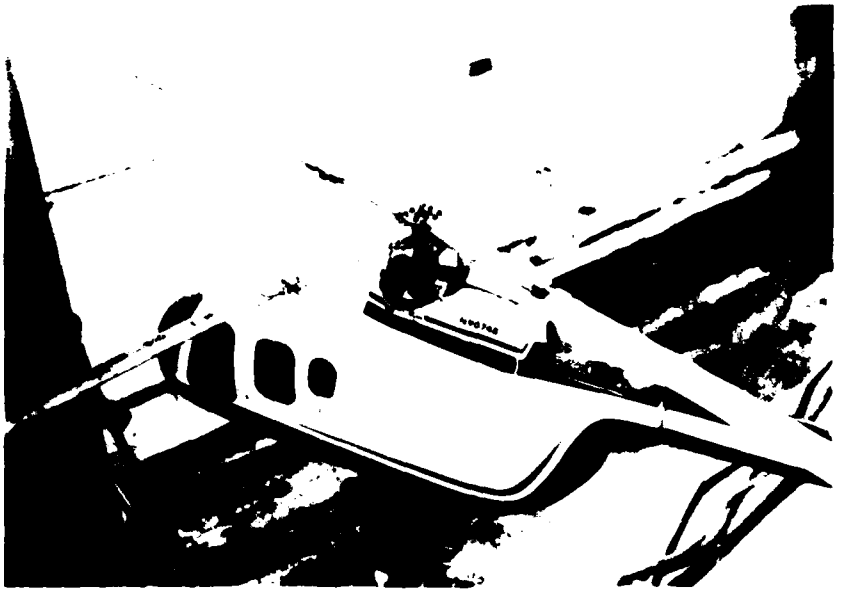

FIGURE 10. 5.5-FOOT-DIAMETER FROUDE SCALED MODEL FOR AEROELASTIC STABILITY INVESTIGATIONS.

4. INTERIM TECHNICAL REPORT FOR TASK II, 1/5.86 FROUDE SCALED MODEL TEST RESULTS, Boeing Vertol Document D210-11245-1, June 1977.

BEARINGLESS MAIN ROTOR (BMR) SYSTEM CHARACTERISTICS

GENERAL DESCRIPTION

The Boeing Vertol Bearingless Main Rotor, under development for nearly 5 years, is as shown in Figure 1. The configuration shows modified BO-105 blades attached to a set of dual fiberglass beams. The blade-to-beam joint is made at the 25-percent radius station. The beam's root end is pinned at the 2.38-percent radius station to a metal hub plate set. Blade pitch is controlled by a filament-wound graphite torque tube. The outboard end of the torque is bolted solidly (cantilevered) at the blade-to-beam joint. The torque tube is supported at its inboard end by a rod-end bearing of the type used in helicopter upper control assemblies. The fiberglass beams are made of 3M-1002SF-1 preimpregnated material and are laid up in matched metal dies. The fiberglass beams have basically a C-channel ([) cross section. All the geometric parameters of the individual beams such as width, height, flange and web thickness, and spacing between the beams vary along the 52-inch nominal length. The fiberglass beams permit flapwise bending, chordwise bending, and full torsional travel. The BMR, as designed to fly on the BO-105 flight vehicle, has flap chord and torsional frequencies at approximately the current BO-105 values; thus the BMR is a soft in-plane rotor.

Geometric Properties

Radius of the rotor system is 193.37 inches. Figure 11 presents the beam flexure cross section geometry in graphical form. Tabulated data is given in Table 1. For the blade having a constant 23012 airfoil distribution and 10.63 inches chord, the geometric twist is shown in Figure 12. With the beam flexure untwisted, and attached at the hub at an inclination of 12-1/2°, the blade chord line at 70-percent radius station has an incidence of 9.55° or the theoretical cruise collective.

Attachment of the blade to the 8-inch-diameter titanium clevis is made at 52.36 inches radius station and that of the clevis to the beam flexure is at 49.30 inches radius station. The inboard attachment of the flexure to the hub is at 4.60 inches radius station.

Stiffness Properties

Table 1 presents the stiffness distribution in flap and chord together with the shear stiffness of the beam flexure. The additional term (EC_w) is the warping constraint which resists a component of the applied twisting moment. Table 2 shows the total contributions of the rigidizing factors as they resist the applied twisting moment of 128 in.-lb, which results in 1° of total twist.

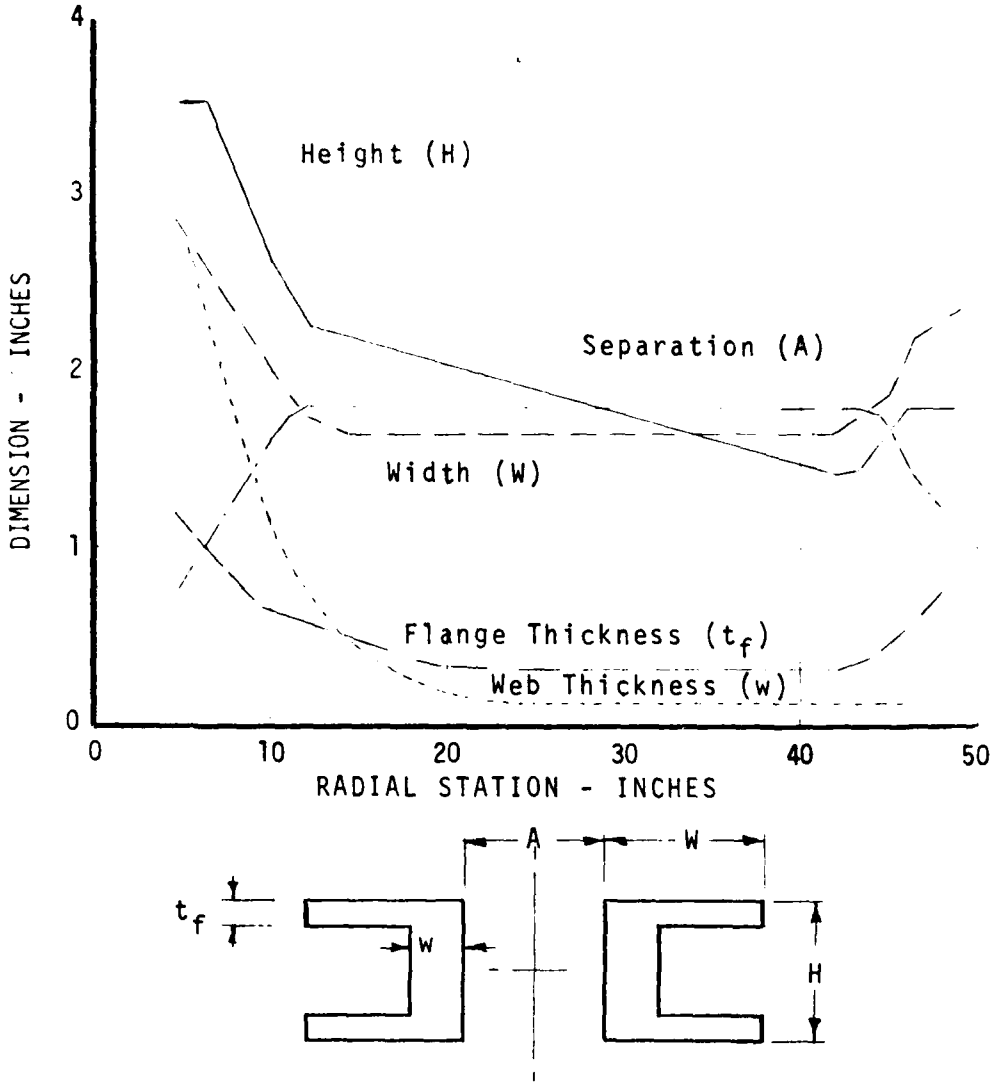

FIGURE 11. FLEXURE BEAM SECTION GEOMETRY.

TABLE 1. PHYSICAL PROPERTIES OF DUAL BEAM ASSEMBLY
CONFIGURATION DEFINED BY DWG. 238-10001, REV. F

RADIAL STN. (IN.)	WIDTH W (IN.)	HEIGHT H (IN.)	t_{FLANGE} t_f (IN.)	t_{WEB} t_w (IN.)	EI_f x 10^{-6} (LB-IN.^{2})	I_f (LB-IN.^{2})	EI_c x 10^{-6} (LB-IN.^{2})	I_c (LB-IN.^{2})
4.6	2.875	3.526	1.201	1.250	58.1600	15.992	380.8900	44.351
5.3	2.770	3.526	1.156	2.718	96.8550	20.223	392.3630	74.521
6.3	2.600	3.526	1.092	2.336	92.0356	18.593	350.1850	63.489
8.3	2.280	3.055	.895	1.651	60.0551	10.617	235.5785	40.144
10.3	1.960	2.583	.699	1.056	30.9167	5.379	151.0927	24.290
12.3	1.720	2.2756	.593	.676	19.5626	3.1545	104.713	15.958
14.3	1.650	2.2182	.516	.469	16.6151	2.673	79.639	12.358
16.3	1.650	2.1608	.439	.359	14.2379	2.320	66.083	10.361
18.3	1.650	2.1034	.362	.256	11.7275	1.949	52.548	8.401
20.3	1.650	2.0460	.337	.182	10.2690	1.723	46.903	7.614
22.3	1.650	1.9886	.311	.140	8.9609	1.520	42.021	6.934
24.3	1.650	1.9312	.286	.126	7.6557	1.313	38.041	6.358
26.3	1.650	1.8738	.286	.126	7.2890	1.249	38.014	6.349
28.3	1.650	1.8164	.286	.126	6.7715	1.159	37.975	6.336
30.3	1.650	1.7590	.286	.126	6.2735	1.072	37.935	6.322
32.3	1.650	1.7017	.286	.126	5.7959	.989	37.896	6.309
34.3	1.650	1.6443	.286	.126	5.3369	.909	37.857	6.296
36.3	1.650	1.5869	.286	.126	4.8974	.833	37.818	6.282
38.3	1.650	1.5295	.286	.126	4.4774	.761	37.778	6.269
40.8	1.650	1.4577	.286	.126	3.9793	.675	37.729	6.252
42.3	1.740	1.6647	.304	.126	5.979	1.009	43.986	7.241
44.3	1.920	1.6970	.410	.126	7.7065	1.362.	71.2332	11.276
46.3	2.150	1.8500	.575	2.150	12.8540	2.269	135.6900	28.659

TABLE 1. (CONTINUED)

RADIAL STN. (IN.)	EI_{co} x 10^{-6} (LB-IN.^{2})	EA x 10^{-6} (LB)	A (IN.^{2})	GK x 10^{-6} (LB-IN.^{2})	WT/IN. (LB/IN.)	I_θ (LB-IN.^{2}/IN.)	SEPARATION OF N. A.'s (IN.)	EC_w x 10^{-6} (LB-IN.^{4})
4.6	45.135	64.253	9.830	29.560	.688	4.224	3.600	419.78
5.3	36.241	81.147	19.408	26.215	1.359	6.632	3.550	404.43
6.3	31.728	76.810	17.627	15.747	1.233	5.746	3.488	157.90
8.3	13.087	61.355	12.338	6.425	.864	3.553	3.499	65.85
10.3	6.908	43.929	7.983	1.627	.559	2.077	3.378	25.68
12.3	3.905	33.485	5.554	.52145	.389	1.338	3.289	11.94
14.3	3.197	27.440	4.518	.3096	.316	1.052	3.224	7.73
16.3	2.767	22.657	3.818	.1936	.267	.888	3.221	5.75
18.3	2.235	17.716	3.095	.1134	.217	.725	3.245	4.18
20.3	1.885	15.228	2.724	.0931	.191	.654	3.328	3.28
22.3	1.587	13.307	2.435	.0756	.170	.592	3.391	2.73
24.3	1.399	11.944	2.226	.0611	.156	.537	3.414	2.40
26.3	1.394	11.926	2.216	.0610	.155	.532	3.416	2.26
28.3	1.387	11.900	2.201	.0609	.154	.525	3.419	2.12
30.3	1.379	11.874	2.187	.0607	.153	.518	3.423	1.98
32.3	1.372	11.847	2.172	.0606	.152	.511	3.426	1.85
34.3	1.364	11.821	2.158	.0605	.151	.504	3.429	1.72
36.3	1.357	11.795	2.143	.0603	.150	.498	3.433	1.60
38.3	1.349	11.768	2.129	.0602	.149	.492	3.436	1.48
40.8	1.340	11.735	2.111	.0601	.148	.485	3.440	1.34
42.3	1.638	13.127	2.358	.0734	.165	.578	3.504	1.91
44.3	2.8528	18.456	3.370	.1673	.236	.885	3.656	2.47
46.3	8.2719	31.577	7.955	9.7500	.557	2.165	3.681	45.34

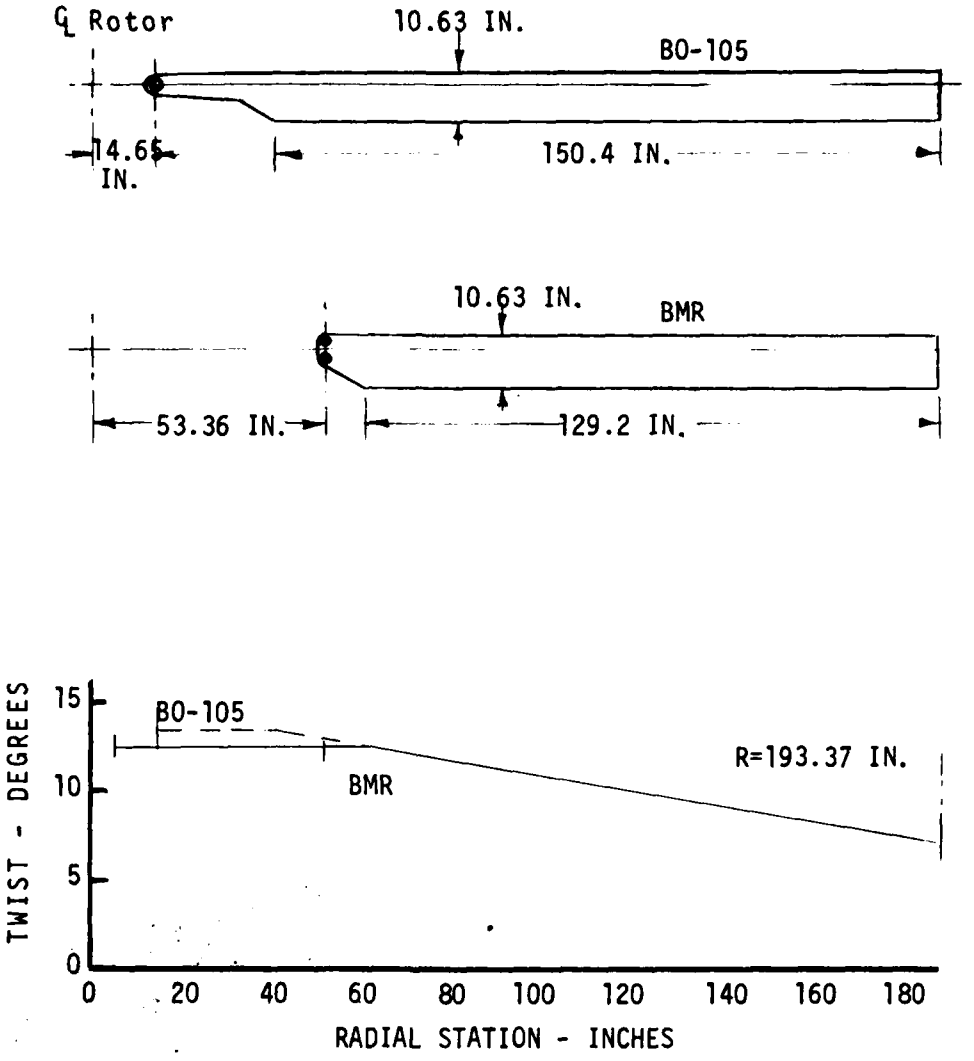

FIGURE 12. BMR AND BO-105 ROTOR BLADE - GEOMETRIC TWIST.

TABLE 2. FACTORS THAT CONTRIBUTE TO A TORSION MOMENT REQUIREMENT OF 128 IN-LB FOR ONE DEGREE OF TWIST

$$M_\theta = GK\left[\frac{d\theta}{d\ell}\right] - E \cdot C_w\left[\frac{d^3\theta}{d\ell^3}\right] + CF\left[\frac{EI_f + EI_c}{EA}\right]\frac{d\theta}{d\ell} - CF\left[\frac{M_f^2 + M_c^2}{CF^2}\right]\frac{d\theta}{d\ell}$$

R (IN.)	$GK\frac{d\theta}{d\ell}$ (IN-LB)	$-E \cdot C_w\frac{d^3\theta}{d\ell^3}$ (IN-LB)	$CF\left[\frac{EI_f + EI_c}{EA}\right]\frac{d\theta}{d\ell}$ (IN-LB)	$CF\left[\frac{M_f^2 + M_c^2}{CF^2}\right]\frac{d\theta}{d\ell}$ (IN-LB)
4.6	0	128	0	0
5.3	306	-180	2	0
6.3	456	-334	7	1
8.3	457	-339	13	3
10.3	216	-103	22	7
12.3	121	-14	31	10
14.3	93	5	42	12
16.3	76	11	54	13
18.3	54	19	67	12
20.3	49	13	78	12
22.3	45	8	86	11
24.3	37	9	92	10
26.3	38	6	93	9
28.3	39	3	92	7
30.3	39	2	92	6
32.3	39	2	92	5
34.3	38	3	92	5
36.3	37	6	89	4
38.3	36	12	83	3
40.3	33	24	73	3
42.3	30	40	60	2
44.3	29	70	30	1
46.3	0	128	0	0

Flap and chord stiffness data from Tables 1 and 2 is presented graphically in Figures 13 and 14 respectively and provides a comparison with the standard BO-105 blade root flexure.

The theoretical twisted mode shape of the BMR beam flexure with and without the applied centrifugal force or the expected flapwise and chordwise bending moment distribution is given in Figure 15.

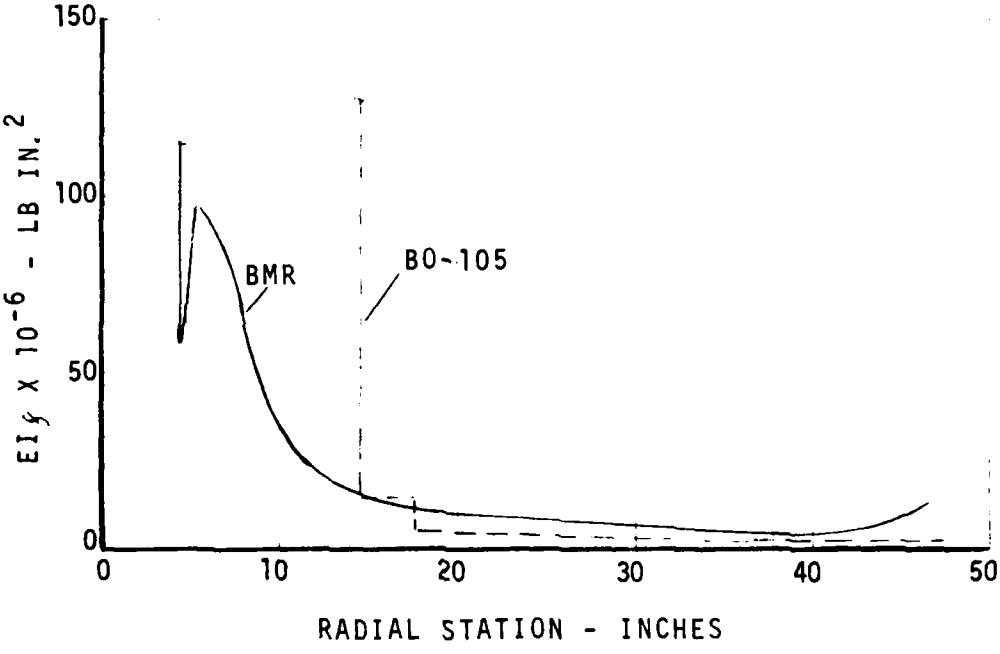

FIGURE 13. BEAM FLEXURE FLAPWISE STIFFNESS DISTRIBUTION.

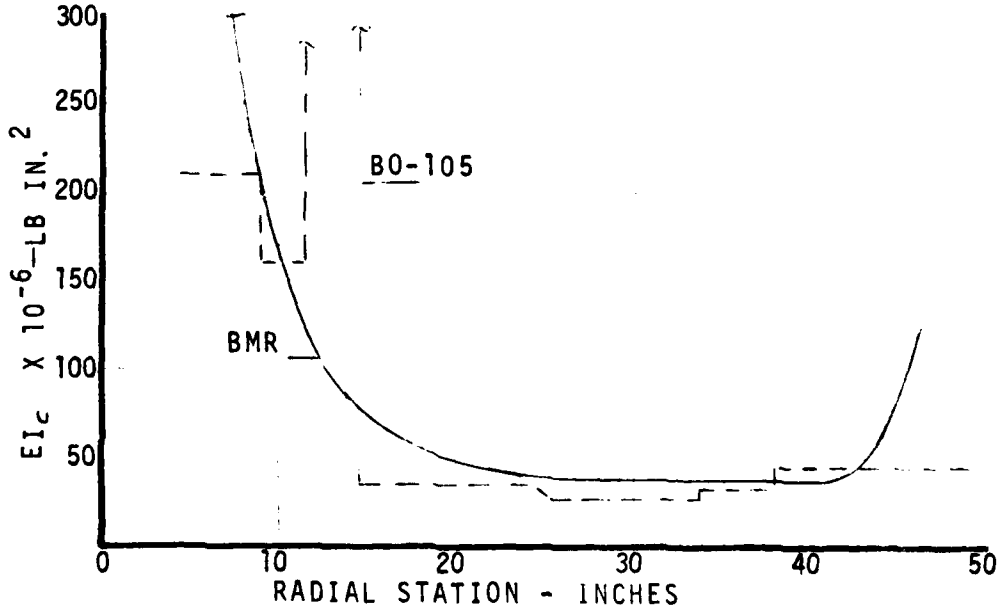

FIGURE 14. BEAM FLEXURE CHORDWISE STIFFNESS DISTRIBUTION- EQUIVALENT SINGLE BEAM.

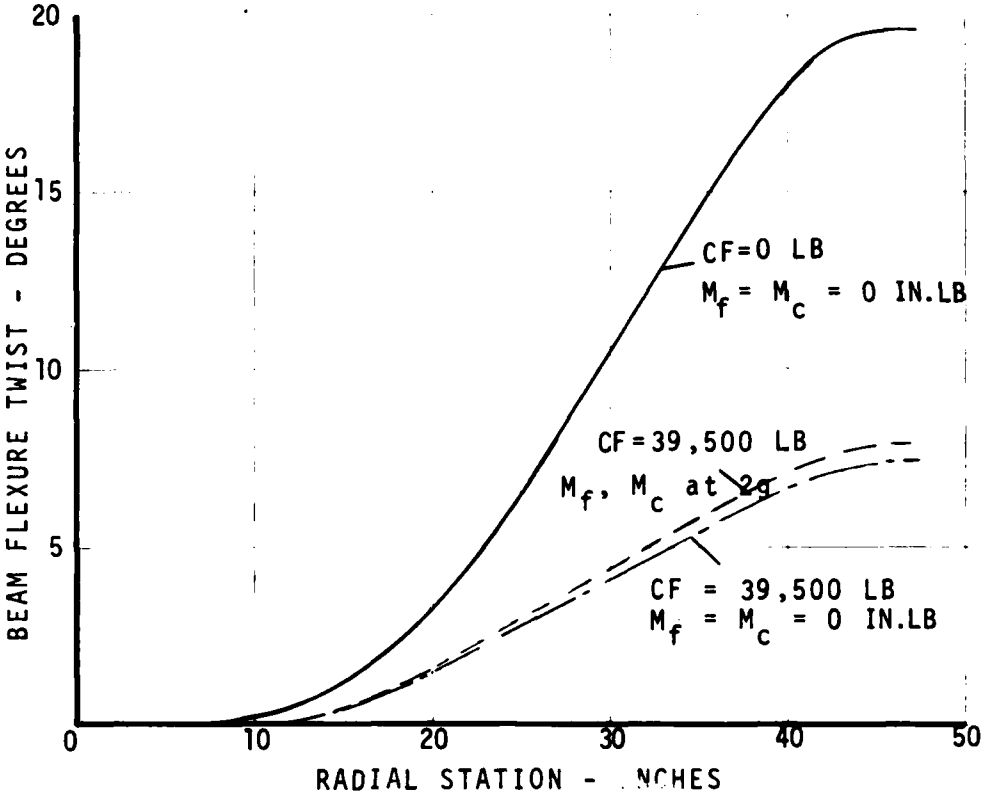

FIGURE 15. BEAM FLEXURE TWIST UNDER APPLIED TORQUE OF 1000 IN.-LB.

Stiffness properties of the blade section of the rotor are listed in Table 3.

Weight and Inertia

The radial distributions of rotor weight and pitching moment of inertia are listed in Tables 1 and 3.

TABLE 3. BLADE AND CLEVIS PROPERTIES

R (IN.)	r/R % RADIUS	WT./IN. (LB-IN)	EI-FLAP (10^6 LB-IN.^{2}) EI_F	EI-CHORD (10^6 LB-IN.^{2}) EI_C	TORSIONAL STIFFNESS (10^6 LB-IN.^{2}) GK
193.37	1.0	.71	2.38	59.4	1.36
192.02	.993	.71	↑	↑	↑
192.02	.993	.511			
188.92	.997	.511			
186.99	.967	.32			
153.92	.796	.32			
153.92	.796	.309			
97.65	.505	.309			
97.65	.505	1.447			
95.72	.495	1.447			
95.72	.495	.309			
87.79	.454	.309	↓	↓	1.36
81.99	.424	.309	2.38	59.4	1.55
76.19	.394	.372	3.39	56.71	1.74
66.52	.344	.4762	5.084	52.21	3.02
62.85	.325	.5159	5.725	50.51	3.80
59.94	.304	.5474	6.234	49.16	4.07
53.95	.279	.6121	7.281	46.375	4.10
53.95	.279	2.573	82.28	68.375	5.10
52.	.269	2.573	157.28	266.375	5.77
50.4	.2607	2.573	164.4	291.38	6.32
50.4	.2607	1.3725	164.4	521.38	41.13
49.75	.2573	1.359	167.28	566.95	41.13

BO-105 BASELINE AIRCRAFT CHARACTERISTICS

GENERAL DESCRIPTION

Figure 16 shows the standard production Messerschmidt-Boelkow-Blohm BO-105 Helicopter. Figure 17 is a 3-view drawing of the aircraft.

Maximum design gross weight is 5070 lb (C_t/σ = 0.073). Power is from two Allison 250-C20 turbines, each capable of 400 SHP output. Placard rotor rpm range is 95 to 102 percent of the normal 425 rpm - power on, and 85-percent to 110 percent normal - power off. This aircraft, owned by the Boeing Vertol Company, is an engineering research tool and has been used to develop and demonstrate techniques to attenuate rotor induced vibration. An Improved Rotor Isolation System (IRIS) is configured into the existing aircraft, but for the purpose of demonstrating the BMR this system has been rendered ineffective. However, the nonstandard control linkage has been retained. The aircraft, thus configured, was used for both baseline (BO-105 standard rotor) and BMR flight evaluations.

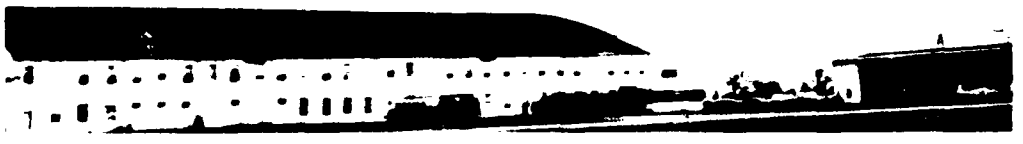

FIGURE 16. THE MBB BO-105 FLIGHT RESEARCH HELICOPTER.

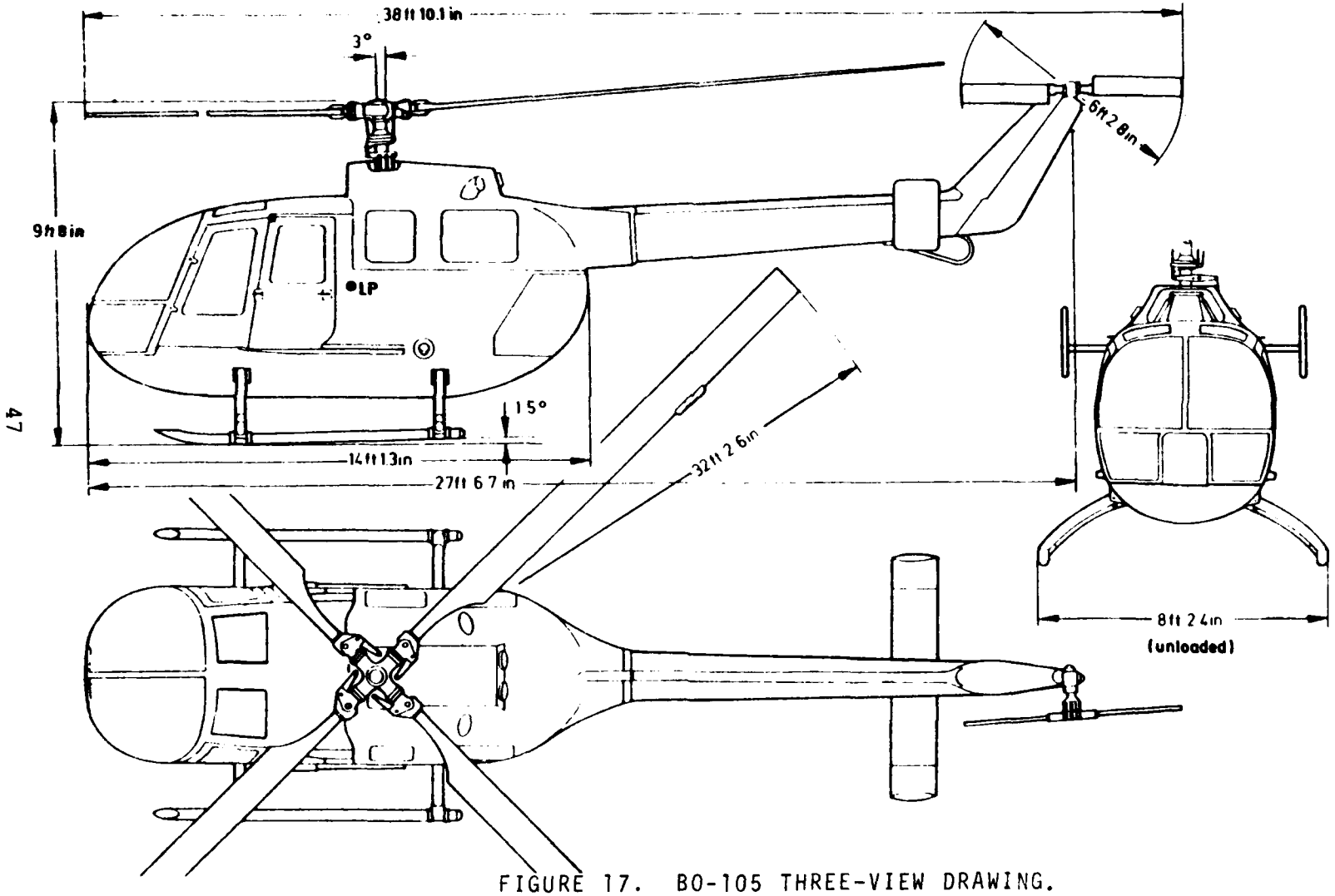

FIGURE 17. BO-105 THREE-VIEW DRAWING.

FURTHER AIRCRAFT MODIFICATIONS

Due to the torsional rigidity of the BMR beam flexures (141 in.-lb/degree) being greater than the BO-105 (45 in.-lb/degree), control loads were expected to be higher than normal. Analytical studies reinforced with bench test data showed that the standard hydraulic boot pressure of 1500 psi was only just sufficient. It was considered prudent to provide a greater control margin by increasing the system boost pressure to 2000 psi.

The attachment of the BMR hub to the rotor shaft was through the same hole pattern as the standard hub; however, shorter pitch links had to be fabricated to accommodate the difference in the pitch arm attachment location.

Preliminary ground resonance flight tests showed the need for stiffening of the landing gear to result in an increase in the critical rotor speed for ground resonance. Figure 18 shows two steel cables, each stretched between the ends of the gear bows at skid level, which resulted in an increase in aircraft pitch and longitudinal mode frequency.

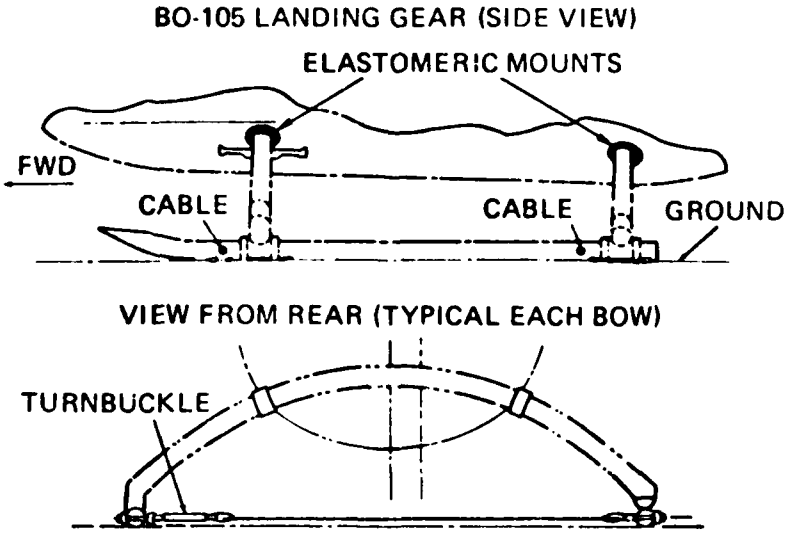

FIGURE 18. STIFFENING MODIFICATION FOR BO-105 LANDING GEAR.

BASELINE ROTOR SYSTEM CHARACTERISTICS

The BO-105 rotor system, radius 193.37 inches, is a soft-in-plane hingeless rotor having feathering bearings only. Flap and lag motions are accommodated through a blade root flexure of rectangular cross section; thus, this flexure is stiff in torsion. Figure 19 presents a photograph of the system.

FIGURE 19. BO-105 ROTOR BLADE AND HUB.

Geometry

The rotor blade has a 23012 airfoil of a constant 10.63 inches chord from the blade root cutout station (42.95 inches radius) to the tip. Geometric twist is given in Figure 12.

Stiffness

Flap and chord stiffness distribution for this baseline is shown compared to the BMR in Figures 13 and 14 respectively. It is also listed in Table 4 together with torsional stiffness.

TABLE 4. BO-105 CAMBERED BLADE PROPERTIES DISTRIBUTION

(IN.)	(% RADIUS)	(LB-IN)	FLAP STIFFNESS (10^6 LB-IN.^{2}) EI_F	CHORD STIFFNESS (10^6 LB-IN.^{2}) EI_C	TORSIONAL STIFFNESS (10^6 LB-IN.^{2}) GK	I_α (LB-IN.^{2}/IN.)	C.G. (IN. AFT OF BLADE 1/4 CHORD)	BAR CENTER (IN. AFT OF BLADE 1/4 CHORD)
193.37	1.0	.71	2.38	59.4	1.36	1.934	.01	-.60591
192.02	.993	.71						
192.02	.993	.511						
188.92	.977	.511						
186.99	.967	.32						
153.92	.796	.32						
153.92	.796	.309						
97.65	.505	.309				1.934		
92.86	.555	1.447				2.345		
90.72	.469	1.447				2.345		
85.01	.395	.309				1.934		
85.01	.26				1.36			
44.45	.23				1.05		.01	-.60591
41.788	.216			59.4	1.039		-.291	-.49
41.091	.2125			46.	1.051	1.934	-.3663	-.49
40.008	.21			46.	1.077		-.42	-.44
38.674	.20			46.	1.74		-.5414	-.44
37.991	.196		2.38	46.	1.842		-.59	-.27
37.991	.196		2.5	33.8	1.842			-.27
34.607	.18		2.5	33.8	2.252			-.2
33.453	.173		2.5	33.8	2.491			-.2
33.453	.173		2.65	28.3	2.491			-.2
32.039	.166	.325	2.65	28.3	2.61			-.2
32.039	.166	.325	2.65	28.3	2.61			-.2
30.552	.158	.325	2.65	28.3	2.815			-.2
30.552	.158	.325	3.0	27.2	2.815			-.2
29.096	.15	.325	3.0	27.2	3.02			-.2
27.845	.144	.325	3.0	27.2	3.254			-.2
27.845	.144	.37	4.1	28.5	3.4			-.2
26.912	.139	.37	4.1	28.5	3.644			-.2
26.912	.139	.394	4.1	28.5	3.644			-.2
26.139	.135	.394	4.1	28.5	3.8			-.61
26.139	.135	.394	4.6	33.5	3.8			
23.091	.1192	.402	4.6	33.5	3.974	.85	-.59	
22.131	.1136	.402	4.6	33.5	4.1	.85	-.3663	
22.131	.1136	.406	5.0	34.2	4.1	.85	-.3663	
19.724	.102	.415	5.0	34.2	4.087	.85	-.3	
19.724	.102	1.28	5.0	34.2	4.087	45.9	-.3	
17.403	.09	1.28	5.0	34.2	4.087	45.9	-.25	
17.403	.09	1.4	14.1	34.2	4.087	45.9	-.25	-.61
17.017	.088	1.4	14.1	34.2	4.089	45.9	-.22	-.61

TABLE 4 (Continued)

(IN.)	(% RADIUS)	(LB-IN)	FLAP STIFFNESS (10^6 LB-IN.^{2}) EI_F	CHORD STIFFNESS (10^6 LB-IN.^{2}) EI_C	TORSIONAL STIFFNESS (10^6 LB-IN.^{2}) GK	I_θ (LB-IN.^{2}/IN.)	C.G. (IN. AFT OF BLADE 1/4 CHORD)	(IN. AFT OF BLADE 1/4 CHORD)
17.017	.088	1.7	14.1	34.2	4.089	45.9	-.20	-.61
16.92	.069	1.7	14.1	34.2	4.093		-.075	-.61
16.95	.063	2.8	14.1	34.2	4.093		-.075	-.61
15.083	.078	2.8	14.1	34.2	4.097		0.	-.61
15.283	.078	5.0	14.1	34.2	4.097		0.	0.
13.3	.078	5.0	14.1	34.2	4.097		0.	0.
[illegible]	[illegible]	5.0	14.1	34.2	4.10		.76	
14.1	.075	5.0	406.	880.			.76	
13.[illegible]	.07	5.0	406.	880.			1.52	
12.[illegible]	.066	-	406.	880.			1.712	
12.762	.066	-	500.	1060.			1.712	
11.[illegible]62	.06	3.1	500.	1060.		45.9	2.0	
11.[illegible]32	.05	4.1	343.	1060.		.85	.8	
11.265	.058	4.1	343.	160.			.793	
11.[illegible]15	.058	3.9	160.	160.			.793	
10.[illegible]32	.0555	-	160.	160.			.785	
10.732	.0555	-	160.	160.			.785	
9.832	.051	3.1	160.	160.			.77	
9.832	.051	5.1	160.	160.			.77	
8.[illegible]95	.046	5.1	160.	160.			.753	
8.[illegible]45	.044	5.7	206.	210.			.753	
7.9[illegible]8	.041	5.7					.737	
7.928	.041	2.6					.737	
6.9[illegible]1	.036	2.6					.72	
6.961	.036	2.0					.72	
5.[illegible]94	.031	2.0					.7	
5.934	.031	1.65					1.30	
4.9[illegible]1	.026	1.56					0.	
4.0[illegible]	.021	3.214					0.	
2.514	.013	3.214	206.	210.			0.	
2.514	.013	3.214	851.	885.			0.	
0.	0.	3.214	850.	885.	4.10	.85	0.	0.

SIGN CONVENTION:

+ IS AFT OF BLADE 1/4 CHORD

- IS FWD. OF BLADE 1/4 CHORD

Weight and Inertia

This data is presented in Table 4.

Dynamics

BO-105 Rotor System modal frequencies are calculated as follows based on a rotor speed of 425 rpm.

1st Flap	1.124 per rev
1st Chord	0.704 per rev
2nd Flap	2.760 per rev
2nd Chord	4.299 per rev
3rd Flap	5.057 per rev
1st Torsion	3.193 per rev

Structural damping in the rotor system is thought to be as high as 3-percent critical in the 1st mode and is due to at least three sources: (1) pitch bearings, (2) composite fiber structure, and (3) the blade root end retention. The latter is expected to vary with CF, which is explained as follows. Figure 20 shows the BO-105 rotor blade and its root retention hardware.

The final process in assembly procedure is to encaster the blade loop in the retention socket with an epoxy potting resin. When the blade is assembled into the rotor head, a rigid attachment is achieved with the main retention pin restraining the blade in flap, and the lag pin restraining the blade through the socket, in lag. However, when a centrifugal force field is applied to the blade, extension of fibers in the root loop result in a reduction in fiber volume encapsulated by the fitting. This further results in looseness in the blade root chordwise restraint and hence motion between the blade root and retention fitting occurs as the blade moves through its normal flap and lag excursions. High friction damping is therefore present.

Looseness in the root attachment also results in a reduction in 1st chord mode frequency but this reduction is believed to provide a small but positive change in air resonance damping.

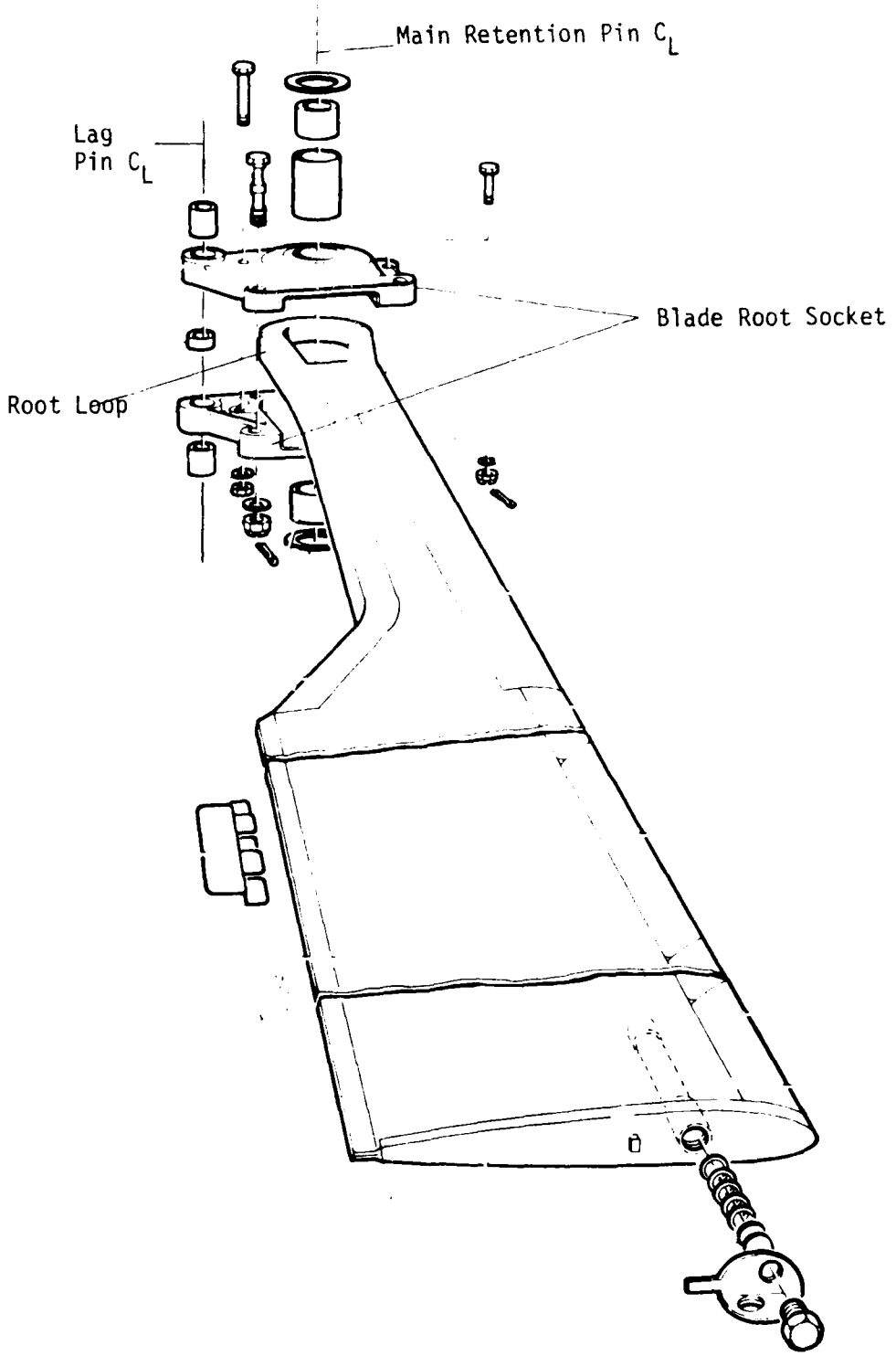

FIGURE 20. BO-105 MAIN ROTOR BLADE ASSEMBLY.

DESIGN CRITERIA FOR THE BMR ROTOR SYSTEM - FINAL DESIGN

Key Design Criteria and Constraints to which the preliminary design effort was directed were discussed previously. Understanding of the characteristics of the BO-105 aircraft and rotor system subsequently improved. The criteria were corrected in part for the detail design criteria below.

1. The BMR was to have no pitch bearings or flap or lag hinges.

2. The aeromechanical stability of the baseline BO-105 aircraft system was to be retained.

3. The BO-105 rotor system coupled frequencies were to be approximated as follows:

	At 425 RPM		At 425 RPM
1st Flap	1.12 per rev	2nd Flap	2.76 per rev
1st Chord	0.70 per rev	2nd Chord	4.30 per rev
		3rd Flap	5.06 per rev

4. The BMR first torsion frequency was to be greater than 3.2 per rev at 425 rpm when coupled with the drive system.

5. All BMR components were to be designed to a minimum fatigue life goal of 3600 hours following the contract Statement of Work flight profile shown pictorially in Figure 21.

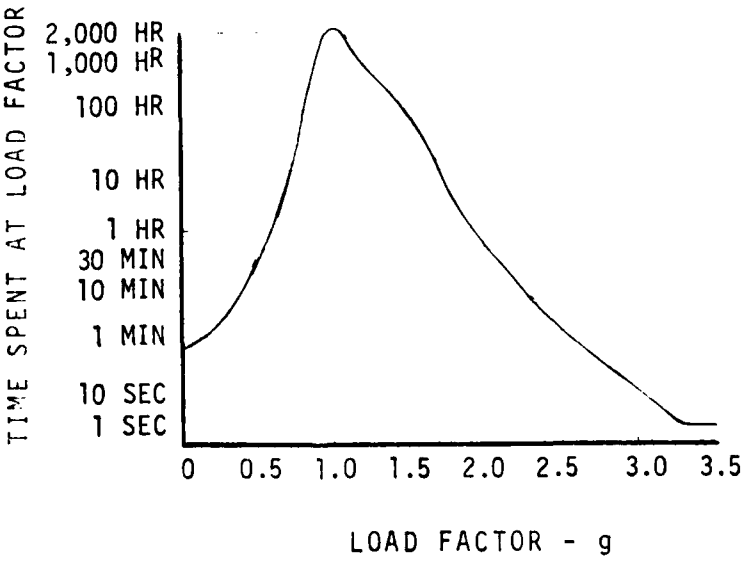

FIGURE 21. DESIGN FLIGHT SPECTRUM OF THE BMR/BO-015 HELICOPTER.

6. The BMR was to be adaptable to the BO-105 flight aircraft without changing the current control system, actuators, or drive system components.

7. The BMR was not to degrade the current BO-105 flying qualities and performance.

8. The BO-105, designed to the requirements of Federal Aviation Regulations Part 27, Airworthiness Standards, was not to be compromised while demonstrating the feasibility of the BMR system.

STRUCTURAL INTEGRITY

BY ANALYSIS

Positive margins in fatigue, limit, and ultimate loading conditons were obtained through analysis. The design flight conditions for fatigue were 1.6 g steady turns with the chord and flap loadings achieved by flying at the design gross weight and 100 knots, with CG at 3.35 inches aft and 6.3 inches forward of the rotor shaft respectively. By assuming that both conditions could occur simultaneously a conservatism was introduced. A life greater than 3600 hours was projected for all components of the BMR. Figure 22 presents a summary of the expected fatigue lives of prime components of the rotor system and Reference 5 provides details of the structural analysis.

5. STRUCTURAL ANALYSIS REPORT OF BMR/BO-105 (HELICOPTER), Boeing Vertol Document D210-11398-1, June 1978.

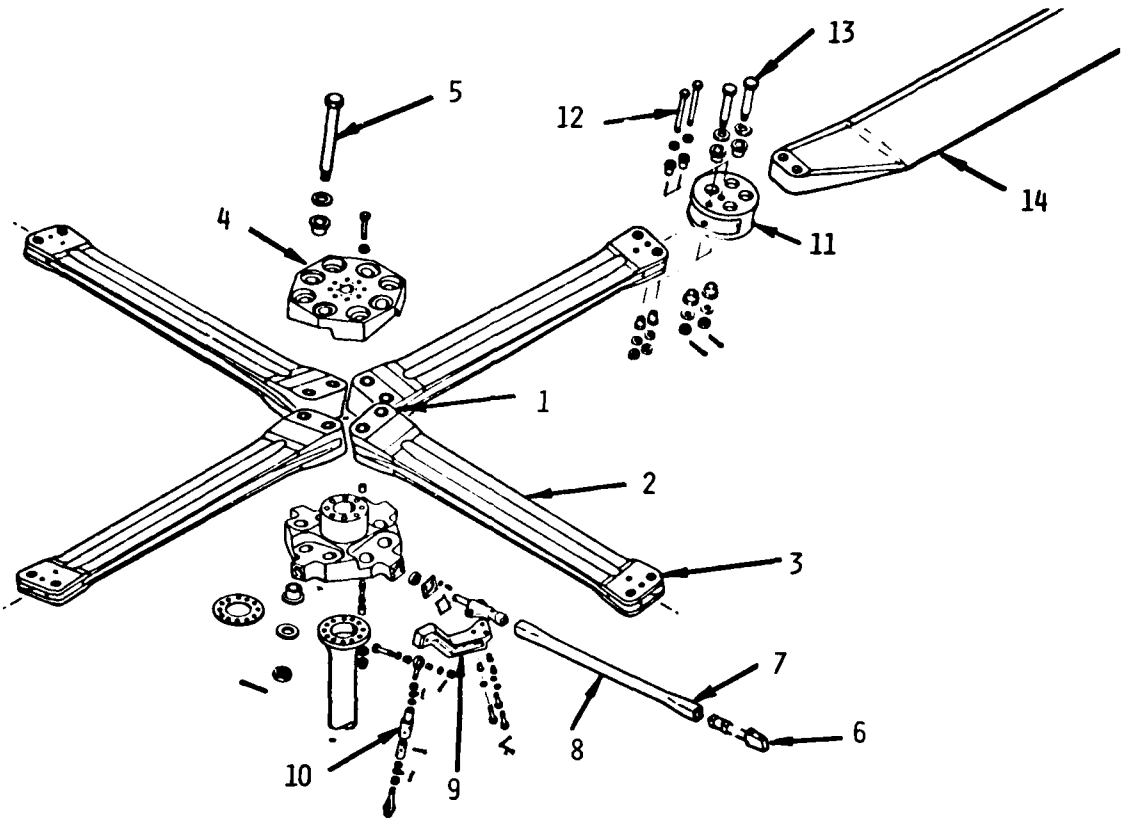

ITEM	DESCRIPTION	ESTIMATED LIFE (HR)
1	FLEXURE, INBOARD ATTACHMENT	4,480
2	FLEXURE	3,872
3	FLEXURE, OUTBOARD ATTACHMENT	383,370
4	STEEL HUB	20,796
5	FLEXURE/HUB ATTACHMENT BOLTS	46,903
6	TORQUE TUBE, OUTBOARD FITTING	1,000,000
7	TORQUE TUBE, OUTBOARD ATTACHMENT	161,630
8	TORQUE TUBE	383,700
9	PITCH ARM ASSEMBLY	14,178
10	PITCH LINK ASSEMBLY	1,000,000
11	CLEVIS	3,965
12	TORQUE TUBE/CLEVIS ATTACHMENT BOLTS	161,500
13	BLADE/CLEVIS ATTACHMENT BOLTS	43,924
14	ROTOR BLADE ASSEMBLY	(NOT ESTIMATED)

FIGURE 22. FATIGUE LIVES OF FINAL BMR CONFIGURATION COMPONENTS BY ANALYSIS.

BY BENCH TEST

To verify these predictions, bench fatigue, limit, and ultimate tests were conducted as reported in Reference 6. The prime objective of the bench testing was to prove that the rotor system had adequate structural integrity for at least 100 hours of flying. All components were subjected to at least 2.55×10^6 cycles of fatigue loading, which qualified the system for at least 500 hours of flight.

No failures occurred but the testing was not continued to demonstrate the design goal of 3600 hours, due to schedule and budget. By treating each run-out as a failure, demonstrated fatigue lives as presented in Figure 23 were estimated using the loading spectrum shown graphically in Figure 21.

The limit and ultimate tests were conducted without failure. Subsequent whirl and flight testing showed that the bench test load levels for torque tube bending moments were low compared to measured data. Fatigue limit and ultimate tests were repeated on the torque tube components at representative load levels again without failure occurring.

BY WHIRL TEST

Figure 24 shows the rotor system installed on the whirl tower facility. An extensive loads survey on the rotor and BO-105 control system was conducted over a thrust range from zero until limited by maximum rotor torque allowed in the BO-105 system shaft (in 1000-lb increments). At normal (425 rpm) rotor speed and at 110 percent overspeed, loads were measured at positive and negative cyclic pitch settings until rotor shaft, beam flexure, or torque tube bending limits were reached. Extensive strain gage instrumentation provided loads data, which is discussed in References 7 and 8.

6. MODEL AND BENCH TEST EVALUATION OF THE PRELIMINARY DESIGN, Boeing Vertol Document D210-11245-2, November 1977.

7. BMR WHIRL TEST REPORT, Boeing Vertol Document D210-11428-1, September 1978.

8. INSTRUMENTATION DESIGN DOCUMENT, BMR FLIGHT TEST PROGRAM, Boeing Vertol Document D210-11299-1, 22 September 1977.

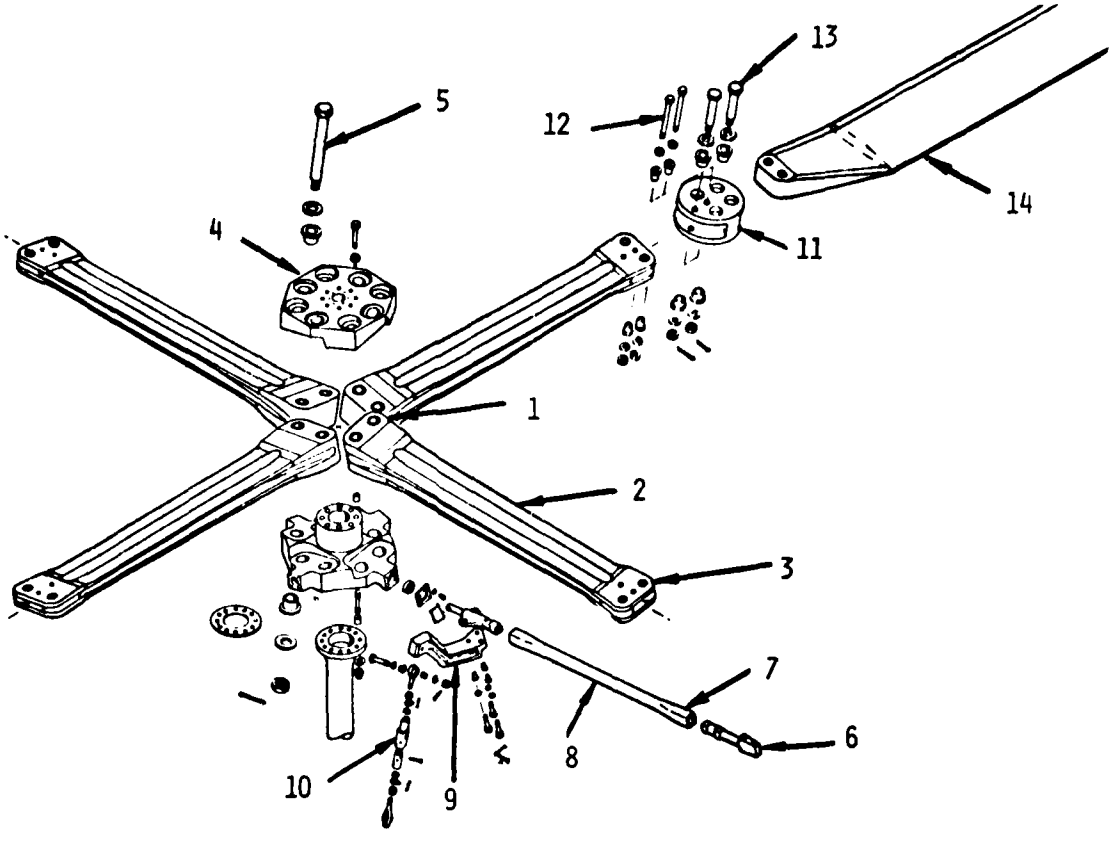

ITEM	DESCRIPTION	ESTABLISHED LIFE (HR)
1	FLEXURE, INBOARD ATTACHMENT	82,000
2	FLEXURE	1,150
3	FLEXURE, OUTBOARD ATTACHMENT	21,000
4	STEEL HUB	26,000
5	FLEXURE/HUB ATTACHMENT BOLTS	82,000
6	TORQUE TUBE, OUTBOARD FITTING	532
7	TORQUE TUBE, OUTBOARD ATTACHMENT	532
8	TORQUE TUBE	532
9	PITCH ARM ASSEMBLY	37,000
10	PITCH LINK ASSEMBLY	58,000
11	CLEVIS	10,000
12	TORQUE TUBE/CLEVIS ATTACHMENT BOLTS	21,000
13	BLADE/CLEVIS ATTACHMENT BOLTS	100,000
14	ROTOR BLADE ASSEMBLY	100,000

NOTE: THESE ARE CONSERVATIVE ESTIMATES FROM RUNOUTS OBTAINED FROM UNCOMPLETED TESTS

FIGURE 23. FATIGUE LIVES OF FINAL BMR CONFIGURATION COMPONENTS DEMONSTRATED BY BENCH TESTING.

To assess the integrity of the system under prolonged loading conditions, the rotor was whirled for 6.5 hours with loads in the most critical components at their endurance limits. At its uneventful conclusion, an overspeed test to 125 percent of normal operating rpm was conducted.

A subsequent teardown inspection, in which extensive nondestructive methods were used (e.g., X-ray, magnaflux, and visual), revealed minor fretting in attachment hardware necessitating only minimum refurbishment prior to installation of the system on the flight vehicle.

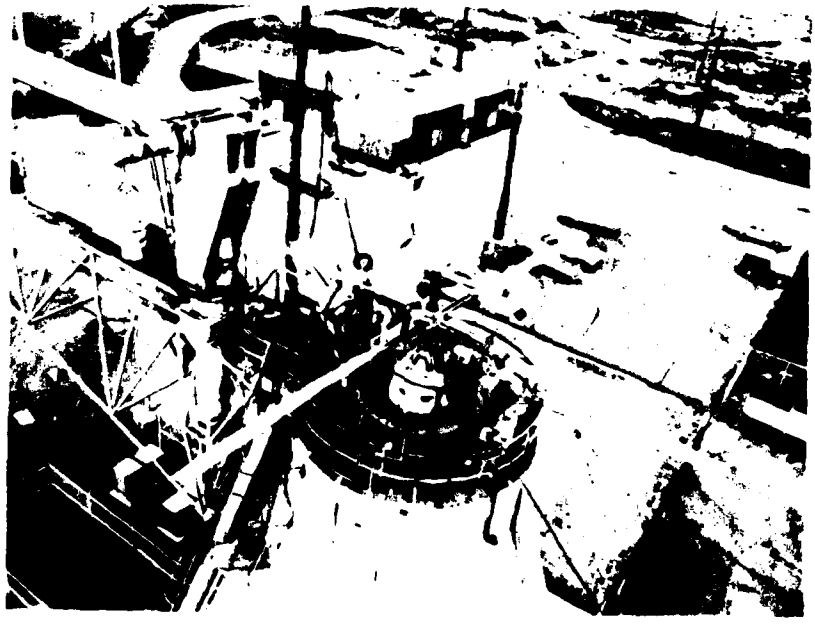

FIGURE 24. THE BEARINGLESS MAIN ROTOR INSTALLED ON THE WHIRL TOWER.

EXPECTED DYNAMIC CHARACTERISTICS BY PREDICTION AND TEST

MODAL FREQUENCIES

The dual beam configuration required unique attention to the prediction of chordwise modal frequency but the other modes were straightforward. In chord, the beam flexures react the bending loads at the beam/blade attachment clevis by differential axial loading in each of the two beam components. However, due to the absence of a continuous shear web between them the capability of the assembly to react chordwise shear forces at the clevis is greatly reduced. The frequency of the second and higher chord bending modes is consequently reduced.

By Analysis

The Boeing Vertol Y-71 coupled frequency analysis was used to predict flapwise and torsional modal frequencies but this program was limited to a single beam flexure arrangement. By assuming an interconnecting web between the leading and trailing beams a single beam flexure was modeled. Figure 25 shows the frequency spectrum thus derived.

To obtain a closer prediction of the chord modes the system was modeled using finite element techniques on NASTRAN. Figure 25 presents these results.

By Bench Test

To verify nonrotating modal frequency predictions a full-scale beam/clevis/rotor blade specimen was cantilevered from the flexure root in the horizontal position. By bang test and shake tests the nonrotating frequencies and mode shapes were determined. The results are shown plotted in Figure 25, which suggests that the NASTRAN prediction for the chordwise modal frequency was applicable.

By Whirl Test

The rotor system frequency spectrum as measured during the whirl tests on the isolated rotor mounted on the B.V. whirl test facility is presented in Figure 26, where a comparison with prediction is made.

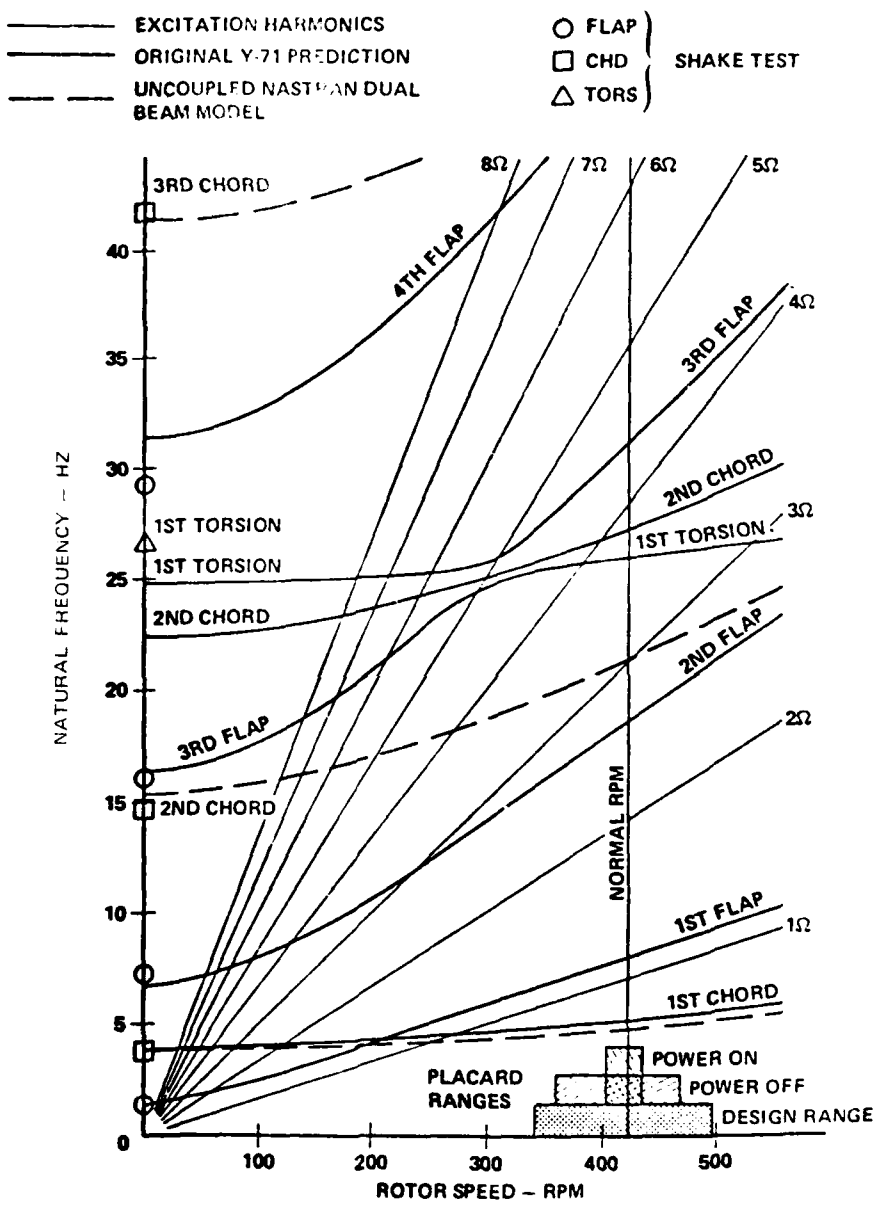

FIGURE 25. BMR ROTOR NATURAL FREQUENCIES - UNCOUPLED FROM THE DRIVE SYSTEM.

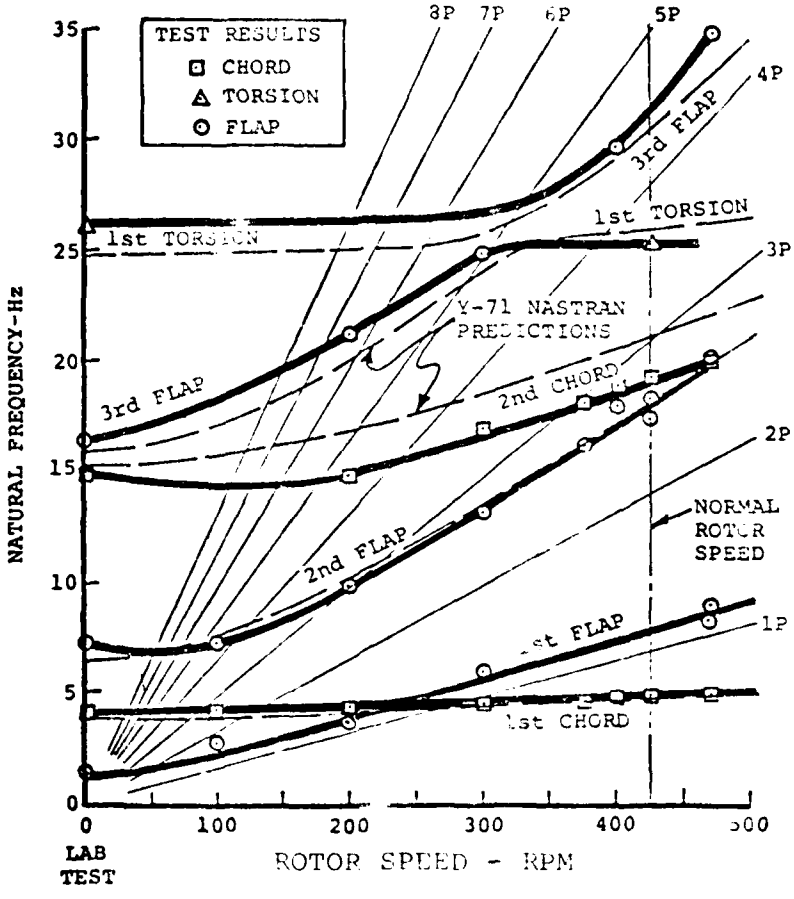

NATURAL FREQUENCIES (PER REV) AT N_{NORM} = 425 RPM

MODE	WHIRL TEST	ANALYSIS
FIRST FLAP	1.12	1.12
SECOND FLAP	2.58	2.58
THIRD FLAP	4.45	4.34
FIRST CHORD	0.69	.67
SECOND CHORD	2.72	3.01
FIRST TORSION	3.56	3.70

FIGURE 26. BMR NATURAL FREQUENCIES ESTABLISHED BY WHIRL TOWER TESTING.

STRUCTURAL DAMPING

Although 1-percent critical structural damping has been used in all stability analyses a simple chord bang test of the cantilevered blade showed a nonrotating structural damping level of between 1.10 percent and 0.64 percent critical. This test was conducted without the high CF field (40,000 lb) normally present, which would reduce motion in the attachments resulting in a decrease in damping. However, friction damping would increase; therefore, nonrotating tests are only an indication of the order of magnitude. Figure 27 shows a typical recording of the decay of the chordwise mode obtained above.

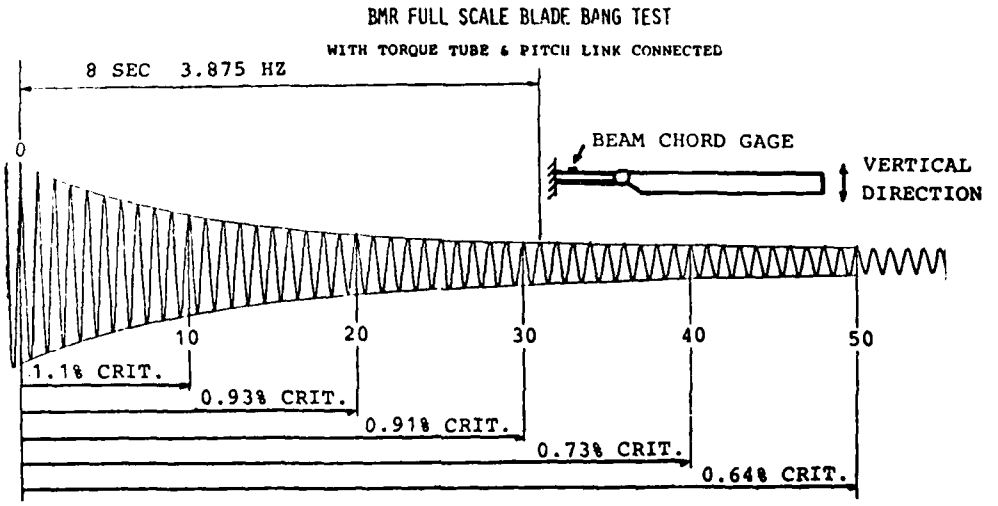

FIGURE 27. DECAY OF BMR NONROTATING FIRST CHORD MODE.

STABILITY

A potential for instability was expected to occur when the frequency of the fixed system excitation from the in-plane or chordwise motions of the rotor system coincides with the natural frequency of the body motion when supported by the landing gear on the ground, by the rotor in the air, or by both means when in the partially airborne conditions. Figure 28 shows the frequencies at which resonance could occur.

The Boeing Vertol C-45 computer program was used to study ground resonance and hover air resonance mode damping of the BMR/BO-105 during preliminary design, model air resonance testing, and in support of full-scale ground and air resonance testing. The analytical model of the

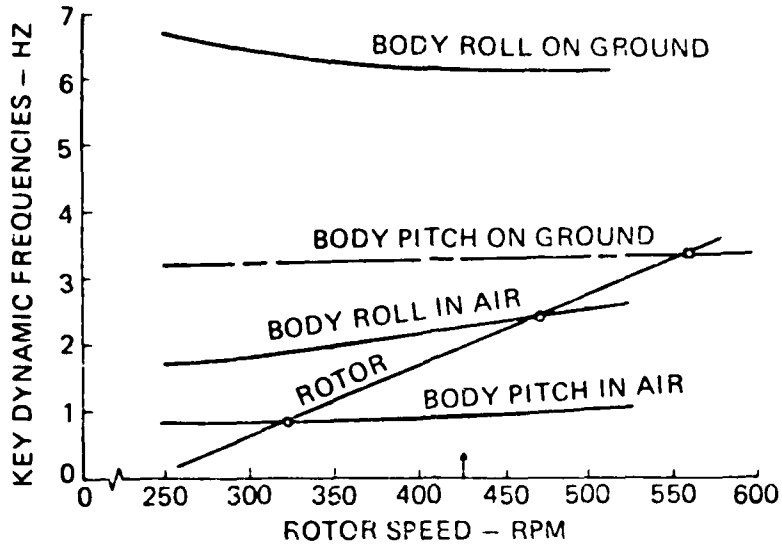

FIGURE 28. ROTOR AND BODY FREQUENCIES VS. ROTOR SPEED.

airframe and rotor blade is shown schematically in References 3, 4, and 9. The airframe is represented by a fuselage with a flexible pylon and a flexible tail boom; however, the pylon and tail boom were considered rigid in most analytical studies. The airframe may be connected to the ground with flexible springs representing landing gear stiffnesses for ground resonance studies. For air resonance studies, springs to ground have zero stiffnesses. The rotor blade is represented by its first flap, chord, and torsion modes with an equivalent hinge model which has an arbitrary flap, lag, and torsion hinge sequence. Hinge locations and rotational springs around the hinges are chosen to give correct variations of blade mode frequencies with rotor speed. Hinge orientations are chosen to give appropriate flap-lag-torsion coupling. Blade mode frequencies for the BMR were computed using Boeing Vertol's Y-71 computer program. Steady state deflections were computed using Boeing Vertol's C-60 computer program; these were used to define equivalent hinge orientations and blade steady coning angle.

9. AEROELASTIC STABILITY AND VIBRATION CHARACTERISTICS OF A BEARINGLESS MAIN ROTOR, Boeing Vertol Document D210-11498-1, June 1979.

Isolated Rotor on Whirl Tower

The BO-105 control system as applied to the whirl tower installation had the lateral cyclic actuator replaced by a fixed link. The remaining monocyclic system was modified so that a cyclic excitation of up to 25 Hz frequency and ±1/2° amplitude could be added. By oscillating the swashplate at a responsive frequency for the rotating blade chordwise motions and then stopping the excitation, the rotor chordwise damping characteristics were examined.

Figure 29 shows how the damping increases with collective and how damping is reduced with increase in rotor speed. This data was used to improve the C-45 analytical predictions of ground and hover air resonance stability of the BMR/BO-105 helicopter system. For comparison, updated C-45 predictions are provided.

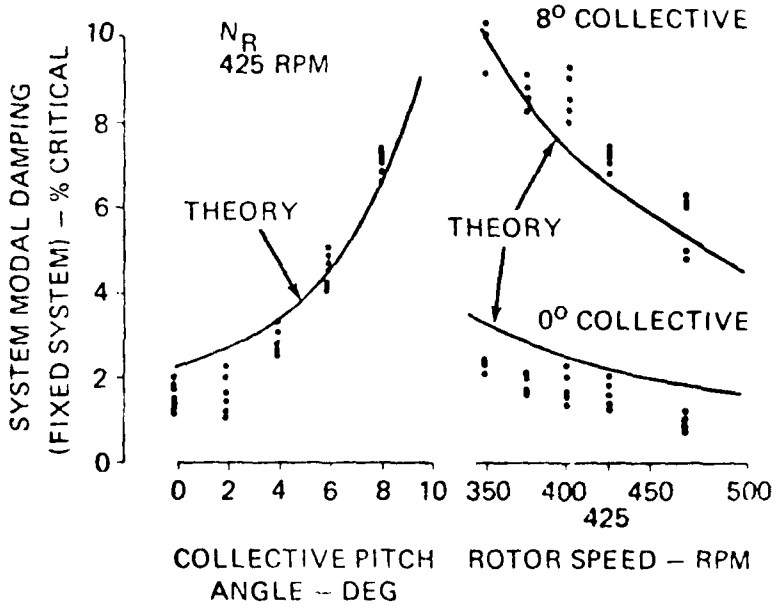

FIGURE 29. EFFECT OF COLLECTIVE PITCH AND RPM ON ROTOR SYSTEM DAMPING - WHIRL TEST.

Ground Resonance

Ground resonance predictions were based on the assumption that the landing gear is in full contact with the ground and that its stiffness is fully effective. This is not the case for partially airborne conditions, which change according to how many of the four corners of the landing gear are in ground contact. Typical C-45 results, within the above limitations, are shown in Figure 30.

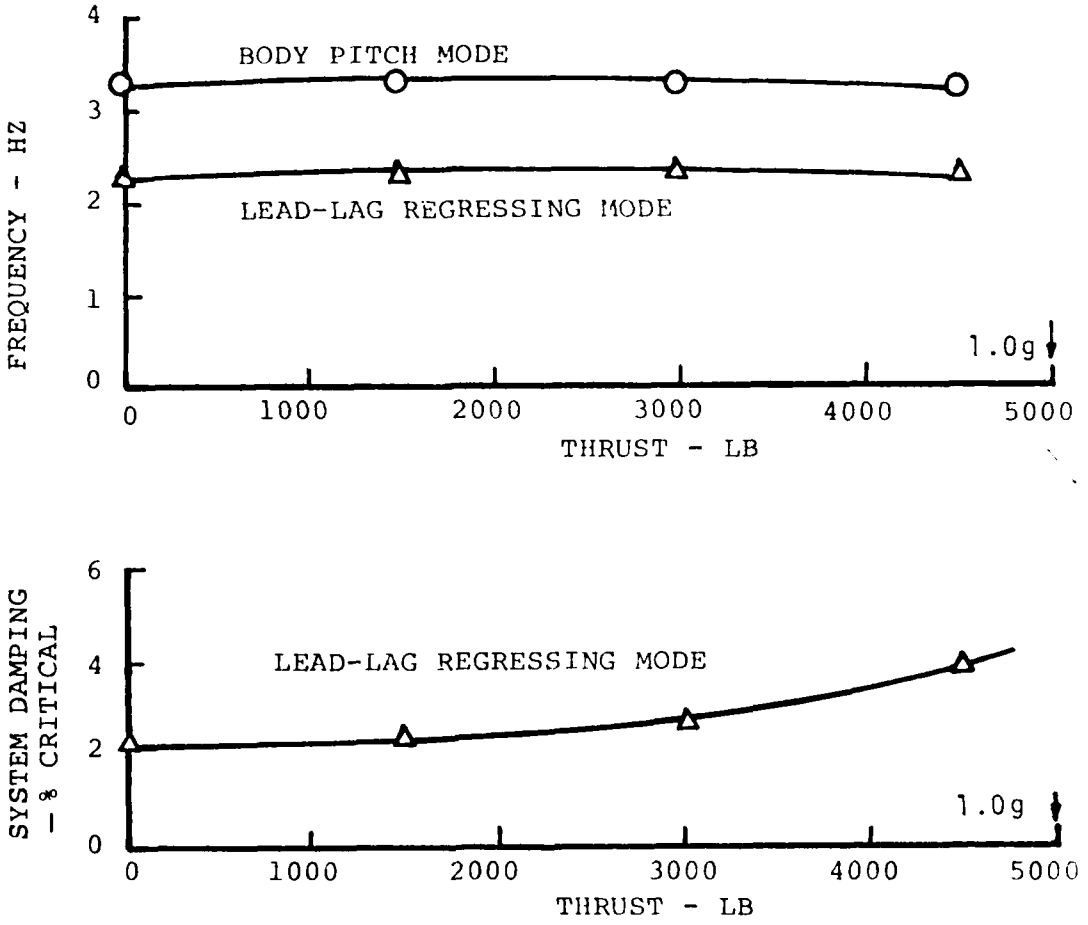

FIGURE 30. TYPICAL PREDICTED GROUND RESONANCE MODE DAMPING VERSUS THRUST AT NORMAL ROTOR SPEED.

Damping versus thrust at normal rotor speed was expected to increase from 2 percent critical at zero thrust to 5 percent in the fully airborne or hover condition. Figure 31 shows the C-45 ground resonance predictions at zero thrust as damping decreased with increase in rotor speed.

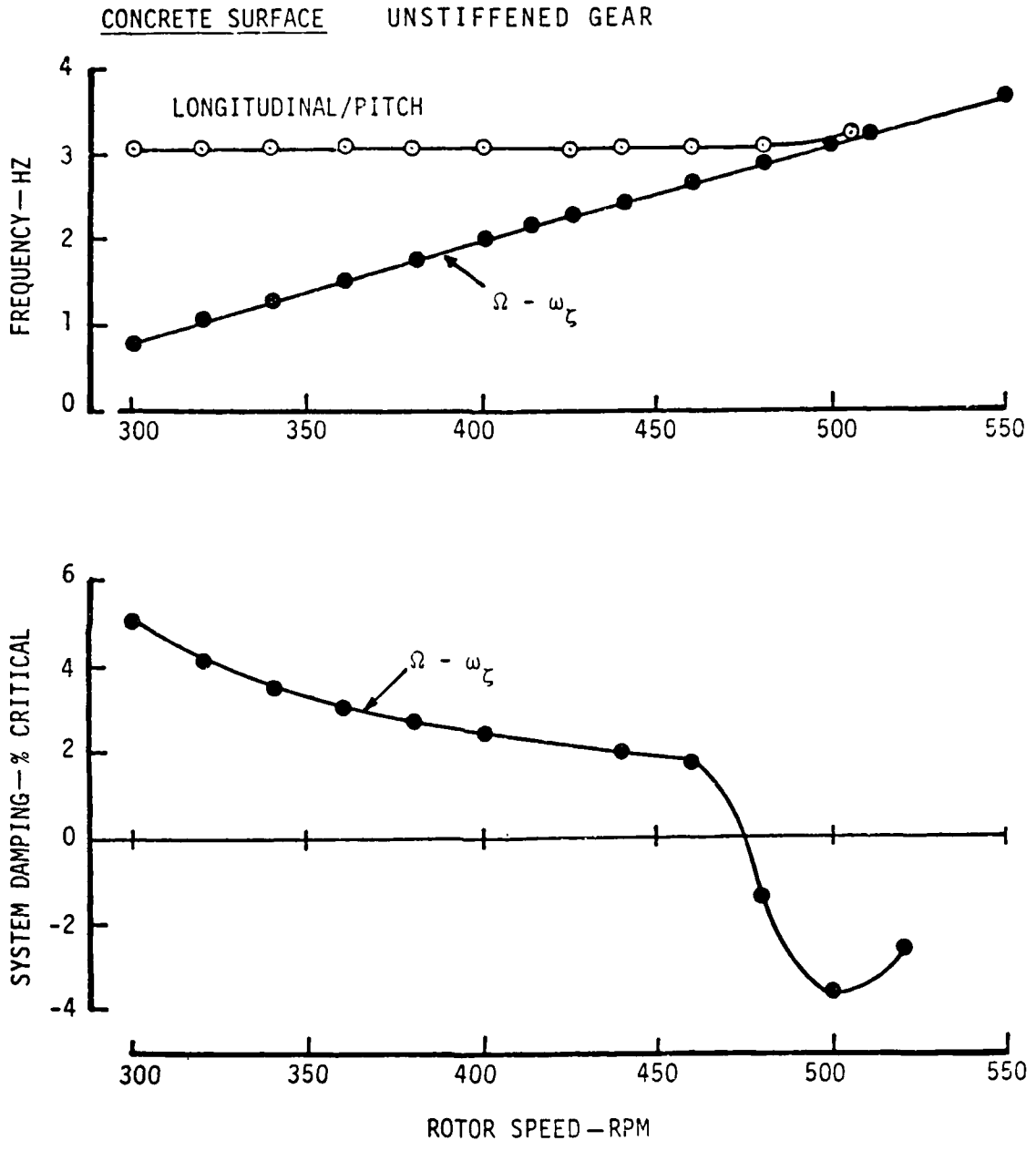

FIGURE 31. TYPICAL PREDICTED GROUND RESONANCE MODE DAMPING VERSUS ROTOR SPEED AT ZERO THRUST.

A gradual decrease was expected with increase in rpm until at 455 rpm, a sudden drop in damping produced instability at 475 rpm where the regressing chord mode coincides with the body longitudinal/pitch mode frequency.

Air Resonance in Hover

Typical C-45 results for air resonance in hover are shown in Figures 32 and 33. Damping versus thrust at normal rotor speed shows damping increasing with thrust. Model test results for damping are included for comparison. Damping versus rotor speed shows that the system was expected to be unstable at 78 percent of normal and stable at all other speeds of interest. The region where damping becomes unstable corresponds to the rotor speed where the lead-lag regressing mode frequency crosses the body pitch mode frequency. There is no corresponding instability where the lead-lag mode coincides with the body roll mode frequency.

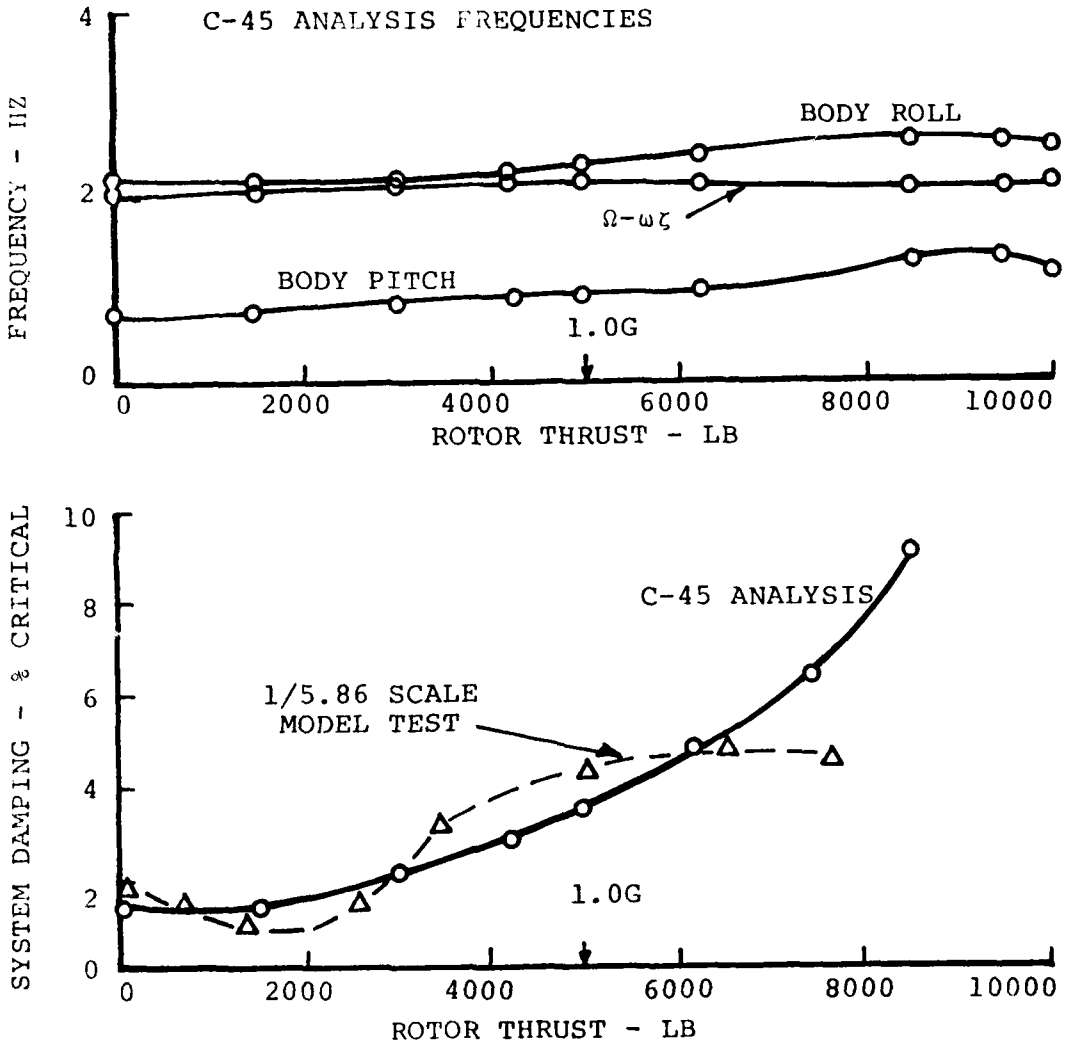

FIGURE 32. TYPICAL AIR RESONANCE MODE DAMPING VERSUS THRUST (GROSS WEIGHT) AT NORMAL ROTOR SPEED IN HOVER.

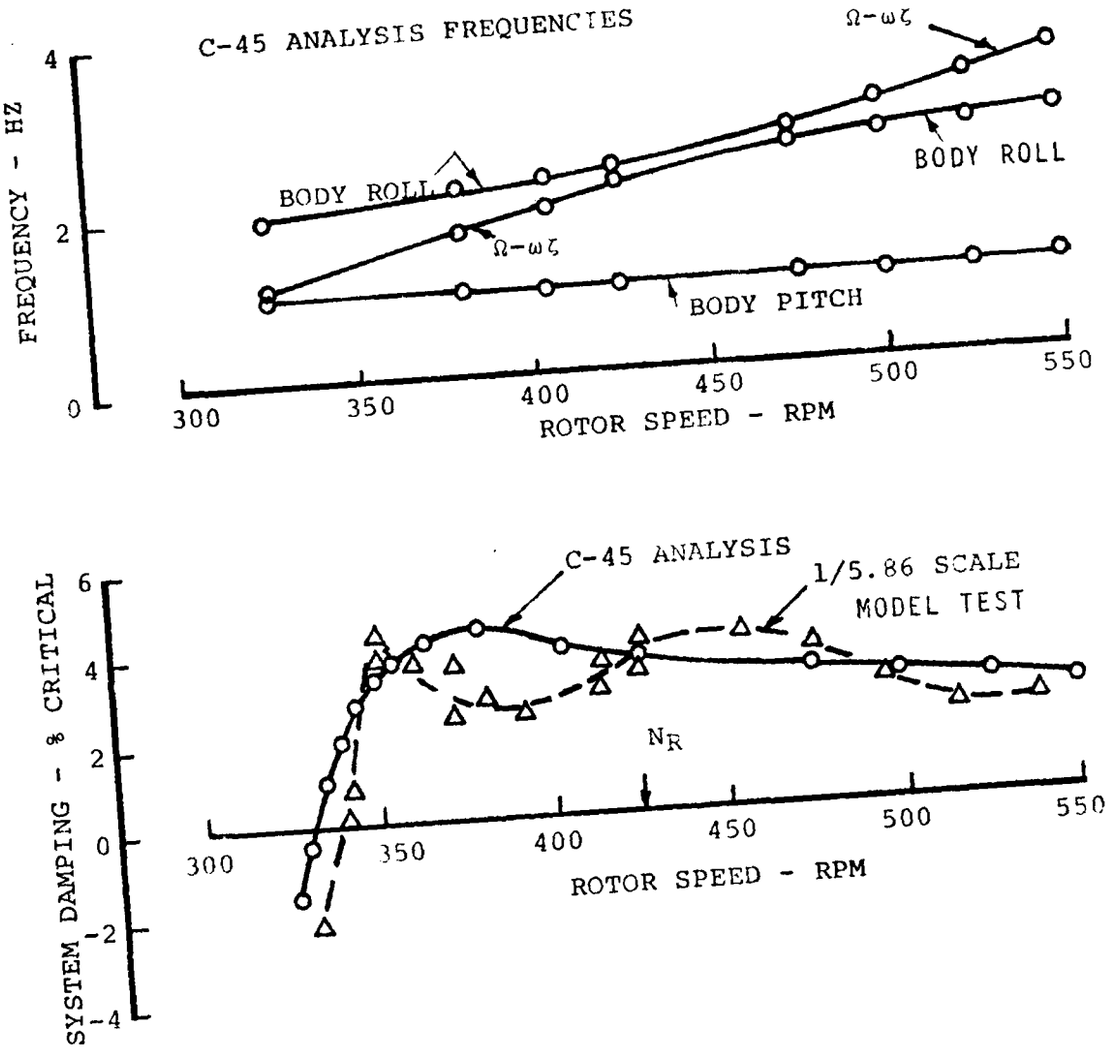

FIGURE 33. TYPICAL AIR RESONANCE MODE DAMPING VERSUS ROTOR SPEED AT 1.0g THRUST IN HOVER.

Air Resonance in Forward Flight

The analysis is not able to provide stability predictions for forward flight. The agreement between model test data and analysis in the hover mode provided confidence in the forward flight model test data shown in Figure 34.

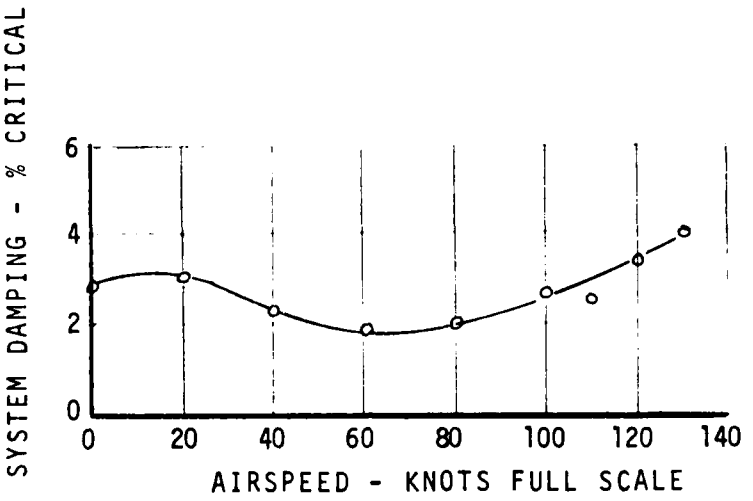

FIGURE 34. TYPICAL AIR RESONANCE MODE DAMPING VERSUS FORWARD SPEED AT 1g THRUST AND NORMAL ROTOR SPEED (MODEL TEST).

It was expected, therefore, that in level flight a minimum stability level would occur in the region of 60 knots forward speed.

Air Resonance in Climb and Descent

By examining the wind tunnel model test data for climb and descent at 60 knots a prediction for the full-scale aircraft behavior was obtained. Figure 35 shows that stability was likely to decrease with rate of descent (or collective pitch). However, a positive stability level of 0.5 percent critical damping was expected in autorotation at near zero collective pitch settings.

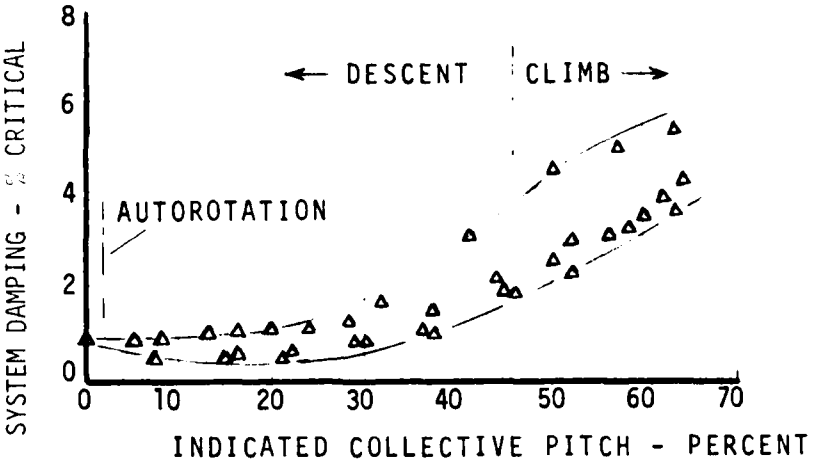

FIGURE 35. AIR RESONANCE MODE DAMPING VERSUS COLLECTIVE PITCH -1/5.86 FROUDE SCALE MODEL DATA AT 60 KNOTS (FULL SCALE SPEED).

Rotor Divergence

This phenomenon is a static twisting divergence of the rotor blade under aerodynamic and centrifugal forces.

For instability in this mode the center of pressure would have to be forward of the blade elastic axis. The C-60 rotor loads analysis includes the relevant terms and showed that the BMR would be stable in this mode. Furthermore, the whirl tower test on the full scale rotor did not identify any potential instabilities up to 125 percent of normal rotor speed.

Pitching Moment Divergence

This occurs when the advancing blade experiences a nose-down pitching moment that results from a combination of aerodynamic pitching moment and the moment produced by drag forces acting on the vertically displaced blade. Both flight tests on the baseline BO-105 helicopter and whirl tests of the BMR showed no divergence problems and analysis of both the BO-105 and BMR rotor configurations at up to 120 percent of maximum level flight speed shows no significant blade pitching moment differences between the two rotors.

Therefore, no divergence problems were anticipated during the flight test program.

Classical Flutter

By the Boeing Vertol L-01 uncoupled frequency analysis, which determines flutter damping and sensitivity to

chordwise center of gravity placement, no classical flutter was predicted for the BMR rotor blade with its CG located at 25 percent chord from the leading edge.

The analysis showed that if the CG was at or aft of 28 percent chord, classical flutter would then be a problem.

Stall Flutter

For this phenomenon, the stall flutter boundaries were defined by the L-01 analysis. Since blade torsional frequency is the significant parameter and for both BMR and BO-105 they are the same, the BMR was expected to have the same stall flutter boundaries as the BO-105 rotor system. The analysis agrees with BO-105 measured pitch link load data and the waveforms were almost identical.

Second Chord Mode Stability

Both analysis and whirl test data showed the second chord and second flap mode frequencies coinciding at 2.6 per rev at 475 rpm, which is within the operating range. To allay concern about resultant instability and severe load amplification, the phenomenon was examined through the Y-71 coupled mode frequency analysis, which indicated sufficient damping of each mode to preclude instability.

EXPECTED FLIGHT LOADS

Flight loads prediction for the BMR were based on measured BO-105 flight data. The common denominator was the shaft (or blade root flapwise) bending moment variation with load factor and aircraft center of gravity location. The BMR flap and chord bending moment radial distribution, as predicted from the C-60 loads analysis, was nondimensionalized in terms of root moment for which the real magnitude at a particular flight condition was obtained from BO-105 flight data.

Since the BO-105 single beam root end had been replaced by the dual beam BMR flexure, distribution of chord bending and axial loads between the beams was an important consideration in both the structural and frequency analysis.

Figure 36 shows the comparison between single and dual beam configuration nonrotating second chord mode.

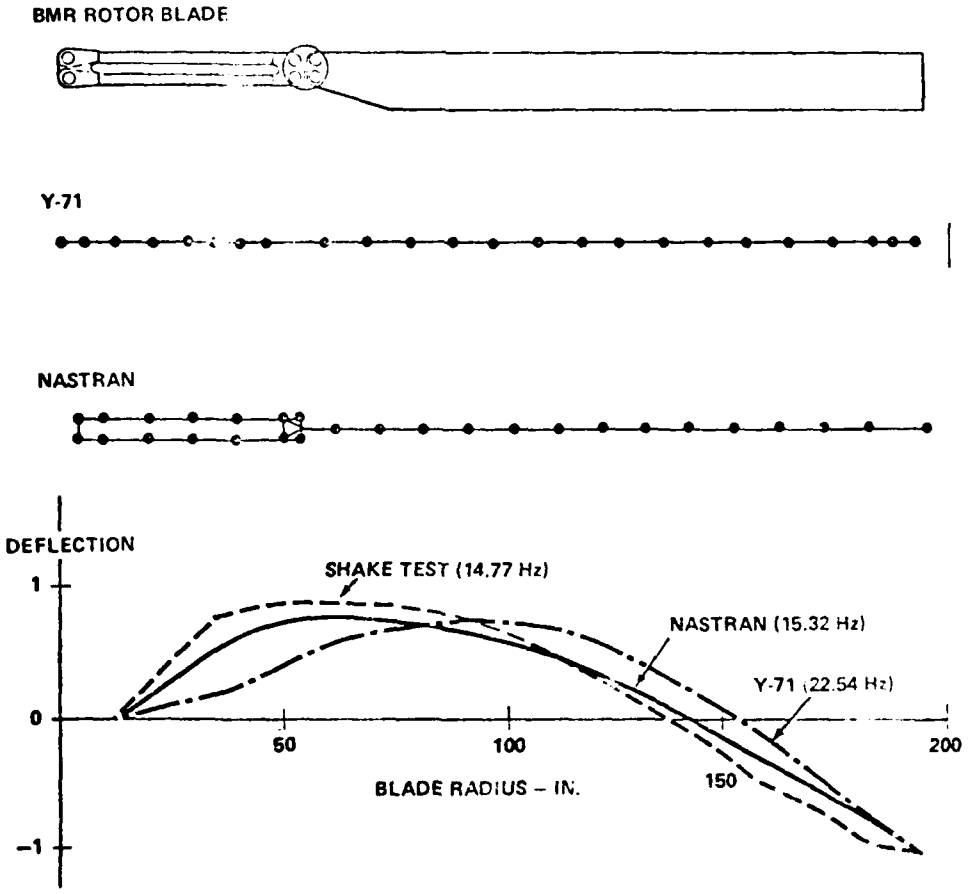

FIGURE 36. NONROTATING SECOND CHORD MODE CORRELATION.

The differences in the predicted flexure deflections explains the corresponding differences in frequency and loads prediction for the rotating as well as nonrotating case.

Structural analysis in the preliminary and detail design phases was achieved by assuming an equivalent single beam flexure and computing radial distribution of steady and vibratory chordwise loadings. Considering the loads at the flexure/blade juncture thus obtained, and applying them to a specially constructed analysis, the distribution of these loads between the beams could be determined.

CONTROL SYSTEM LOADS AND RATES

Dynamically induced pitch link loads measured on the BO-105 were added to the load required to overcome the torsional stiffness of the BMR beam flexure when a control input was applied. Figure 37 presents the expected alternating pitch link load versus level flight speed and load factor at 100 knots. Transferring the predicted steady pitch link load down to the collective actuator a prediction for the collective actuator load versus collective was obtained, as shown in Figure 38. Although this requirement was within the capability of the system pressurized at the normal 1500 psi it was considered prudent to provide a larger margin, so the system pressure was increased to 2000 psi. This regained the BO-105 capability of 10 in. per second velocity of the longitudinal cyclic control, and allowed full collective travel in 0.63 second.

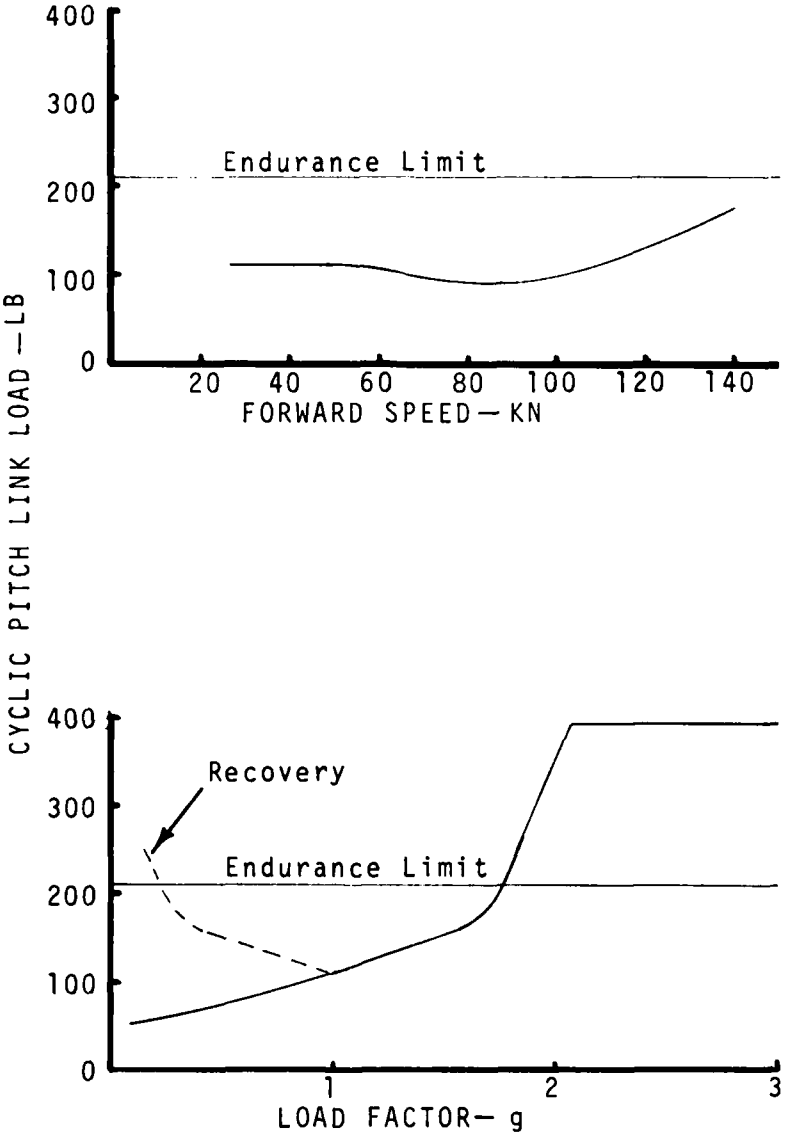

FIGURE 37. EXPECTED VIBRATORY PITCH LINK LOADS.

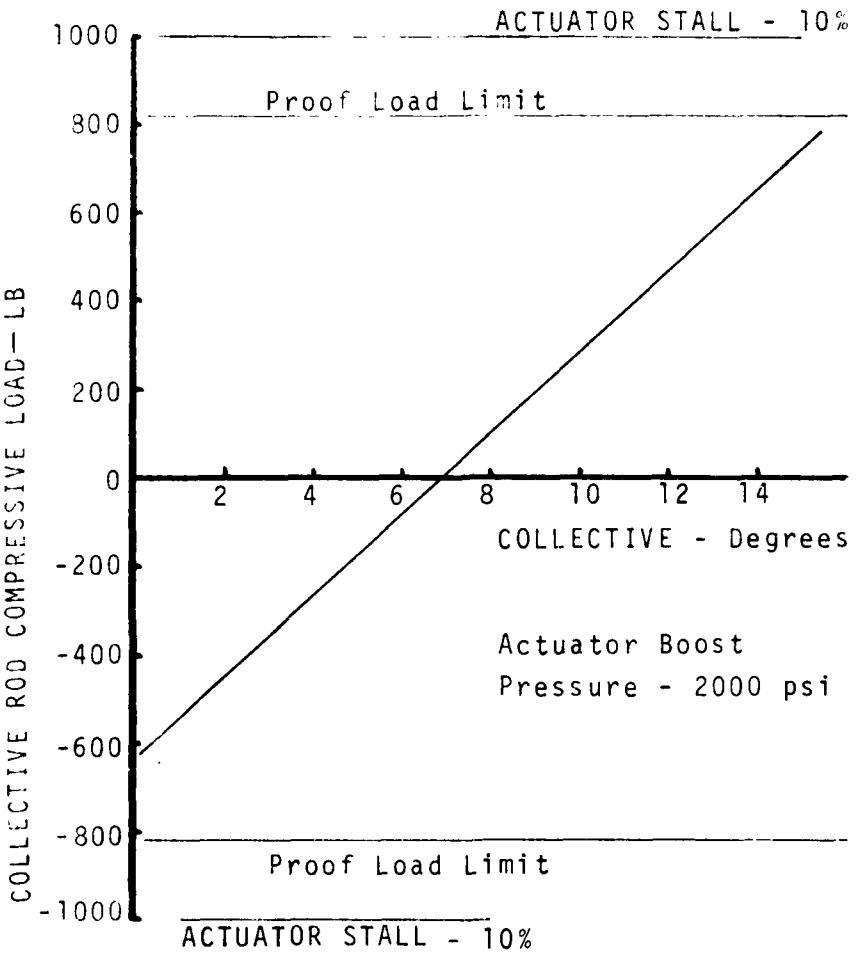

FIGURE 38. EXPECTED COLLECTIVE ACTUATOR LOAD.

SHAFT LOADS

The basis for predicting expected rotor shaft loads was measured BO-105 data. Figure 39 presents the top of scatter of that data and shows the effect of both rotor speed and load factor.

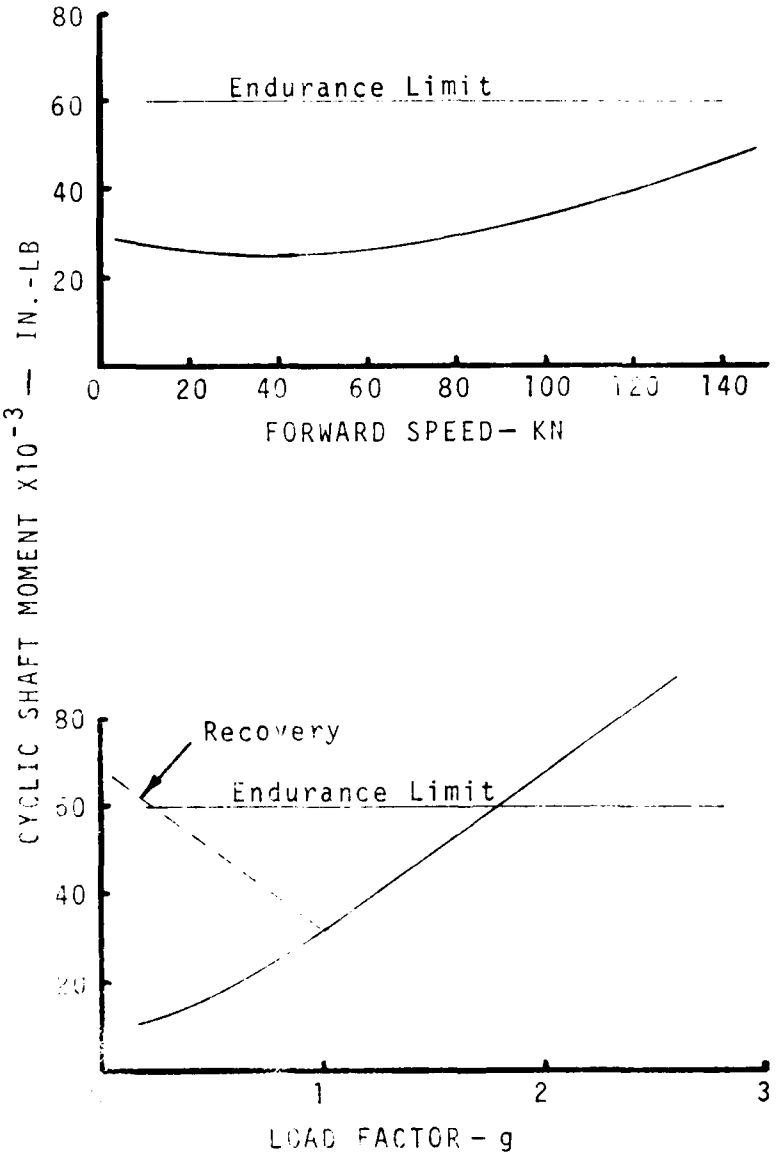

FIGURE 39. EXPECTED VIBRATORY SHAFT MOMENT.

ROTOR LOADS

Figure 40 shows the typical relation between load parameters and shaft bending moment, as determined from whirl test data. Using this together with the shaft moment predictions above, the vibratory loads for the rotor system were predicted.

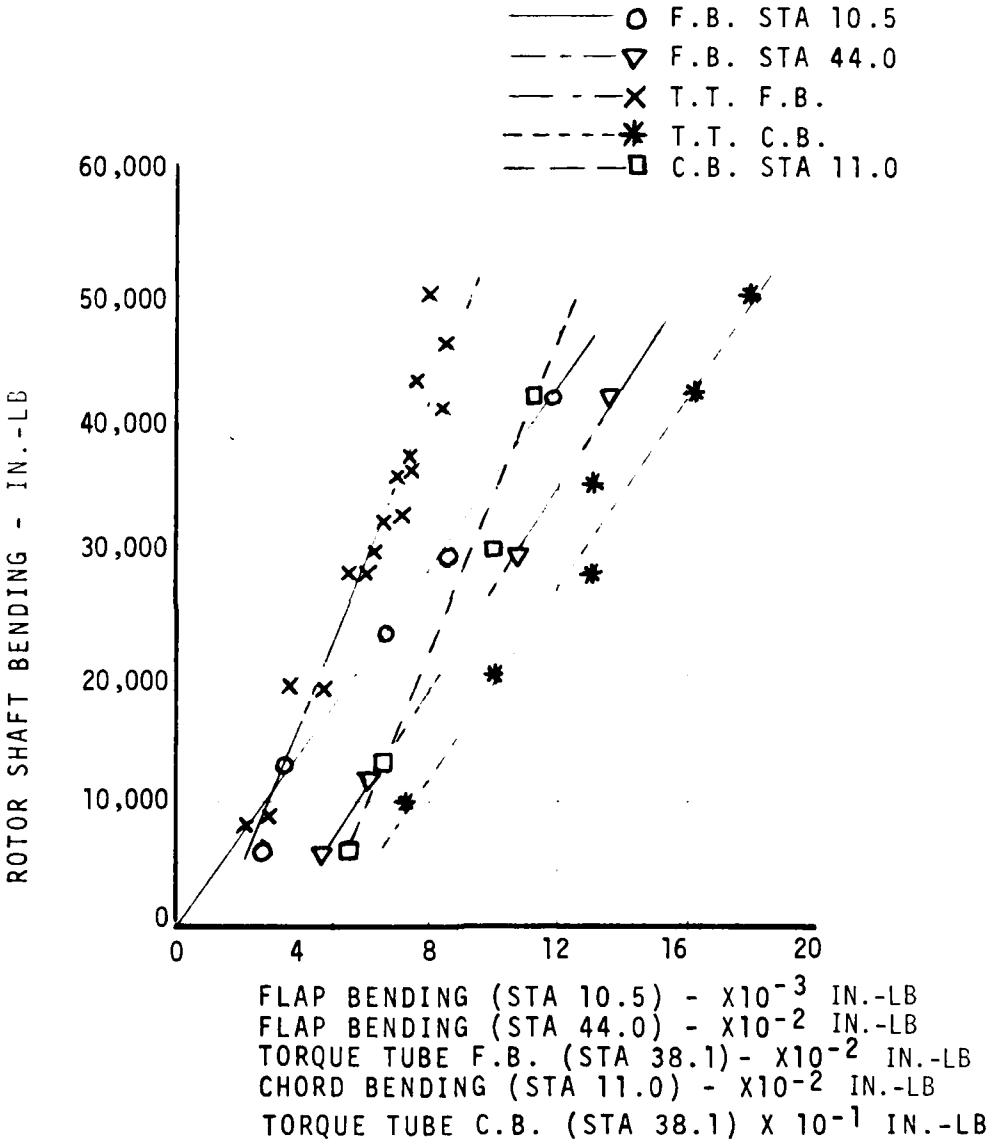

FIGURE 40. BMR WHIRL TEST DATA - FLAP AND CHORD BENDING VERSUS ROTOR SHAFT BENDING.

Steady flap bending moment distribution was predicted through C-60 loads analysis and steady chord moment using the C-60 analysis of the single equivalent beam flexure with the blade attached, and then redistributing the load at the flexure/blade junction inboard into each of the dual beams. Figure 41 presents the expected flap bending moment distribution and Figure 42 shows the chord bending moment distribution. The insets in Figure 42 show the dissimilarity in the distribution of local chord bending between the leading and trailing beam components of the flexure.

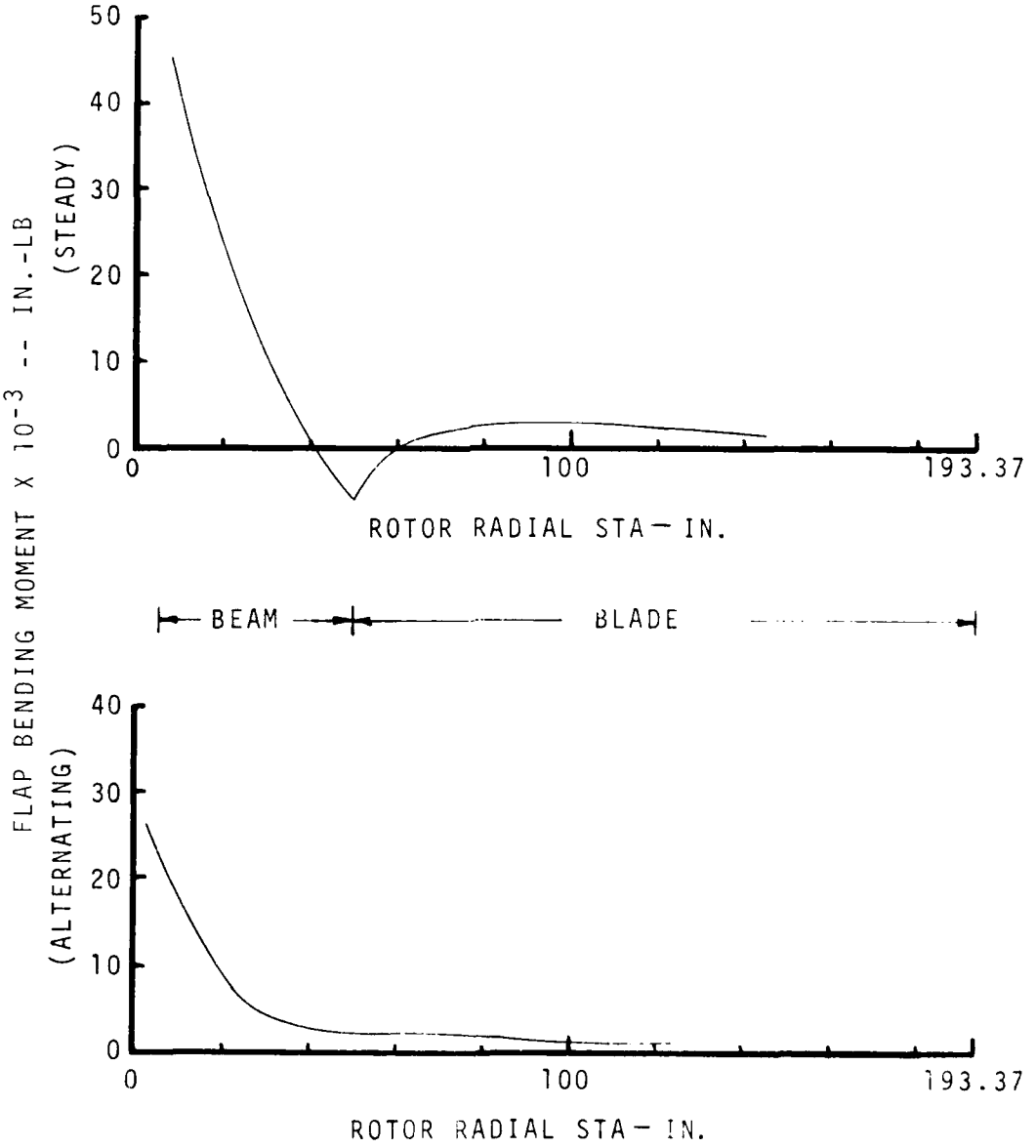

FIGURE 41. EXPECTED FLAP BENDING MOMENT AT 2.0g LOAD FACTOR AND 100 Kn.

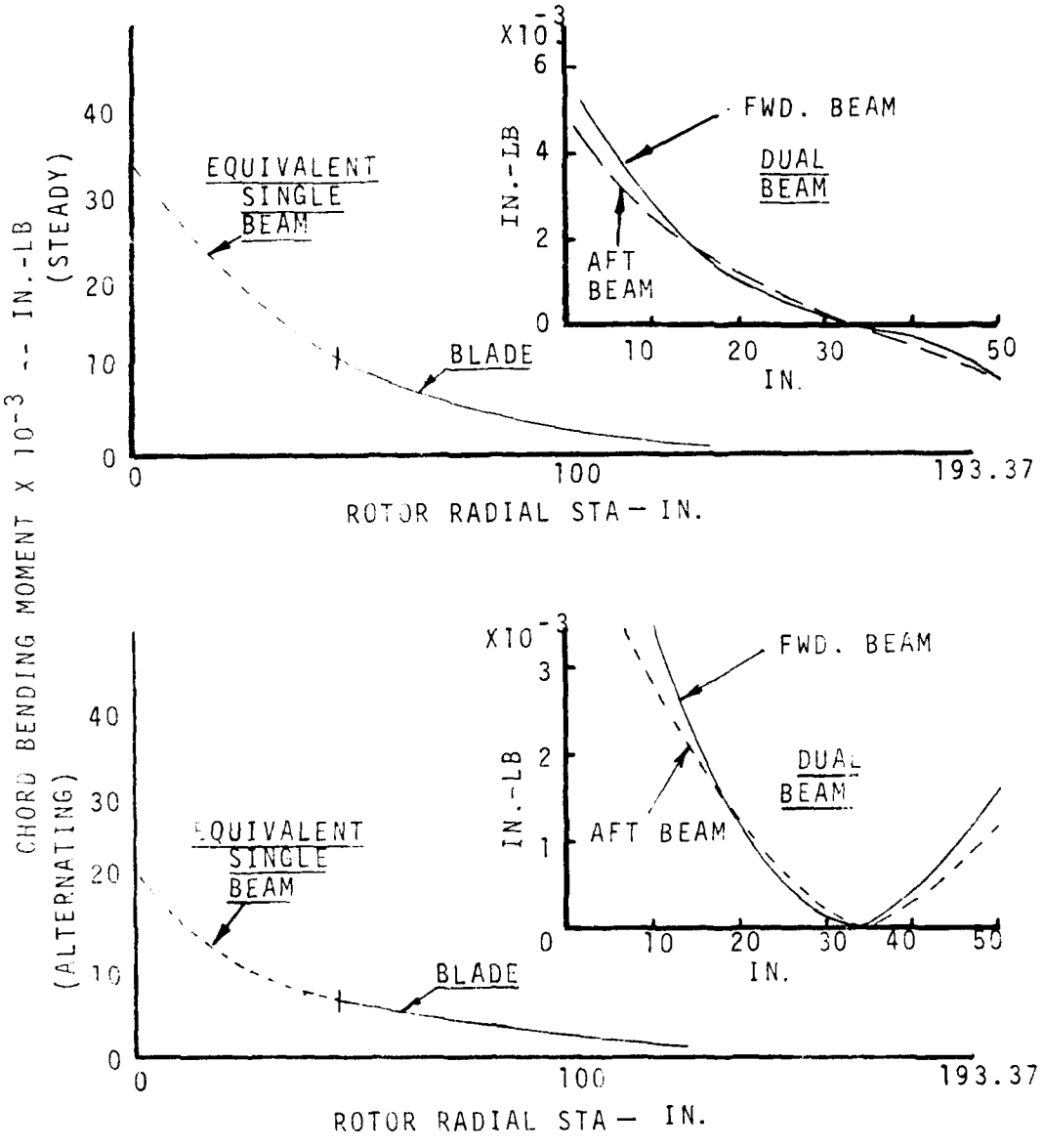

FIGURE 42. EXPECTED CHORD BENDING MOMENT AT 2.0g LOAD FACTOR AND 100 KN.

INSTRUMENTATION (Reference 8)

The airborne instrumentation system used for data acquisition on the flight test program consists of transducers on the rotating and nonrotating components, signal conditioners, FM (frequency modulation) and PCM (pulse code modulation) multiplexers, an onboard tape recorder, and a telemetry transmitter for data transmission to the ground station in real time (see Figure 43). The conditioning, multiplexing, and recording equipment is mounted in a rack assembly installed in the main cabin area.

Instrumentation indicators and controls are provided to the pilot and copilot in the cockpit to control all instrumentation functions during test flights. Instrumentation power, tape recorder, T/M frequency, and time code generator controls are provided in the cockpit.

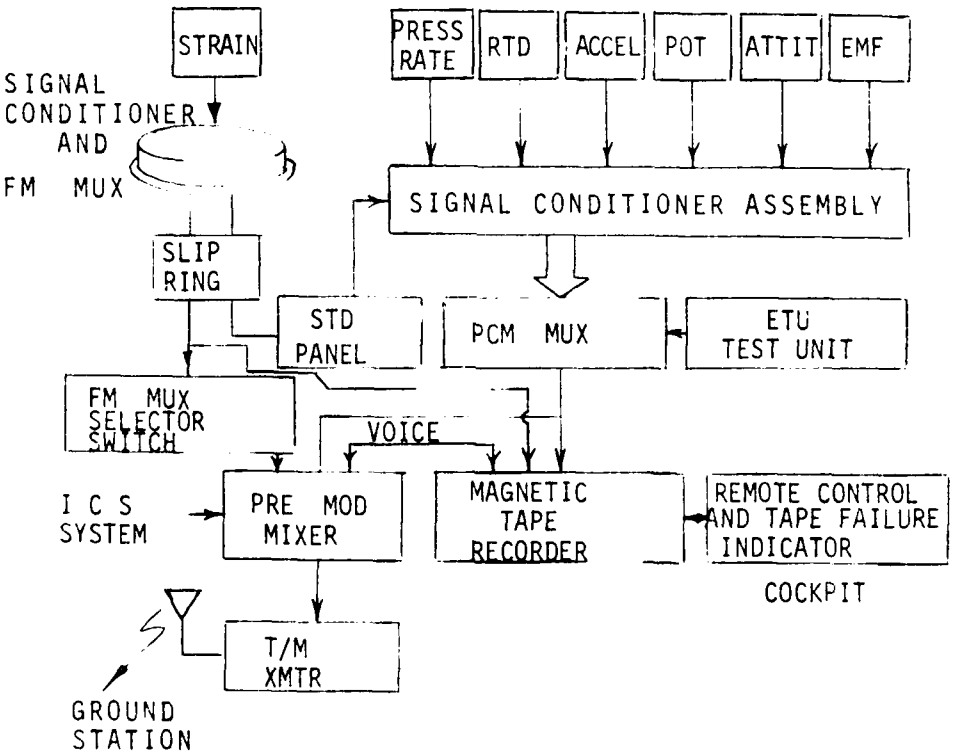

FIGURE 43. AIRBORNE DATA ACQUISITION SYSTEM.

Transmitted data is processed immediately by the STAR (Simulation and Test in Real Time) laboratory system, of which the nucleus is a Xerox Sigma 9-Model 3, a high performance, mapped memory, real time digital computer which checks data against predetermined load limits, converts to linearized floating decimal point engineering units and drives the CRT display and hard copy devices, such as brush recorders.

ROTOR SYSTEM

Two opposite rotor blades were instrumented to measure flap and chordwise bending loads at the mid-span station and at the blade root where a blade root torsion gage was also included. The corresponding flexures had each of their component beams strain gaged to measure flap and chord bending at stations near the blade attachment, at the mid-span, and at the root. Absolute strain measurements were obtained at the extreme upper and lower fibers of both beams at the critical mid and outboard stations. Figure 44 provides the location and type of strain gage bridge, and shows the sign conventions used.

PARAMETER	RADIAL STATION (Inches)			
Beam flap bending (F.B.)	10.50	18.00	44.00	Typical Fwd & Aft flexure beams
Beam Chord bending(C.B.)	11.00	43.00		
Beam Absolute strain	24.00(2)	42.00(2)		
Torque Tube F.B.	38.10			
Torque Tube C.B.	38.10			
Blade F.B.	55.36	110.00		
Blade C.B.	55.36	110.00		
Blade Root Torsion	65.00			
Blade T.E. Tension	110.00			

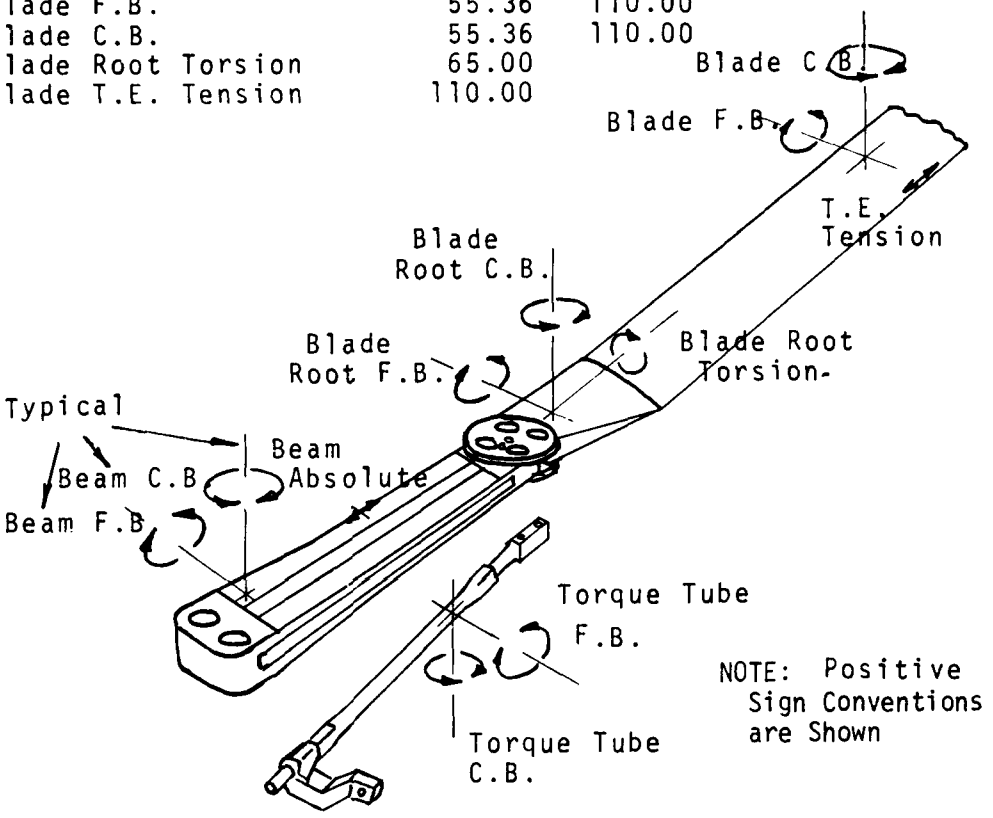

FIGURE 44. ROTOR SYSTEM INSTRUMENTATION.

FLIGHT VEHICLE

The BO-105 flight vehicle was fully instrumented to measure and record flight conditions, associated rotor shaft loads, and control system positions and loads. To record aircraft heading, an instrumentation boom was suspended from the lower left fuselage. To improve the ground stability characteristics, fore and aft skid braces were added and each of these was instrumented to monitor and record cable tension. Data channels in the rotating system were sequence selected by a multiplexing unit attached to the rotor head.

Vibration and aircraft acceleration information was obtained through numerous accelerometers located at positions which included pilot and copilot floor, center of gravity, transmission, rear fuselage, and tail boom. Figure 45 shows the extent of instrumentation coverage.

DATA RECORDING

Permanent records of all data were made on magnetic tape through an on-board recorder and selected data was captured on four brush strip chart recorders after telemetry of data to the STAR laboratory ground recording and flight test operations center.

Flight conditions were also recorded manually by the flight test director.

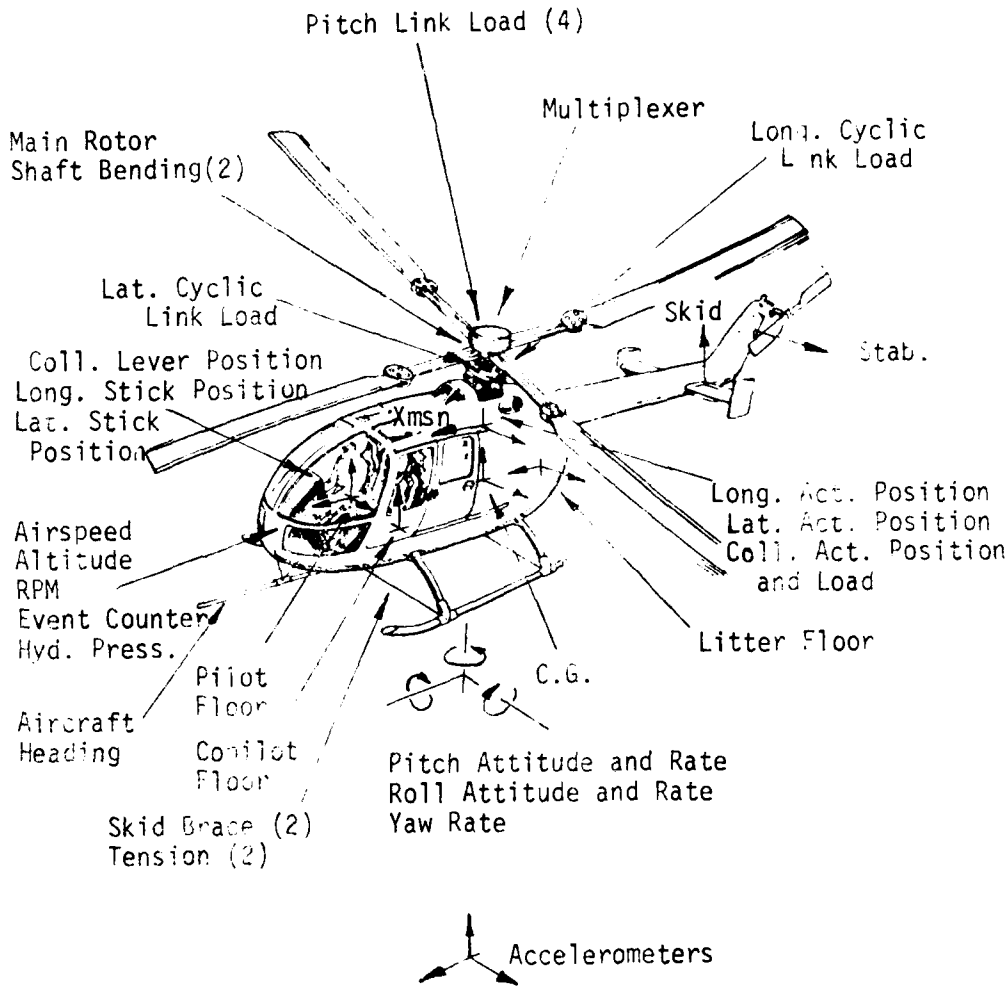

FIGURE 45. FLIGHT VEHICLE INSTRUMENTATION.

ON-LINE DATA REDUCTION

The Sigma-9 computers in the laboratory were used to receive, memorize, and reduce the data. For stability analysis, the pertinent data was analyzed in real time to determine the damping characteristics, through the use of moving block techniques. (See References 8 and 10).

Selected loads were monitored continuously from the brush charts on which the reduced data was displayed in engineering units. During the loads evaluation and structural demonstration phase of the flight test, the data was graphically displayed and plotted. In addition, the computer compared the magnitudes with the predetermined load limits and provided an immediate indication of exceedance.

This system permits flight testing to be conducted in an efficient, expeditious, and safe manner.

A complete description of this system is provided in Reference 8.

10. BO-105 BEARINGLESS MAIN ROTOR GROUND AND FLIGHT TEST PLAN, Boeing Vertol Document D210-11362-1, August 1978.

FLIGHT TEST PROGRAM

The ground resonance and low-speed stability and flying qualities phase of this program were performed at the Boeing Vertol flight test facility at Wilmington, Delaware. The remainder of these phases, together with the loads characteristics and structural demonstration, were conducted in approved airspace over southern New Jersey.

OBJECTIVES

The objective of this program was to demonstrate through flight testing the loads and stability characteristics (including flying qualities) of a Bearingless Main Rotor. It was anticipated that the results of this investigation would either prove the feasibility of such a system or indicate what technical inadequacies still exist and need to be resolved.

TEST PLAN

Reference 10 provides details of the intended test plan and Reference 11 summarizes the test program performed.

The plan was to clear the aircraft from ground instability, up to 95 percent of normal rotor rpm speed (N_r) and to progress into the hover mode. After demonstrating adequate stability in hover, partial airborne conditions and ground resonance at up to 102 percent rotor speed were then to be investigated. The airspeed and rate of climb and descent investigations were then to follow and the program was to conclude with loads and flying qualities evaluations.

Ground and Hover Stability

Figure 46 presents schematically the test sequence for ground and hover testing. The sequence is shown superimposed on predictions for damping derived from analytical and model test results.

Commencing at 75 percent normal rotor speed (N_r) at flat pitch with the aircraft on the concrete flight ramp, the system was to be excited by clockwise whirl at 5 percent of total stick amplitude at a frequency, determined by experiment, to be most responsive. After about eight cycles, the excitation was to be terminated at the neutral stick position and the blade chordwise modal decay analyzed to determine the damping characteristics.

11. FLIGHT TEST SUMMARY, Boeing Vertol Document D210-11501-1, April 1979.

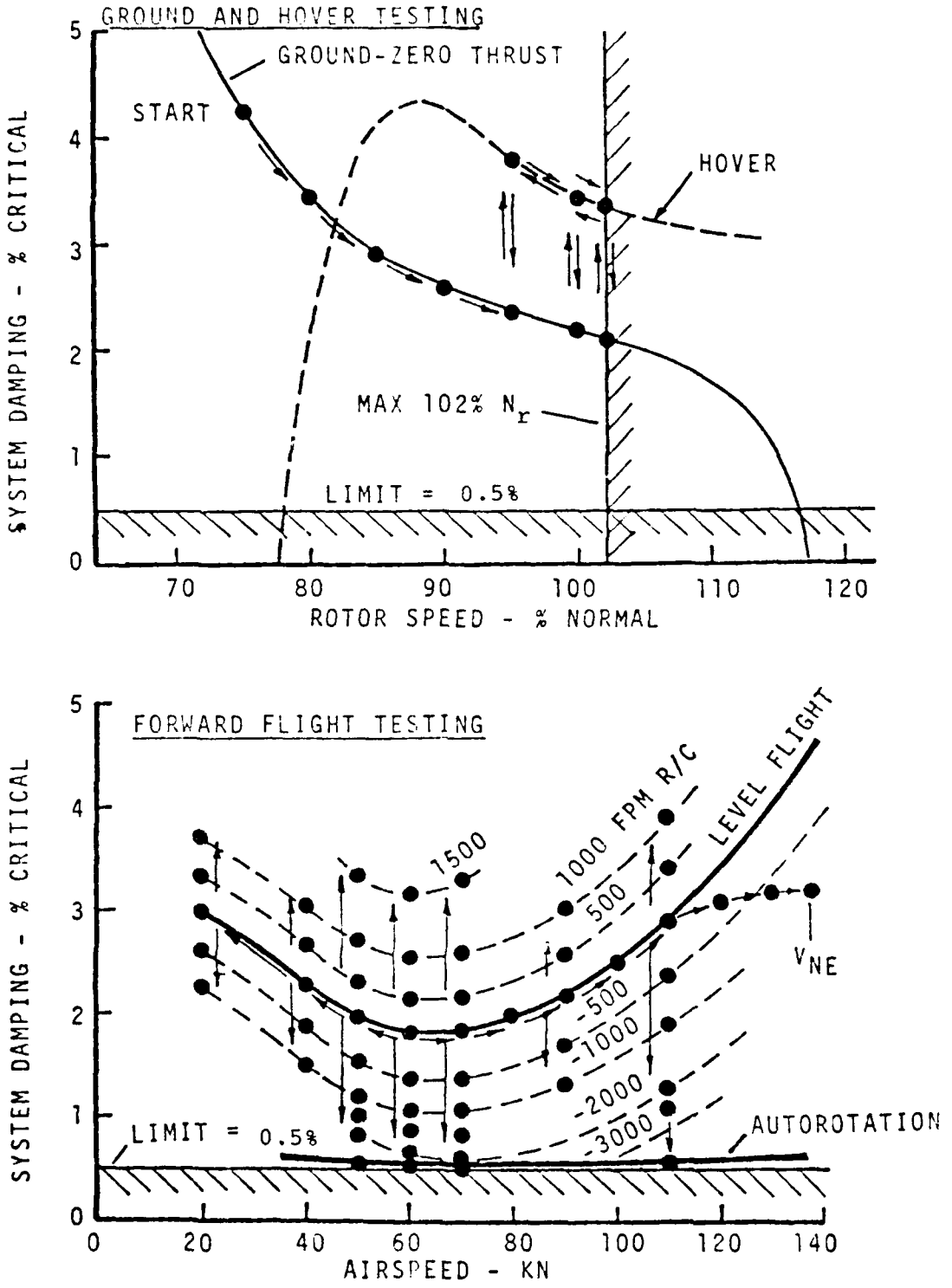

Figure 46. SCHEMATIC OF GROUND, HOVER, AND FORWARD FLIGHT TEST SEQUENCES WITH PREDICTED DAMPING TRENDS.

The technique was to be repeated at increments of 5 percent N_r where damping levels were predicted to remain above 1.5 percent critical and at 2.5 percent N_r increments where they were predicted by data extrapolation to be between 1.5 and 0.5 percent critical. Test points predicted to result in less than 0.5 percent critical damping were not to be attempted.

When a rotor speed of 95 percent N_r was reached, the aircraft was to be lifted off into hover where damping levels were predicted to be higher than on the ground. Using the stick whirl technique, hover stability at this rotor speed was to be demonstrated and then stability in partially airborne conditions was to be investigated. This technique was then to be repeated by lifting off at the highest cleared rotor speed and investigating rotor speeds up to 102 percent N_r. This sequence was carefully devised so that should an instability occur, the pilot could return to a previously cleared condition.

Ground resonance characteristics on both a concrete and turf landing surface were to be examined.

Forward Flight Stability

Using the stick whirl technique, air resonance stability was to be investigated in forward, rearward, and sideward flights.

Maneuver Stability

The stability characteristics in climb and descent from maximum power climbs down to autorotation at rotor speeds up to 110 percent N_r and forward speeds up to V_{ne} were to be measured.

Flight Loads Survey

A flight loads survey was to be performed to determine dynamic component load levels for correlation with design loads at typical flight conditions within the BO-105 flight spectrum and to verify the structural flight limitations of the aircraft. Loads data was to be accumulated in conjunction with rotor stability and flying qualities testing. Supplementary data was to be taken by performing specific flights.

Flight conditions to be investigated included forward, rearward, and sideward level flight, maximum power climbs to autorotative descent, symmetrical pullups to 1.50 g maximum and pushovers to 0.25 g minimum, sideslips to 25°, banked turns to 60°, control reversals, and a maximum load factor demonstration to 2.8 g maximum.

Further details of the plan can be found in Reference 10.

Vibration Survey

Vibration data was to be accumulated during the flight loads survey. Special attention was to be given to transition flight conditions where rotor-induced vibration levels were expected to be high.

Flying Qualities Survey

To augment that data taken during the loads survey, the effects of step and pulse control inputs during hover, level flight, climb, and descents were added to the plan. Longitudinal static stability and maneuvering stability were also to be studied during windup turns to 2.0 g and pushovers to 0.25 g.

SAFETY PRECAUTIONS

An extensive, government-conducted, Safety-of-Flight Review of the aircraft configuration, structural integrity, expected dynamic characteristics, flight test plan, emergency procedures, and safety precautions was conducted during October 1968. Data presented to the board can be found in Reference 12.

TEST LIMITATIONS

The following limitations were applied to flight testing the BMR:

1. All applicable limits with respect to FAA operating limitations.

2. All applicable limits with respect to engine and transmissions, except for Minimum Power on Rotor Speed, which was limited to 92 percent in lieu of 95 percent.

3. Testing conducted inside the envelope defined by the approved flight manual for the BO-105 aircraft.

4. Nominal gross weight of 5070 lb and 4.5 inches forward center of gravity (limited to one configuration due to weight of instrumentation package).

5. V_h was limited to that level flight speed at which the most critical component vibratory load had reached its endurance limit.

Flight conditions were avoided or terminated in the event that:

1. Level flight loads exceeded 100 percent of the endurance limit.

2. Maneuver loads exceeded 150 percent of the endurance limit.

3. The anticipated load for any condition exceeded 80 percent of the design limit load on any component.

4. A control margin of 10 percent or less was reached.

5. The level of resonance damping reduced to 0.5 percent or less.

---

12. SAFETY OF FLIGHT DATA (3 Volumes), Boeing Vertol Document D210-11437-1, October 1978.

6. Short- and long-term stability and controllability as qualitatively assessed by the pilot was approaching an unsafe condition.

7. Mandatory safety monitoring instrumentation became inoperational.

8. Ground winds exceeded 5 knots during the initial ground runs up to 75 percent N_r and +5 knots in increments thereafter during envelope expansion, to a maximum of 30 knots.

9. Gusts exceeded 1/2 peak windspeed.

10. Turbulence exceeded "light".

"SMART BOOK" TECHNIQUE

To preclude the possibility of exceeding those limitations above, a technique of on-line monitoring and recording of mandatory data and the comparison of that data with predictions and predetermined limits was used.

Parameters were divided into the categories A, B, and C:

1. Category A - Predictions required. On-line plotting required as the envelope is being expanded.

2. Category B - Predictions required. On-line plotting required until trend is established.

3. Category C - Predictions required. No on-line plotting required; however, plotting required before next flight during envelope expansion only.

The complete "Smart Book" is to be found in Reference 9.

FLIGHT TEST RESULTS

The flight test program reported in Reference 10 was successfully completed according to the flight test plan detailed in Reference 10. First flight occurred on 26 October 1978 and Figure 47 shows the aircraft after lift-off. References 9, 13, and 14 provide detailed data on the results of the flight test program.

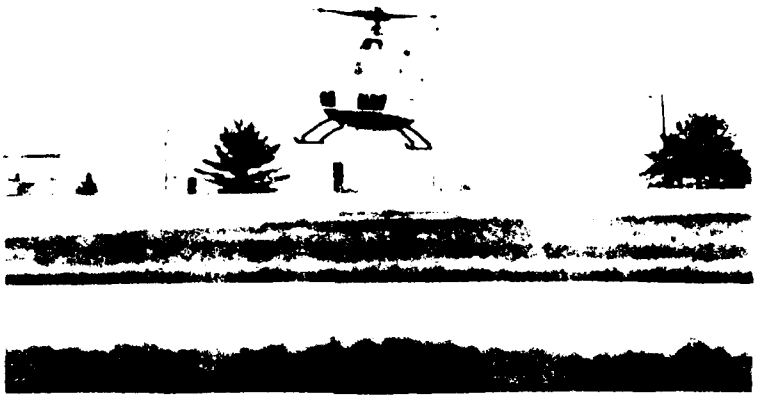

FIGURE 47. FIRST FLIGHT OF THE BMR/BO-105, 26 OCTOBER 1978.

GROUND RESONANCE AND HOVER TESTS

Two series of BMR/BO-105 ground resonance tests were conducted. The first was with the standard BO-105 landing gear where a potential for ground instability was discovered. The second was after the basic gear had been stiffened with [illegible] which resulted in sufficient stability to complete the [illegible] test program.

---

13. LOADS CHARACTERISTICS OF A BEARINGLESS MAIN ROTOR, Boeing Vertol Document D210-11417-1, August 19[illegible].

14. FLYING QUALITIES CHAPACTERISTICS OF A BEARINGLESS MAIN ROTOR, Boeing Vertol Document D210-11499-[illegible], July 1979.

AD-A086 754 BOEING VERTOL CO PHILADELPHIA PA F/G 1/3
DESIGN, DEVELOPMENT, AND FLIGHT DEMONSTRATION OF THE LOADS AND --ETC(U)
JUN 80 P G DIXON DAAJ02-76-C-0026
UNCLASSIFIED USAAVRADCOM-TR-80-D-3 NL

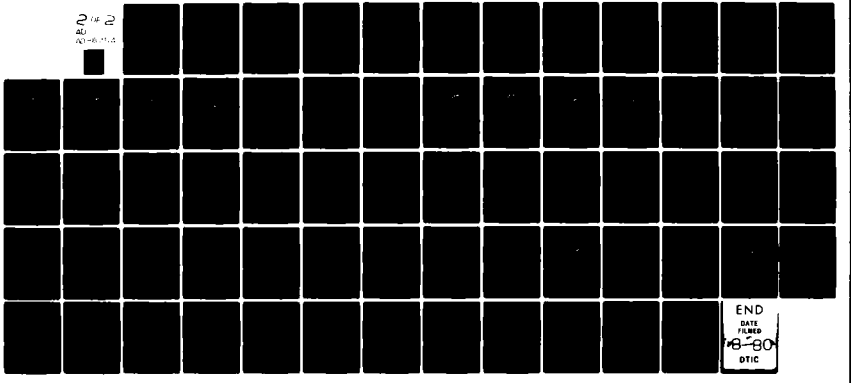

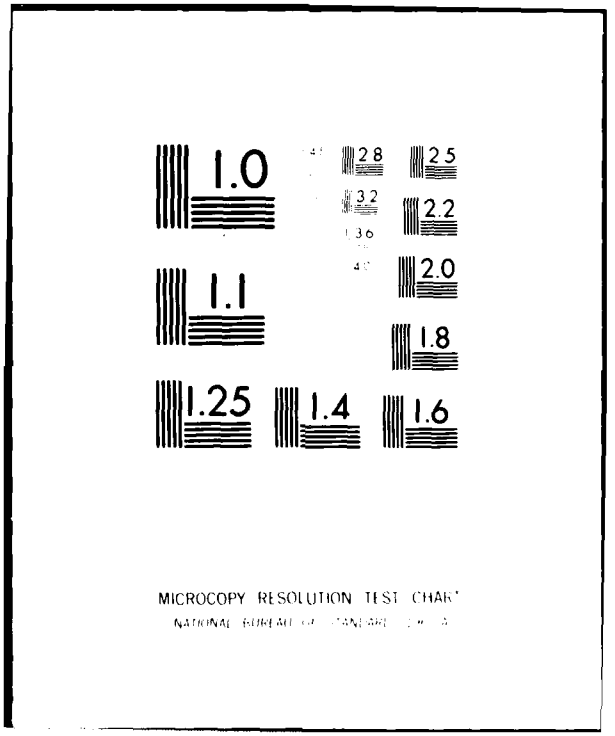
1.0
2.8
2.5
3.2
2.2
3.6
2.0
1.1
1.8
1.25
1.4
1.6
MICROCOPY RESOLUTION TEST CHART
NATIONAL BUREAU OF STANDARDS

Initial Testing

As outlined in the Ground and Hover Stability section, the ground resonance test procedure consisted of a buildup in rotor speed on the ground with the rotor at flat pitch. Excitation was introduced and ground resonance mode damping was determined up to and including 95 percent N_r. Figure 48 shows test values of damping versus rotor speed at flat pitch.

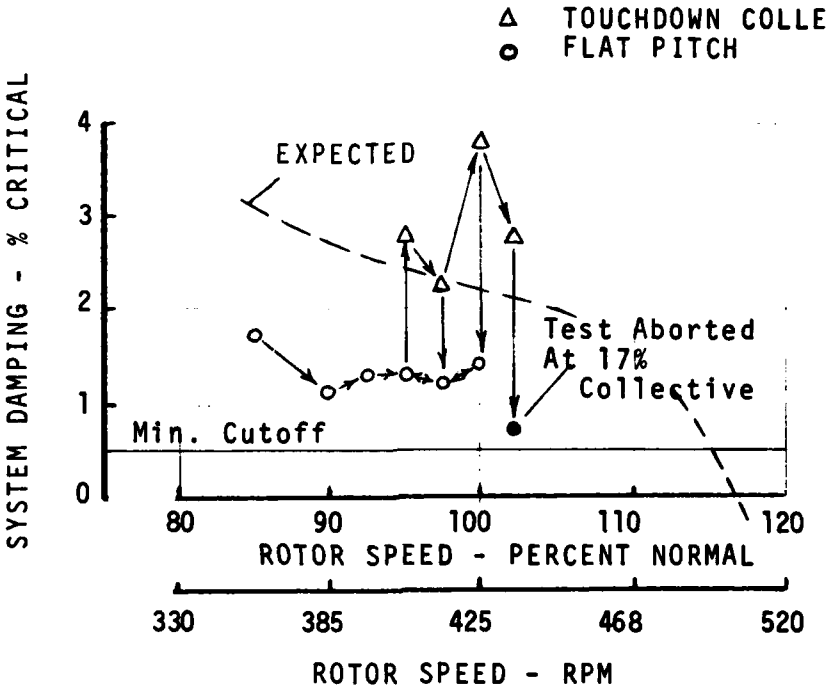

FIGURE 48. DAMPING VERSUS ROTOR SPEED ON CONCRETE WITH STANDARD GEAR - GROUND RESONANCE MODE.

Damping levels were lower than the expected values shown for zero collective pitch. Lifting the aircraft into hover produced an increase in damping level. Landings were made at 95, 97.5, and 100 percent N_r. At 102 percent N_r, the trend approached a resonant condition so the test was cut off at 17 percent collective. It was concluded that the standard landing gear was unacceptable for the BMR/BO-105C configuration. Trimmed conditions were established at several collective settings between touchdown collective pitch (TDCP) and flat pitch and damping evaluations made at each collective. Damping generally decreases with collective pitch as shown by Figure 49, which presents the data for 100 percent N_r on concrete and shows a characteristic dip at an intermediate collective pitch which is different for each rotor speed.

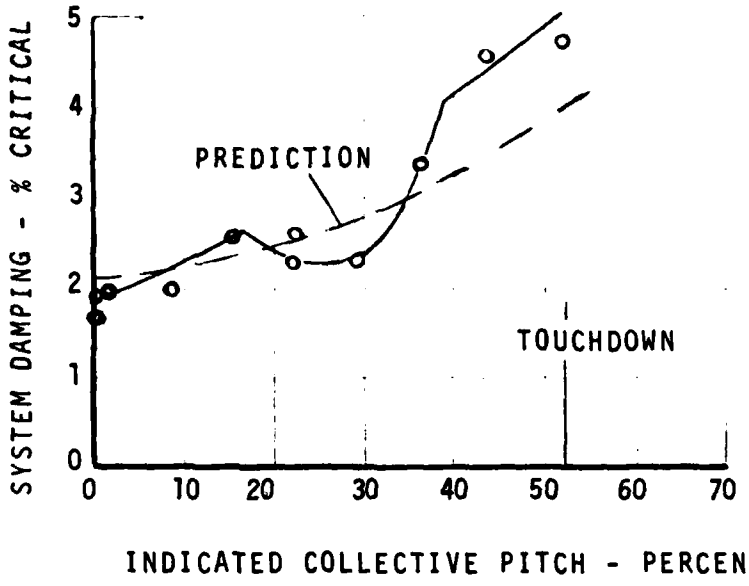

FIGURE 49. DAMPING VERSUS INDICATED COLLECTIVE PITCH AT NORMAL ROTOR SPEED ON CONCRETE - STANDARD GEAR - GROUND RESONANCE MODE.

Figure 50 shows the ground resonance mode damping during landing on turf at 95 percent N_r.

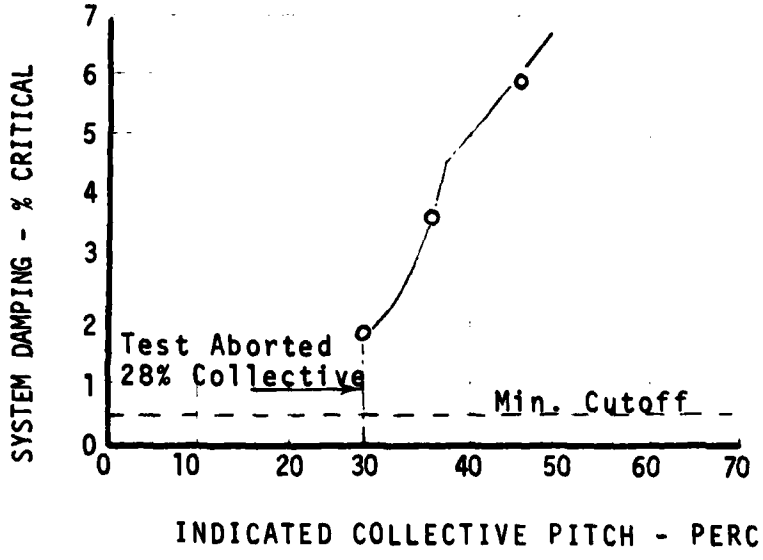

FIGURE 50. DAMPING VERSUS INDICATED COLLECTIVE PITCH AT 95 PERCENT NORMAL ROTOR SPEED ON TURF - STANDARD GEAR - GROUND RESONANCE MODE.

For this test, the aircraft lifted off the concrete runway and began a landing sequence at 95 percent N_r on the turf nearby. A degradation of ground resonance stability was expected on turf because of the reduction of the body pitch frequency on the softer turf surface. Figure 50 shows that the damping trend indicated a possible instability at a collective pitch of about 22 percent collective and the test was terminated at 28 percent collective. The aircraft lifted off and landed on the concrete runway.

The interest in landing on turf was for emergency landings on unprepared areas when the aircraft was scheduled to perform testing out of the Wilmington Airport area.

It was concluded that the landing gear stiffness was nonlinear, and that it varied with percent airborne and had not been accurately modeled in mathematical representation; therefore, the prediction, together with the standard BO-105 landing gear, was incompatible with the BMR system. For comparison with the theoretical predictions, hover stability data is presented in Figure 51.

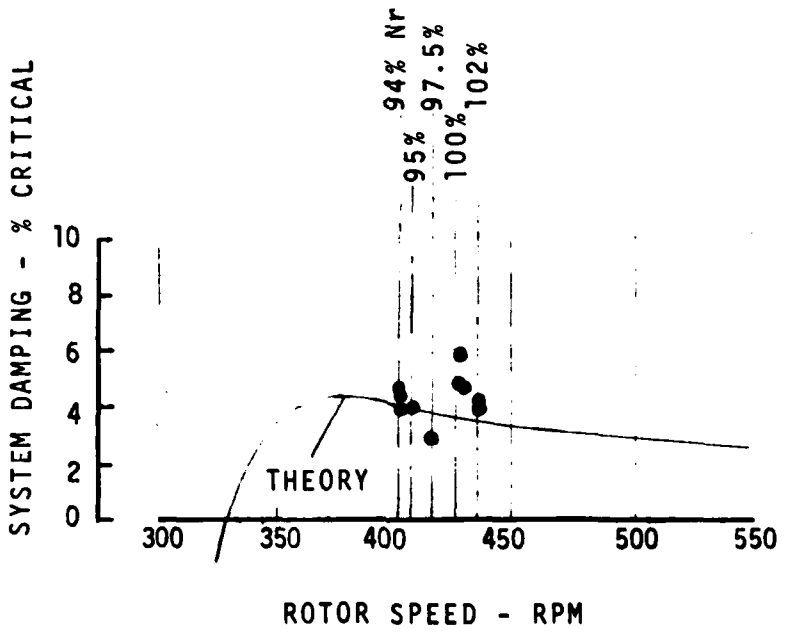

FIGURE 51. DAMPING SENSITIVITY TO ROTOR SPEED IN HOVER.

Landing Gear Modifications

Through more detailed analyses and aircraft shake testing, it was discovered that the predominant mode at the critical frequency on the ground was longitudinal and not pitch as had previously been considered. The gear cross tubes were mounted in an elastomer cuff which provided a soft longitudinal restraint. Stiffening, as illustrated in Figure 18, had been prepared for the pitch mode only, but this would provide some longitudinal mode stiffening.

With this modification installed, shake tests were performed which demonstrated that the longitudinal pitch mode, as it is now termed, was increased from about 3.08 to 3.25 Hz. With this modification, the ground resonance tests were repeated; meanwhile, a design for longitudinal stiffening was initiated.

Effect of Gear Modification

Figure 52 shows ground resonance mode damping versus collective pitch for the stiffened landing gear on concrete at 102 percent rotor speed.

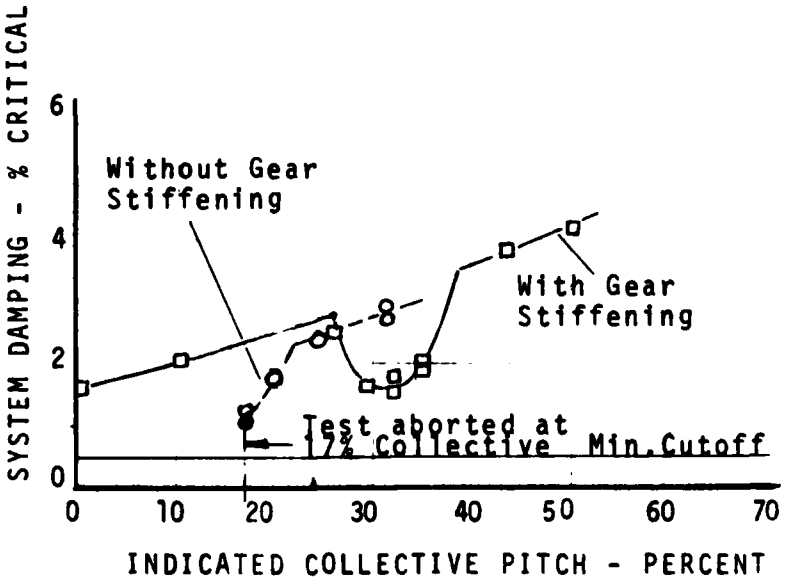

FIGURE 52. SYSTEM DAMPING VERSUS INDICATED COLLECTIVE PITCH AT 102 PERCENT NORMAL ROTOR SPEED ON CONCRETE - EFFECT OF GEAR STIFFENING. GROUND RESONANCE MODE.

A comparison with the previous data is presented which shows that the effect of gear stiffening was to change the dip location on the characteristic damping curve so that it occurred at a higher collective and consequently at a higher level of damping, thus raising the minimum damping level.

Figure 53 presents similar data on turf at 95 percent rotor speed. At 97.5 percent N_r neutral stability was observed. This data showed the aircraft capable of an emergency landing on turf provided that a technique is used to reduce rotor speed to 95 percent N_r or below before collective pitch is reduced to less than 40 percent. This follows the normal sequence of events for a flared landing from autorotation.

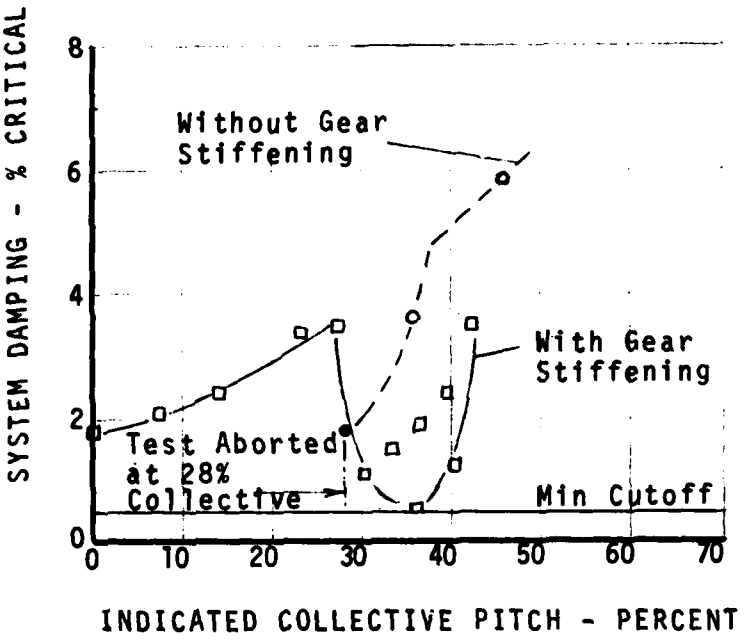

FIGURE 53. SYSTEM DAMPING VERSUS INDICATED COLLECTIVE PITCH AT 95.0 PERCENT NORMAL ROTOR SPEED ON TURF - EFFECT OF GEAR STIFFENING. GROUND RESONANCE MODE.

Figure 54 shows a comparison of ground resonance mode damping for the baseline BO-105 and the BMR/BO-105 with and without gear stiffening.

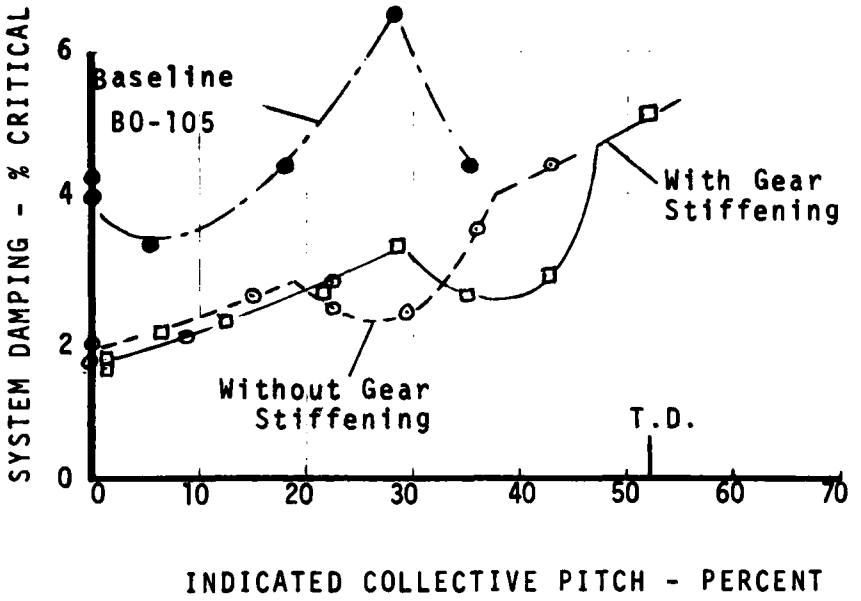

FIGURE 54. SYSTEM DAMPING VERSUS INDICATED COLLECTIVE PITCH AT NORMAL ROTOR SPEED - BASELINE BO-105 AND BMR/BO-105. GROUND RESONANCE MODE.

The baseline BO-105 had somewhat higher stability. However, a tendency toward reduced damping is indicated for the BO-105 baseline above 30 percent collective pitch, but only a limited number of test points were taken and the trend above 30 percent collective was not well defined.

It was decided that this stability level was sufficient to safely meet BMR test objectives and efforts towards alternative gear stiffening were terminated.

AIR RESONANCE TESTS

Before the aircraft could be cleared for testing outside the Wilmington test facility, an initial in-field series of low speed airborne tests were made to give a preliminary indication of the BMR/BO-105 air resonance stability. Checks were made at speeds up to 50 knots in level flight and in climbs and descents up to 500 feet per minute. Based on the successful results of these tests, the test airspace was expanded away from the Wilmington Airport where higher speeds and rates of descents could be flown.

Effects of Forward Speed on Stability

Figure 55 shows damping versus forward speed for airspeeds up to V_h (106 knots IAS) in level flight and for maximum power dives up to V_{ne} at normal rotor speed. Damping is seen to be a minimum of about 3 percent at 50 knots, a characteristic which was predicted by wind tunnel model tests. Damping levels, however, are substantially higher

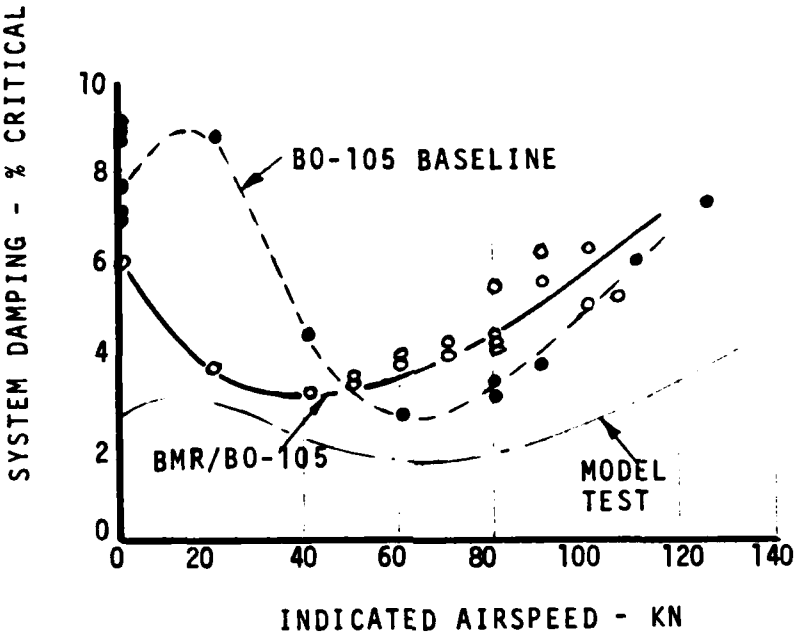

FIGURE 55. BASELINE BO-105 AND BMR/BO-105 DAMPING VERSUS INDICATED AIRSPEED IN LEVEL FLIGHT AT NORMAL ROTOR SPEED. AIR RESONANCE MODE.

at full scale. Included for comparison are the results from the baseline BO-105 tests which shows that the BMR/BO-105 and the standard configuration have similar minimum damping levels in the 50- to 60-knot IAS range. However, the baseline exhibits greater stability levels in hover and transition speeds. The difference may be due to the difference in coning/pre-droop angles between the two configurations.

Effect of Climb and Descent on Stability

Preliminary investigations, using the pilot's rate of climb meter, provided discouraging results due to instrumentation lag and gross inaccuracy producing a large degree of scatter in the data. By relating rate of climb at constant forward speed to collective setting, this scatter was reduced to a minimum and smoother trends were obtained.

The typical data, compared with that obtained from a model and baseline testing, is presented in Figure 56, which shows a gradual decrease in stability from maximum power climbs to autorotative descent. Data at 60 knots, which is in the speed range at which minimum stability was experienced in level flight, is presented here. Reference 9 provides further test results, which show damping slightly higher at lower than the normal rotor speeds and at other speeds than the 60 KIAS presented here.

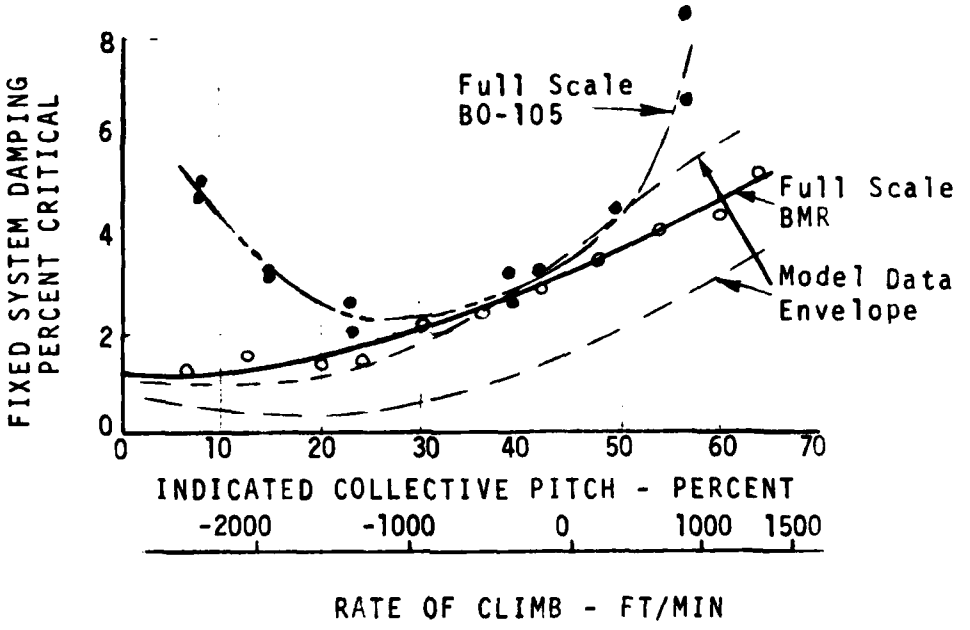

FIGURE 56. DAMPING VERSUS COLLECTIVE PITCH (100 PERCENT N_r) AIR RESONANCE MODE.

Stability in Autorotation

Figure 57 shows damping versus rotor speeds between 85 and 108 percent N_r in autorotation for 60, and 90 to 100 KIAS. Damping is lower at higher rotor speeds in autorotation, but the level increases with increase in forward speed.

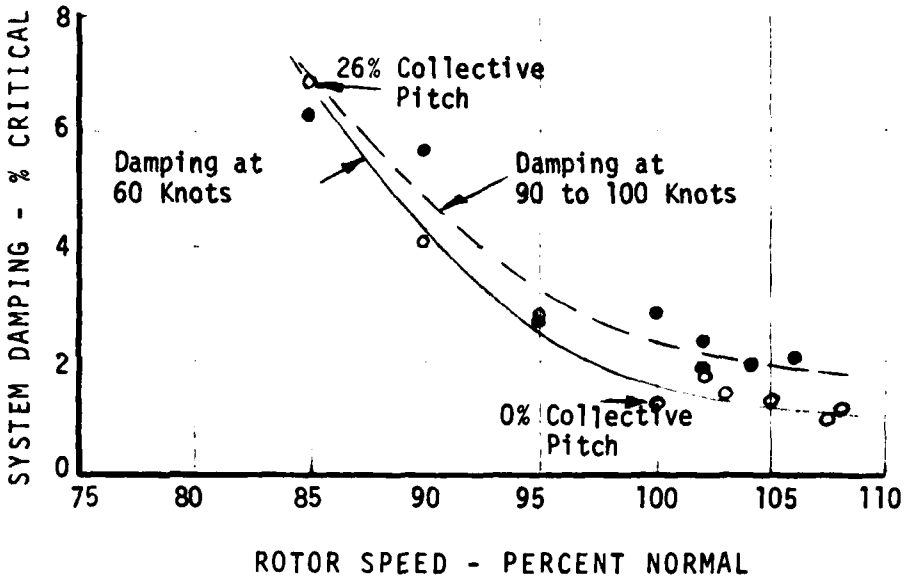

FIGURE 57. DAMPING VERSUS ROTOR SPEED IN AUTO-ROTATION AT 60 AND 90 TO 100 KNOTS.

LOADS SURVEY

The following data has been extracted from Reference 13:

A limited structural demonstration was conducted as shown by the envelope in Figure 58. This flight loads evaluation included level flight from 20 knots rearward to V_{ne}.

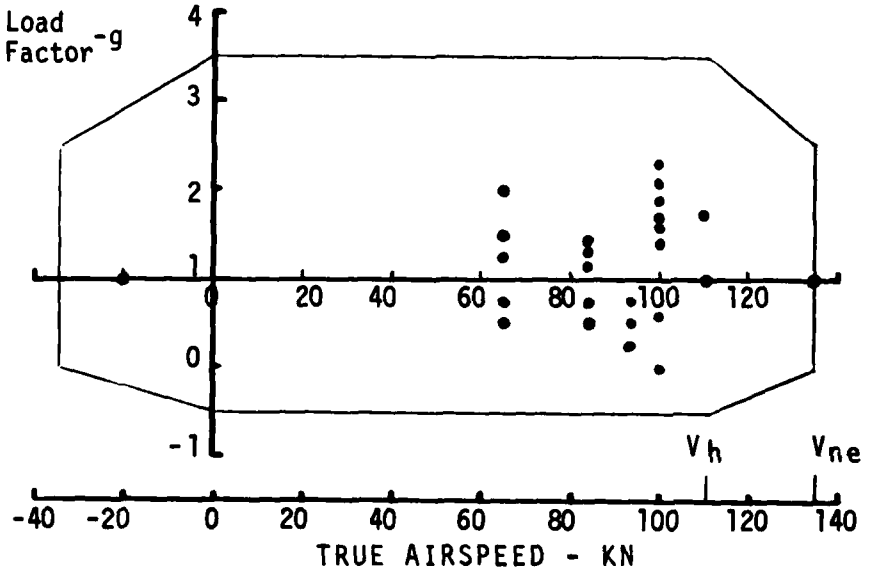

FIGURE 58. BMR/BO-105 STRUCTURAL ENVELOPE.

or 120 percent V_h. Maneuvers included climbs and descents, collective and cyclic pullups to 2.3 g, pushovers to 0 g, banked turns to 60°, and roll angles of up to 90°. In addition, sideward flight, control reversals, landing flares, and effects of rpm were investigated. All loads were monitored continuously throughout the test program commencing with the initial ground resonance evaluations. A cumulative damage count was maintained: for the more than 40 hours of rotor-on time, less than 2 percent of the established life of the most critical component was used. The most damaging conditions were those in which the pilot induced rotor excitations through intentional stick whirl at precisely the cited frequency during the aeromechanical stability investigations.

For the data presented herein, fatigue endurance limits for 10^8 cycles of life were established by bench test. The load levels for maneuver cutoff or 1.5 x E.L. were limitations above which no maneuver was to be attempted. No maneuver was to be sustained between the endurance limit and maneuver cutoff. The abort limit was a fatigue load level at which, if reached or exceeded, the aircraft was to return to base for thorough inspection. Another limitation was at the 80-percent limit load level which was regarded as an abort limit.

Throughout this flight test program, no load exceeded the abort level.

Control System Loads

Figure 59 presents the measured collective actuator loads and shows that the torque to twist a centrifugally loaded flexure of this complexity can be predicted with accuracy.

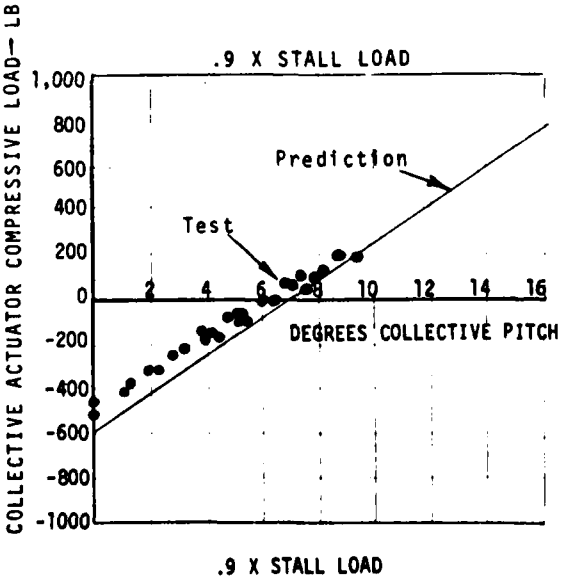

FIGURE 59. COLLECTIVE ACTUATOR LOAD.

The variations in alternating pitch link load with forward speed and load factor were also within prediction. In the regime of blade stall, induced loads were well within the capability of the links as illustrated in Figure 60.

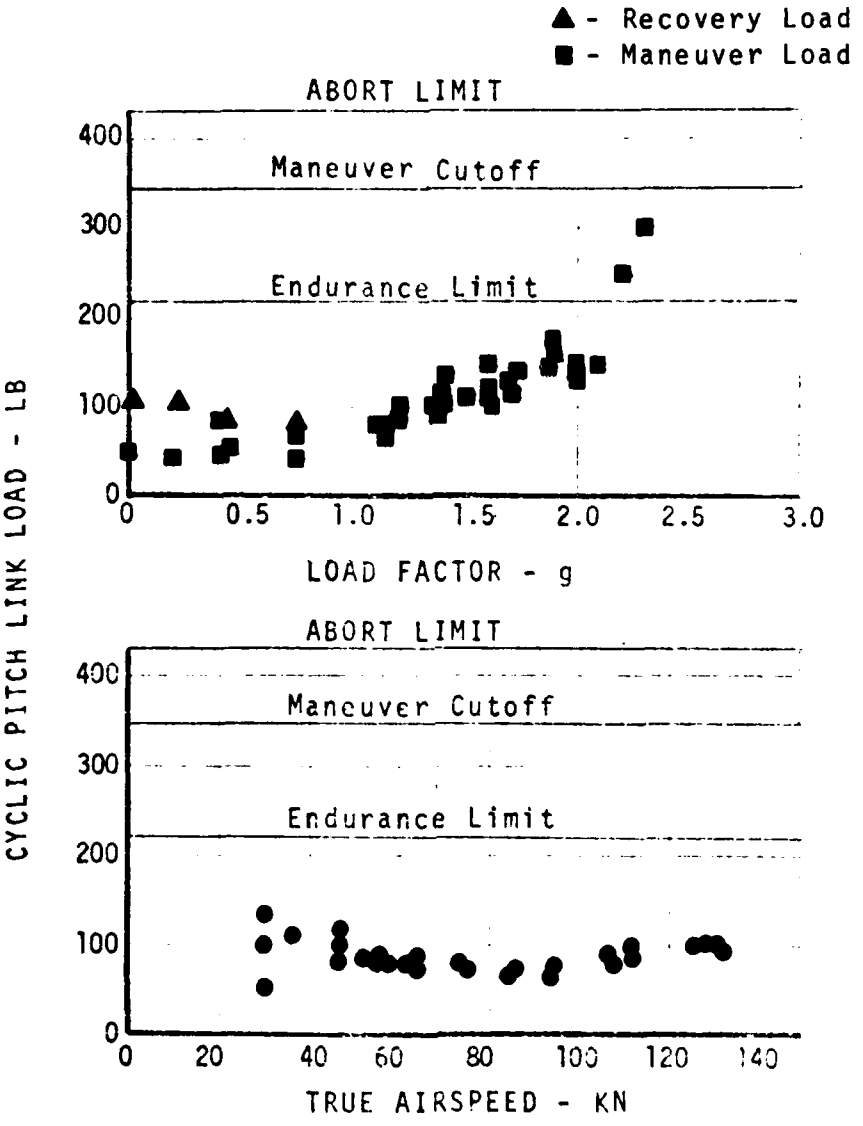

FIGURE 60. PITCH LINK LOAD VERSUS LOAD FACTOR AND AIRSPEED.

The most critical component in the BMR control system was the pitch control torque tube. However, with an extended bench fatigue test to determine the true endurance limit from a failure instead of a runout its structural limitations could likely be raised. Figure 61 presents the flap bending moment data which did not exceed expected levels, but as can be seen in Figure 62 the chord bending moments were at or above the endurance limit throughout the forward flight testing and in one instance approached the abort limit.

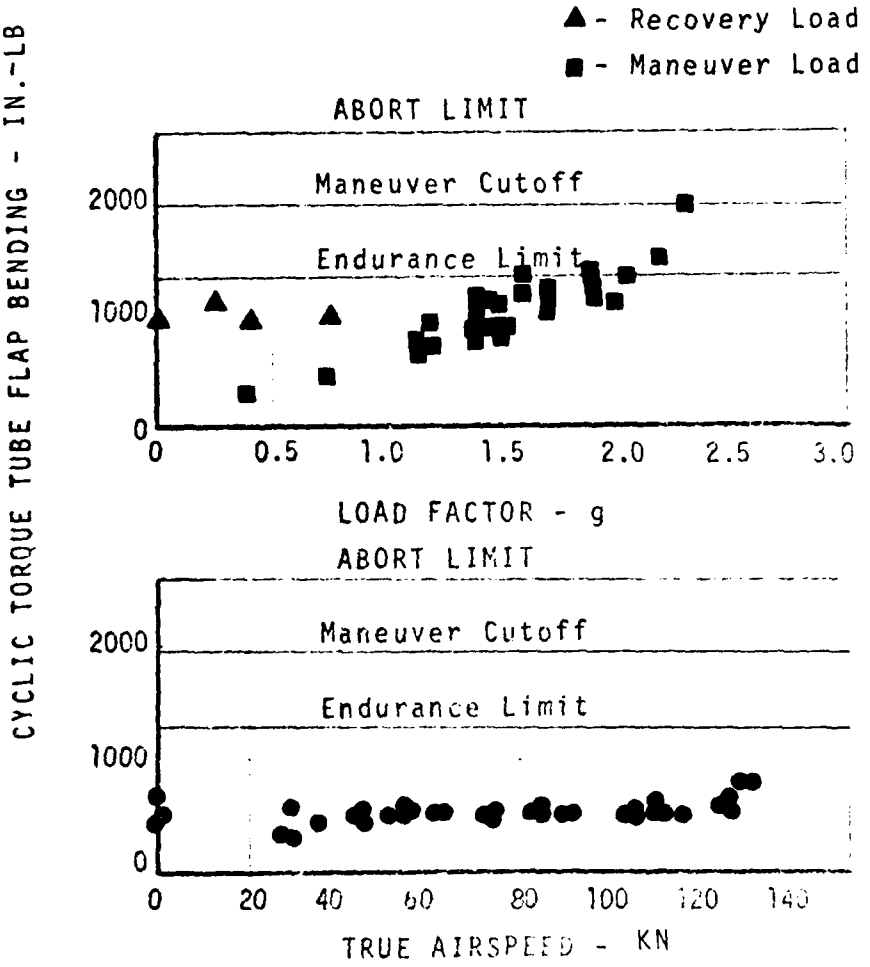

FIGURE 61. TORQUE TUBE FLAP BENDING VERSUS LOAD FACTOR AND AIRSPEED.

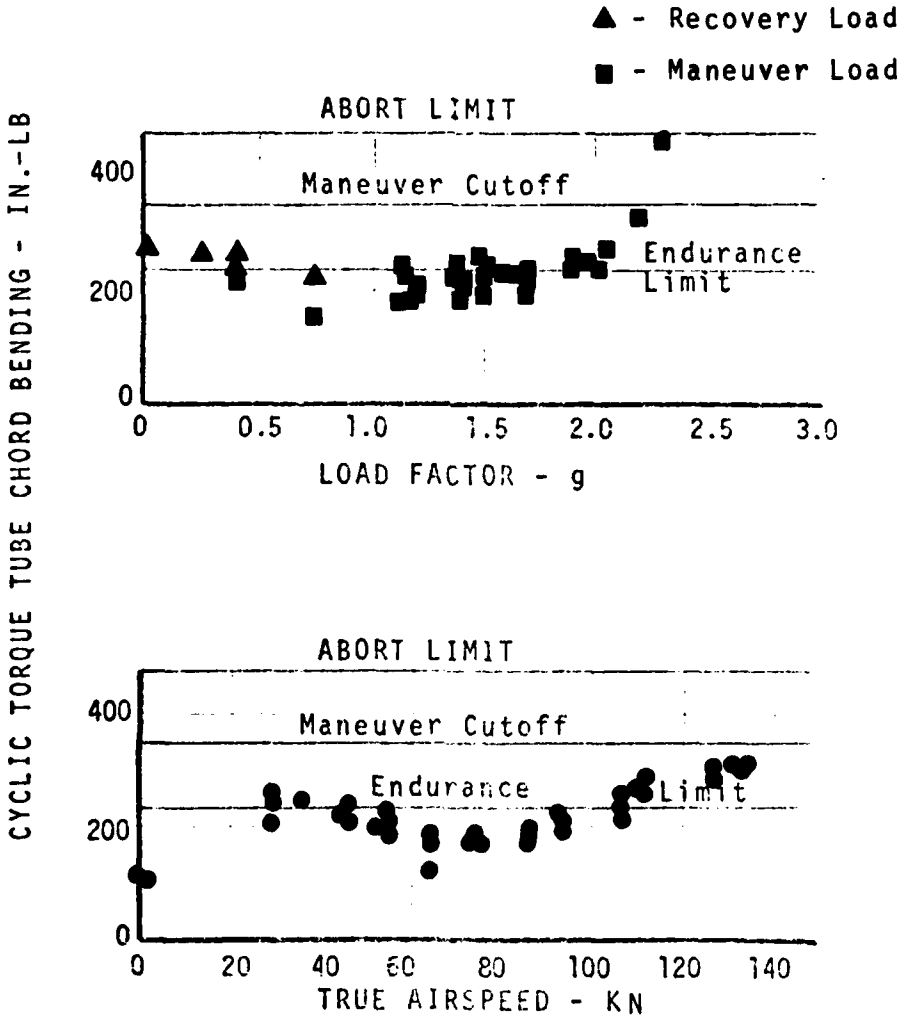

FIGURE 62. TORQUE TUBE CHORD BENDING VERSUS LOAD FACTOR AND AIRSPEED.

Shaft Loads

Figure 63 presents the shaft moment data typical of both the BMR and the standard rotor equipped BO-105. At load factors below 1 g, that is, pushovers, data applicable to the pullups necessary to recover from those maneuvers have been included. It should be noted that in the speed range of 20 to 40 knots peak loads are not observed.

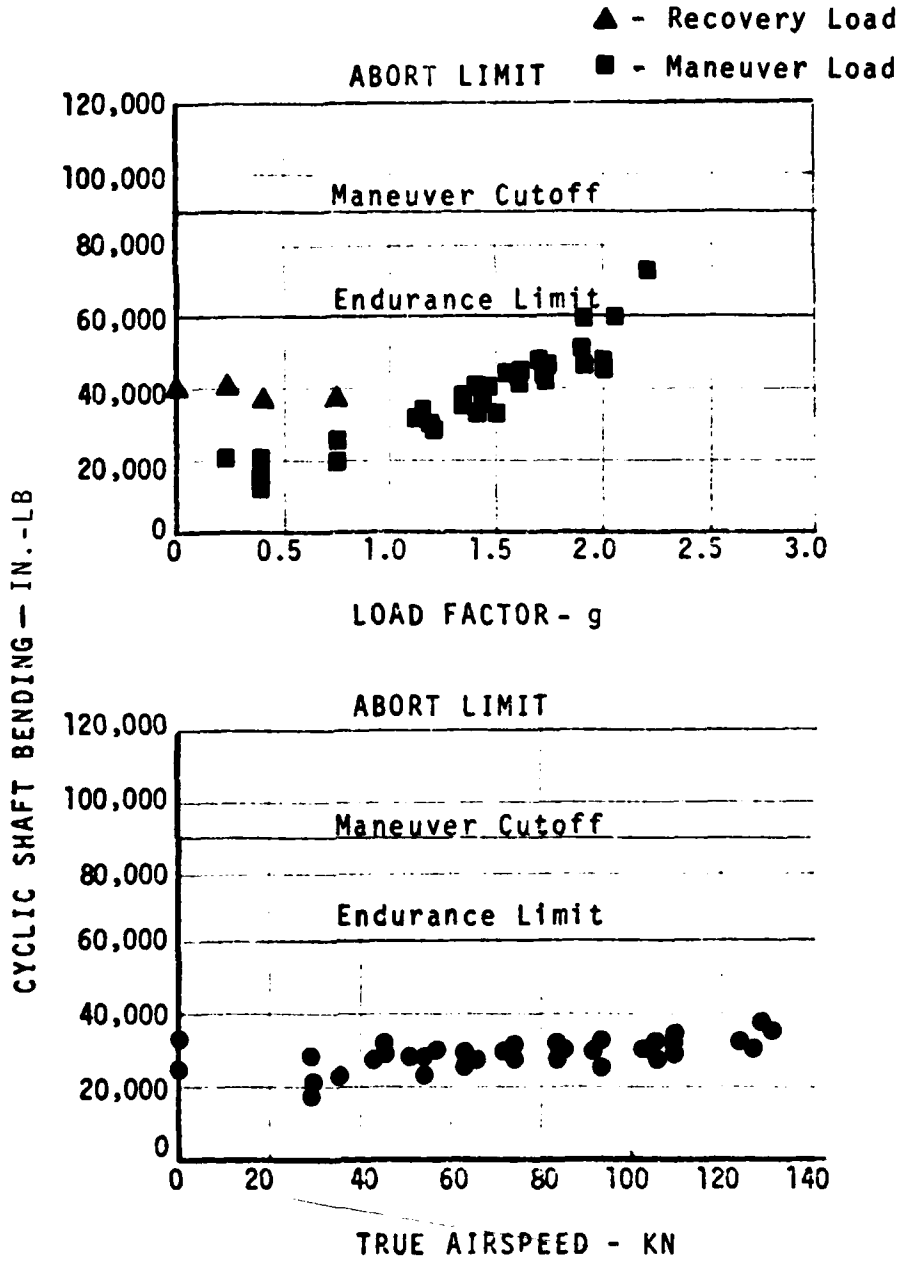

FIGURE 63. SHAFT BENDING VERSUS LOAD FACTOR AND AIRSPEED

Blade Loads

Figure 64 shows how flap bending at the blade root peaks at low forward speeds due to 4-per-rev loads. The effect is not apparent in the shaft bending, which is not sensitive to these loads; however, they are a source of vibration that is discussed in a following section of this report.

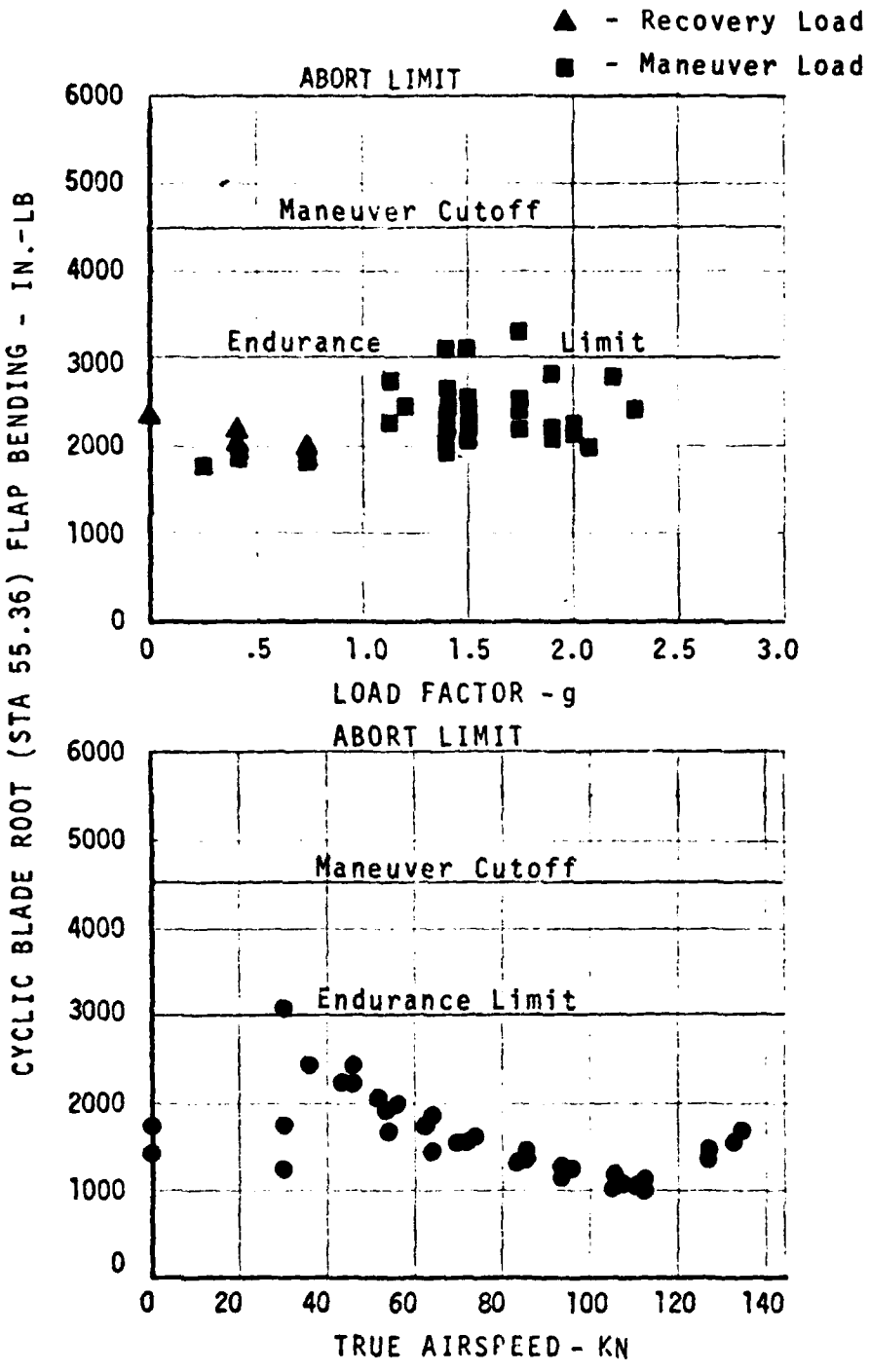

FIGURE 64. BLADE ROOT FLAP BENDING VERSUS LOAD FACTOR AND AIRSPEED.

The excessive mass of the blade to the flexure attachment clevis is thought to aggravate this situation.

Chordwise bending moments do not exhibit this characteristic at low speeds but Figure 65 shows a rapid increase in load in the regime of blade stall at high load factors.

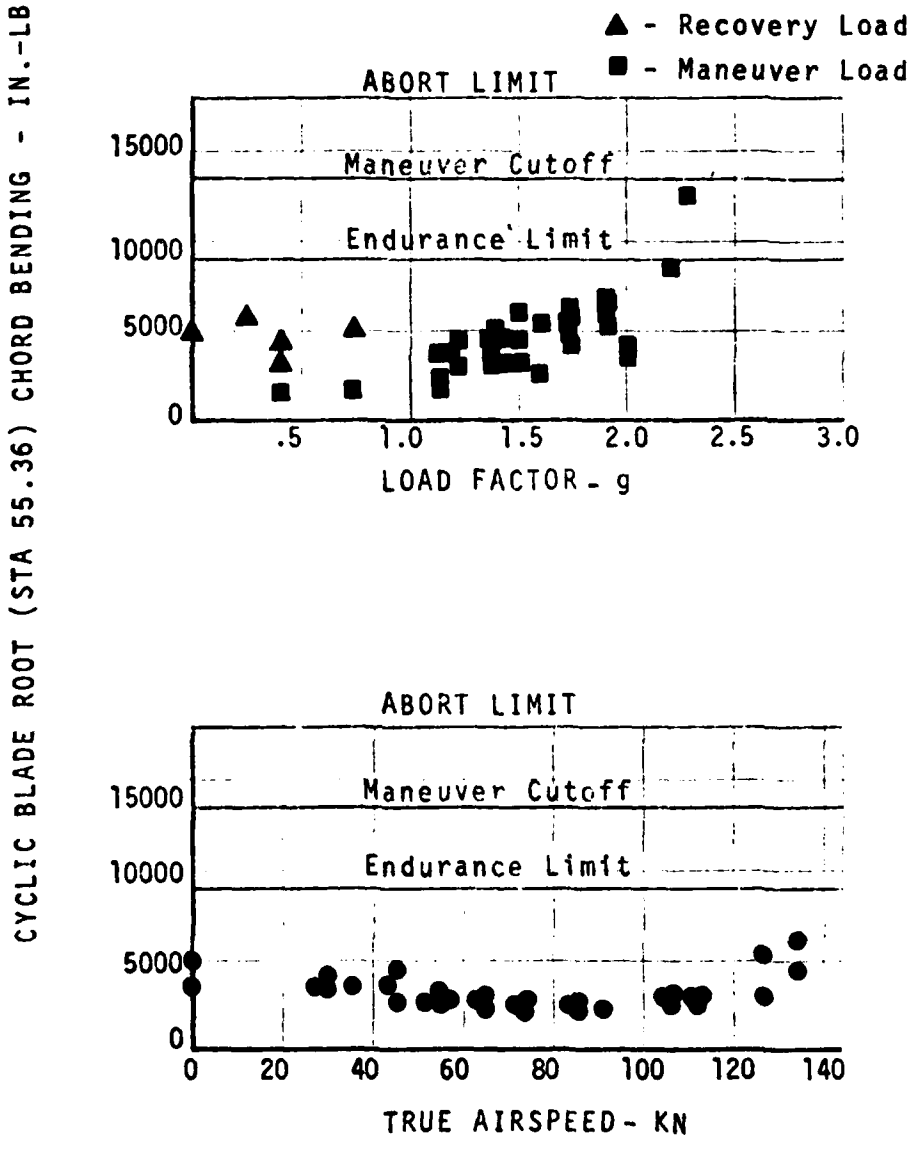

FIGURE 65. BLADE ROOT CHORD BENDING VERSUS LOAD FACTOR AND AIRSPEED.

Blade root torsion loads are insensitive to airspeed but as expected, blade stall raises the fatigue load level above the endurance limit as shown in Figure 66.

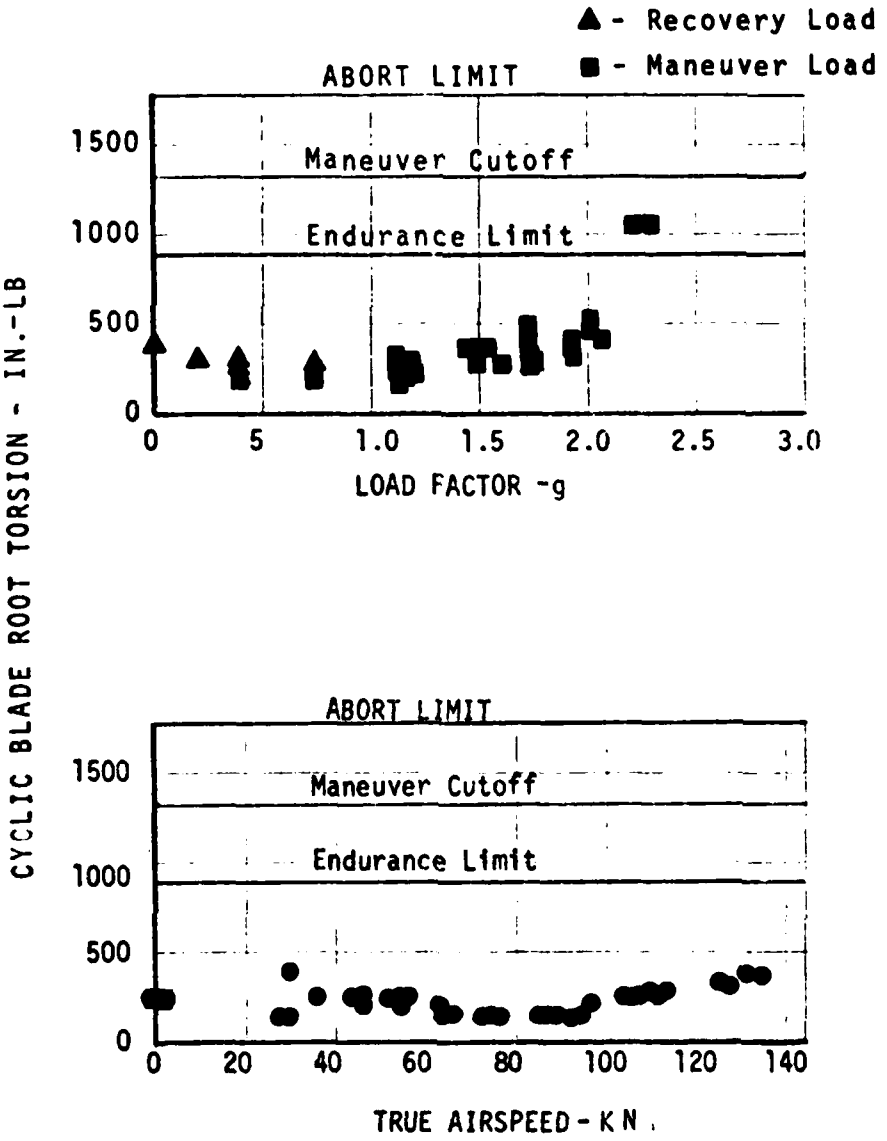

FIGURE 66. BLADE ROOT TORSION VERSUS LOAD FACTOR AND AIRSPEED.

Flexure Loads

The alternating loads presented in this report are those obtained from the one maximum peak in the data trace taken during the maneuver. The cyclic pullups up to 2.3g maximum load factor result in a transient spike in the data and this has been presented here with the result that loads up to the abort limit are shown. Subsequent post-flight inspections, as expected, revealed no structural degradation in any of the rotor system components.

Figure 67 indicates that the inboard station of the flexure is the most critical in bending since loads remain at or above the test established endurance limit throughout the load factor range. Stated in preceding discussions, the fatigue testing of the flexure components resulted in runouts without failure and an expansion of this test program would likely result in increasing the level of those limits presented herein. However, the power limitations, rotor solidity, and rotor stall would preclude demonstration of load factors greater than those achieved in this flight test program, even if these endurance limit levels are increased.

Flap bending loads at the flexure midspan location, as shown in Figure 68, also increase rapidly with high load factors but are more compatible with the established endurance limit for loads up to 2.0 g than at the inboard station.

At the outboard end of the flexure, close to the blade attachment hardware, the even harmonics in flap bending loads are evident by the increase in load at low forward speeds as shown by Figure 69. This characteristic is exhibited by flap bending at the blade root and at the pitch control torque tube as discussed previously.

Figures 70 and 71 show that blade stall at high load factors produces a more rapid increase in chord bending loads at the flexure ends than in flap bending, and the rise in load at low forward speed is not apparent in this bending mode.

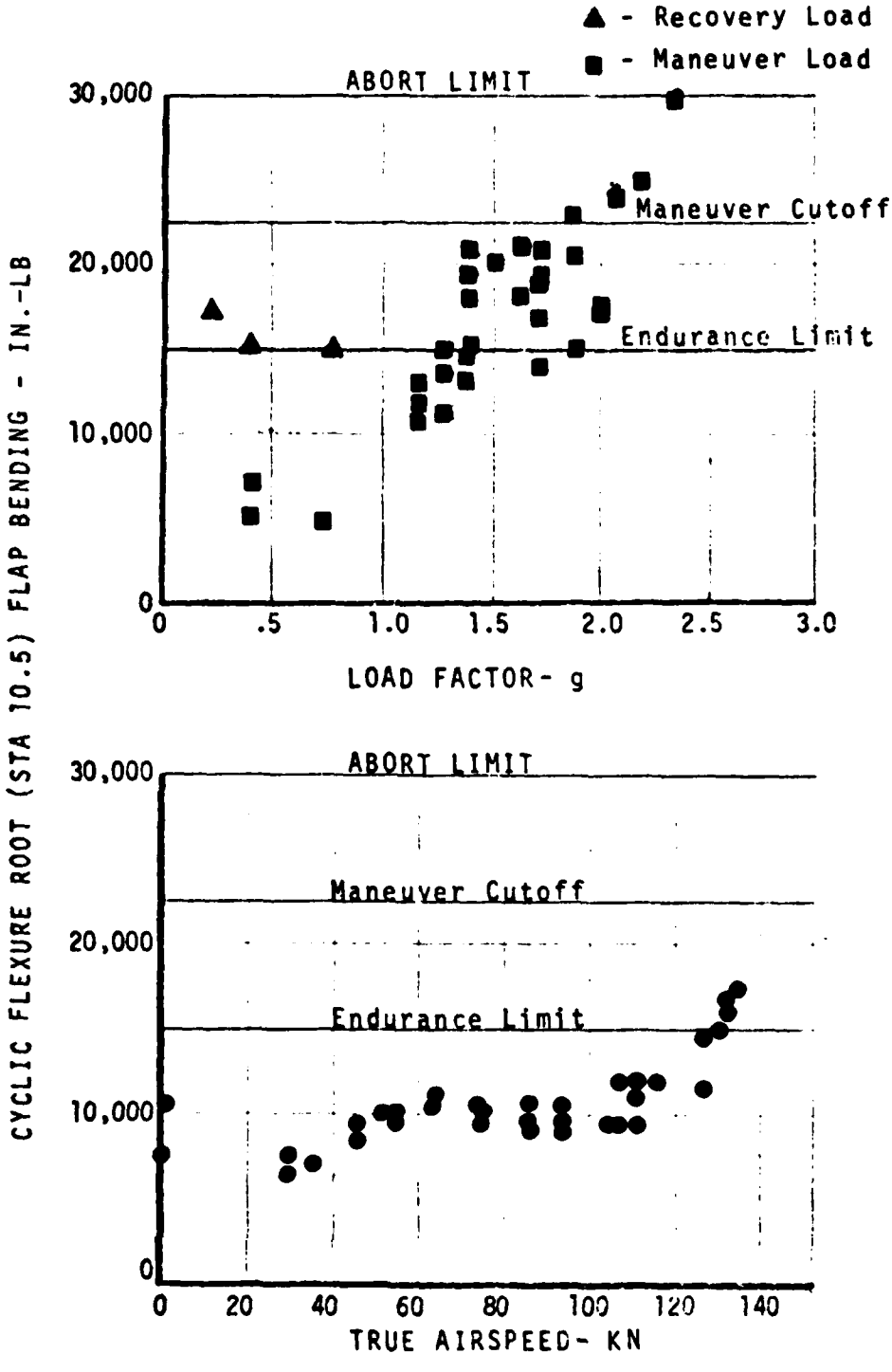

FIGURE 67. FLEXURE ROOT FLAP BENDING VERSUS LOAD FACTOR AND AIRSPEED.

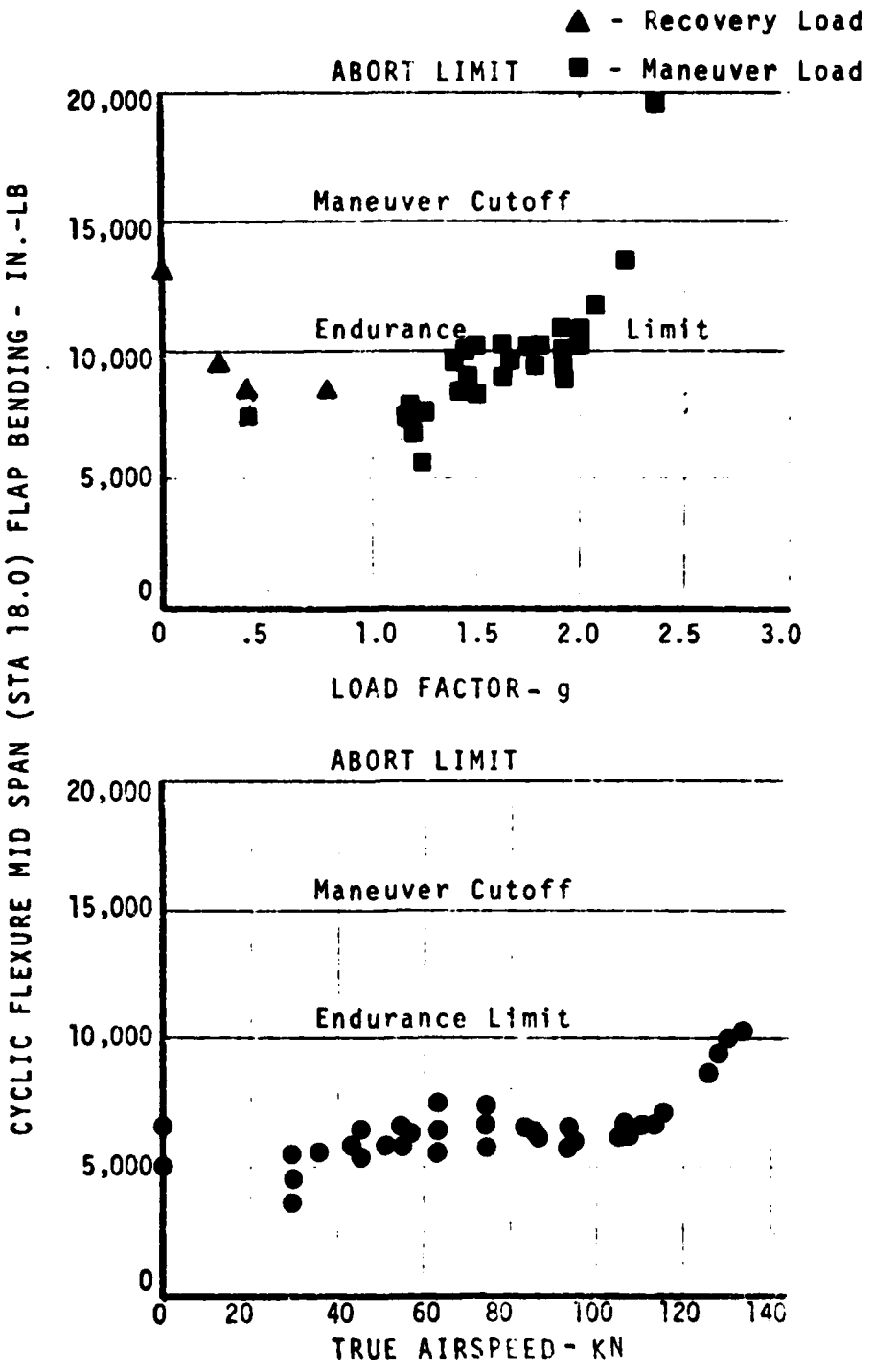

FIGURE 68. FLEXURE MID-SPAN FLAP BENDING VERSUS LOAD FACTOR AND AIRSPEED.

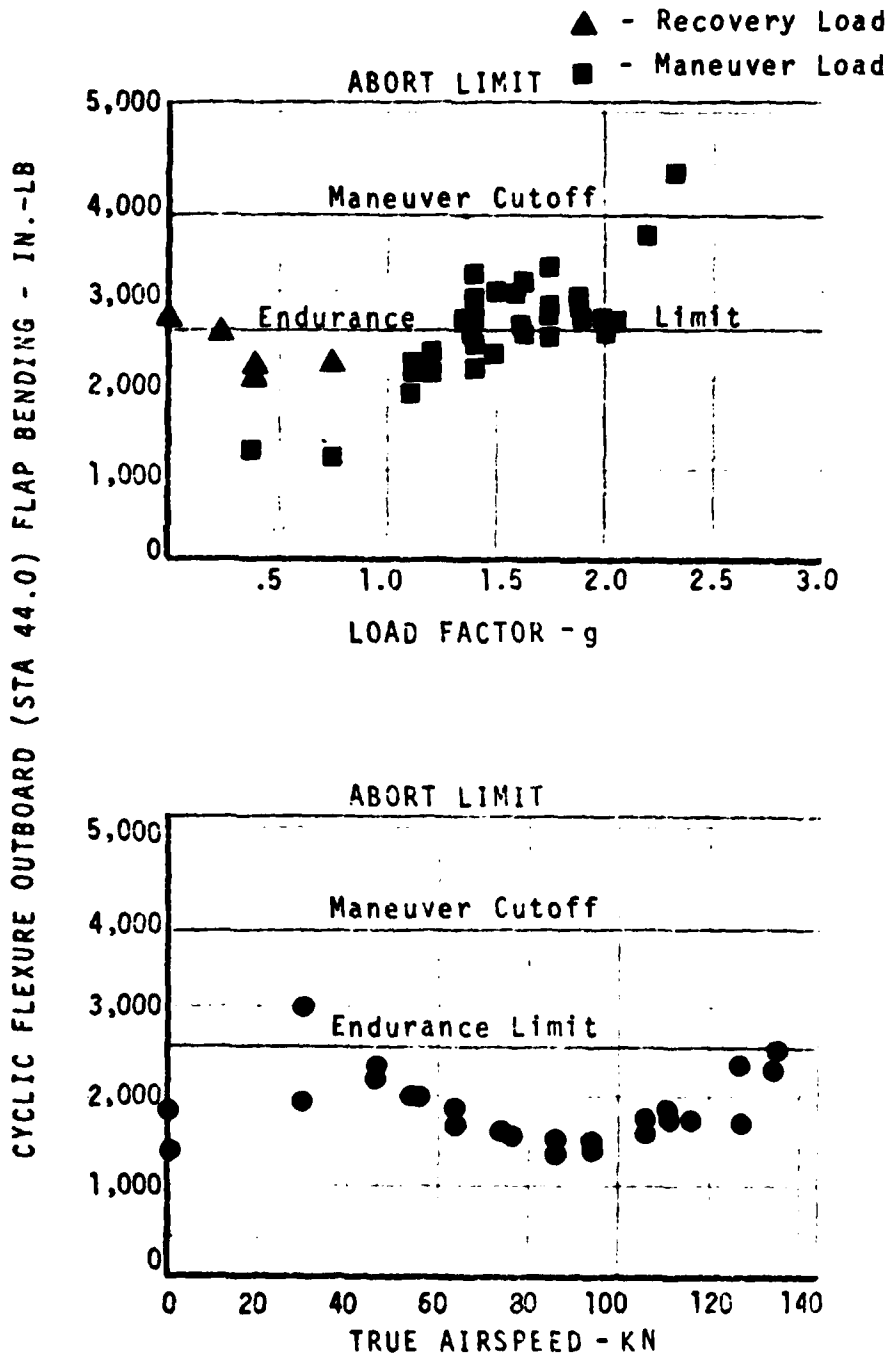

FIGURE 69. FLEXURE OUTBOARD FLAP BENDING VERSUS LOAD FACTOR AND AIRSPEED.

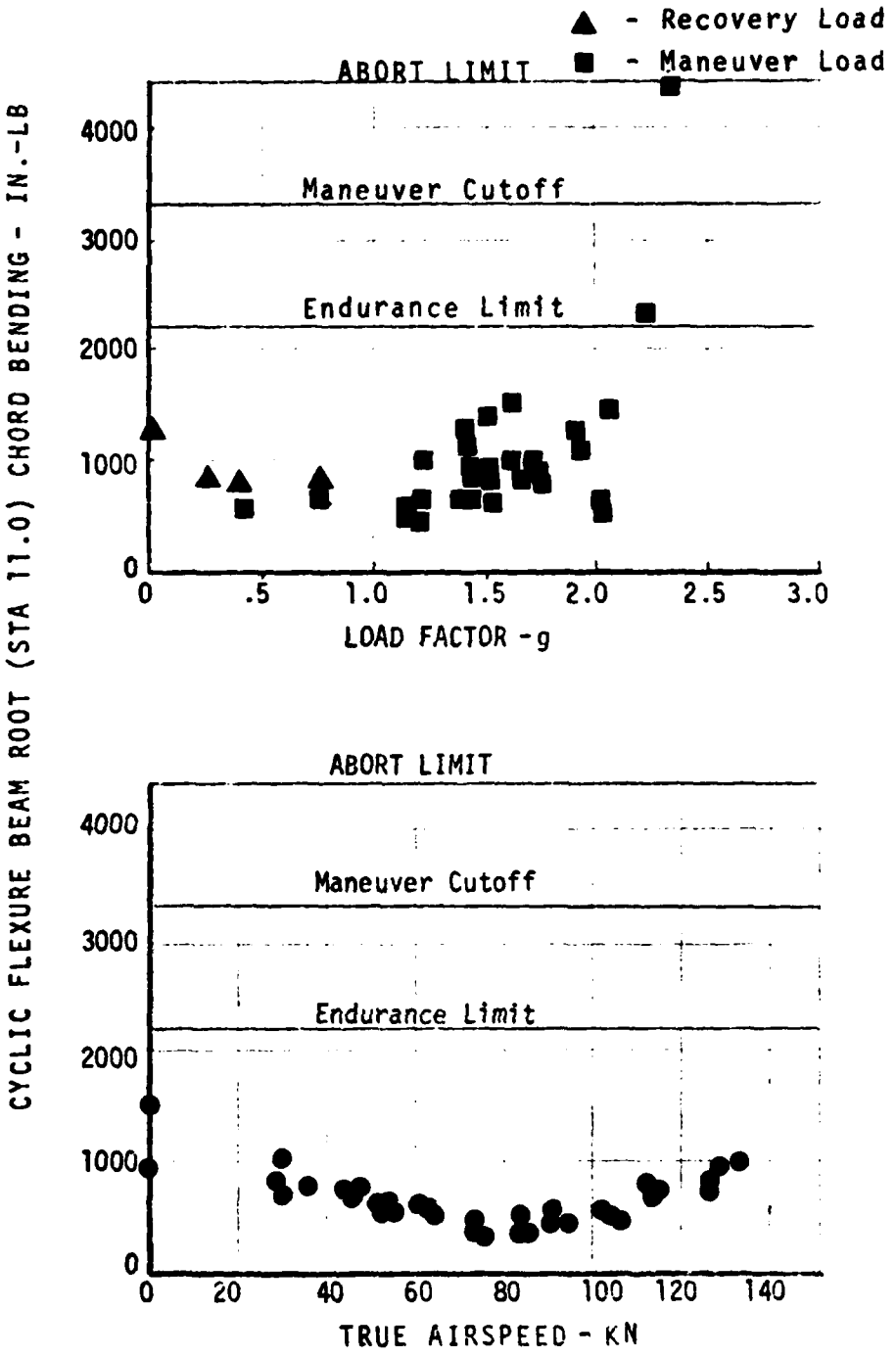

FIGURE 70. FLEXURE BEAM ROOT CHORD BENDING VERSUS LOAD FACTOR AND AIRSPEED.

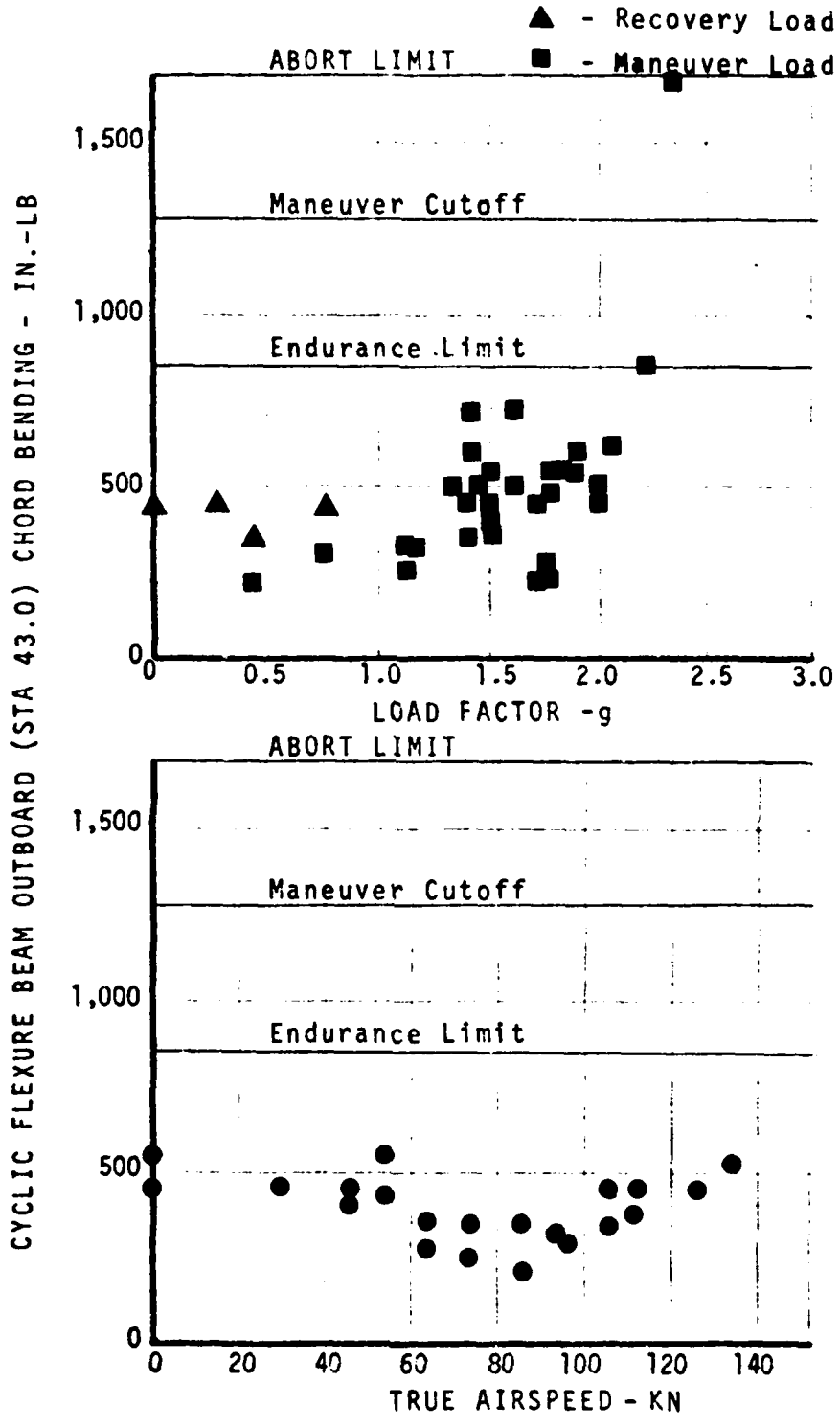

FIGURE 71. FLEXURE BEAM OUTBOARD CHORD BENDING VERSUS LOAD FACTOR AND AIRSPEED.

FLYING QUALITIES

Analysis of the data indicates that the flying qualities of the BMR configuration for the most part are very similar to those of the baseline standard BO-105. This was a design objective and expected, however, there are some areas where outstanding differences were noted. Some of these are readily explainable; others must remain speculative until future investigations can provide resolution.

Lateral and longitudinal controls appear to be displaced approximately 8 percent to the right and 10 percent forward, respectively, over the speed range as shown in Figure 72. This is believed to be simply a matter of rigging and would be rectified on future programs by adjusting the position of the control column at zero cyclic pitch input. Sidewards and rearwards flight envelopes were more restrictive for the BMR/BO-105 as compared to the baseline BO-105. Figure 73 shows the control positions as a function of rate of climb at 60 knots forward speed, which again shows the similarity between the baseline BO-105 and BMR-equipped aircraft characteristics. Figures 74 and 75 show typical data for control positions in right and left turns and symmetrical pushovers.

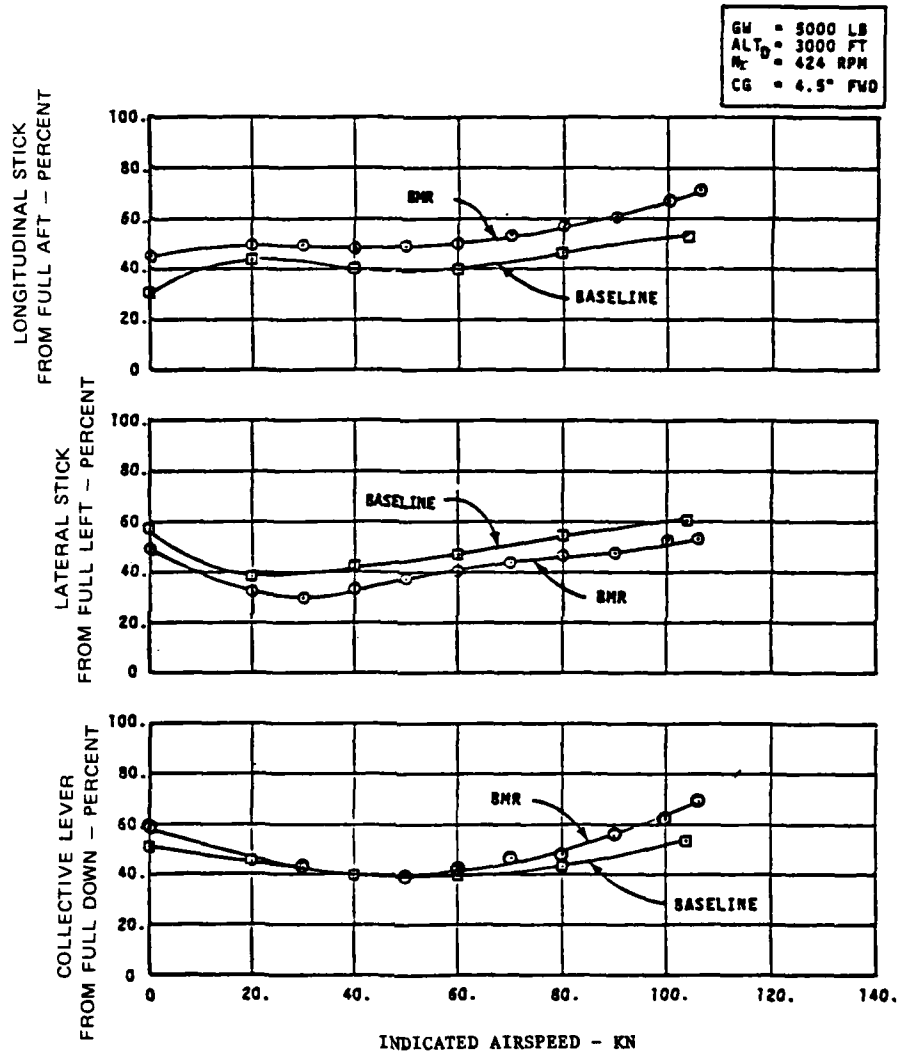

FIGURE 72. CONTROL POSITIONS AS A FUNCTION OF AIRSPEED IN LEVEL FLIGHT.

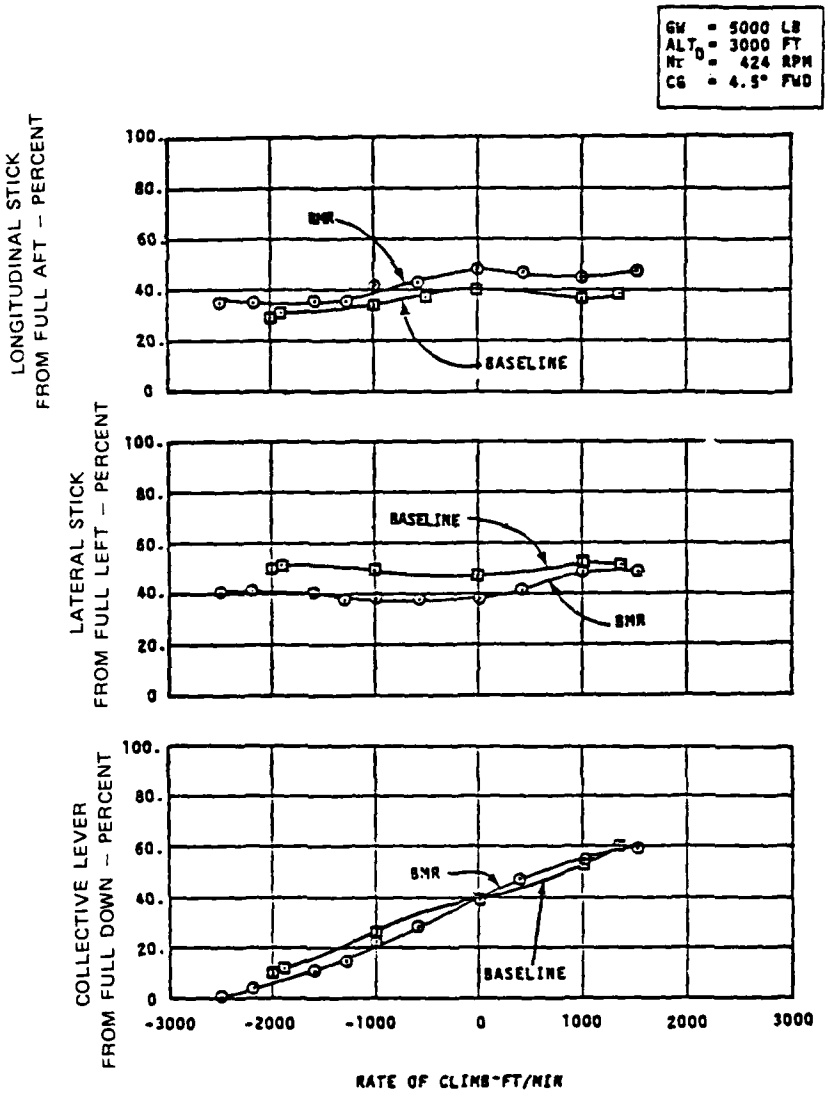

FIGURE 73. CONTROL POSITIONS AS A FUNCTION OF RATE OF CLIMB, IAS = 60 KNOTS.

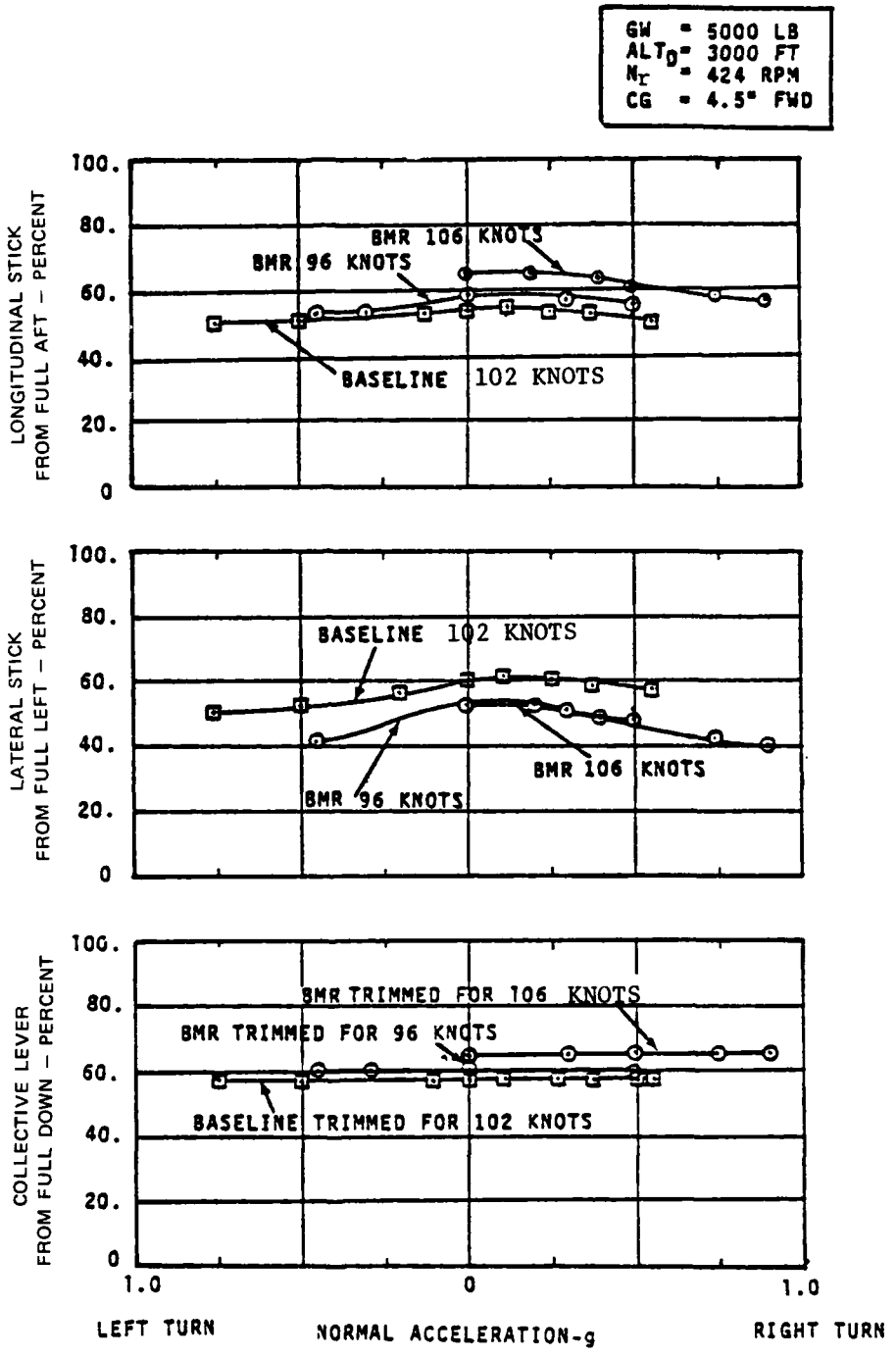

FIGURE 74. CONTROL POSITIONS AS A FUNCTION OF NORMAL ACCELERATION IN RIGHT AND LEFT TURNS, IAS AS SHOWN.

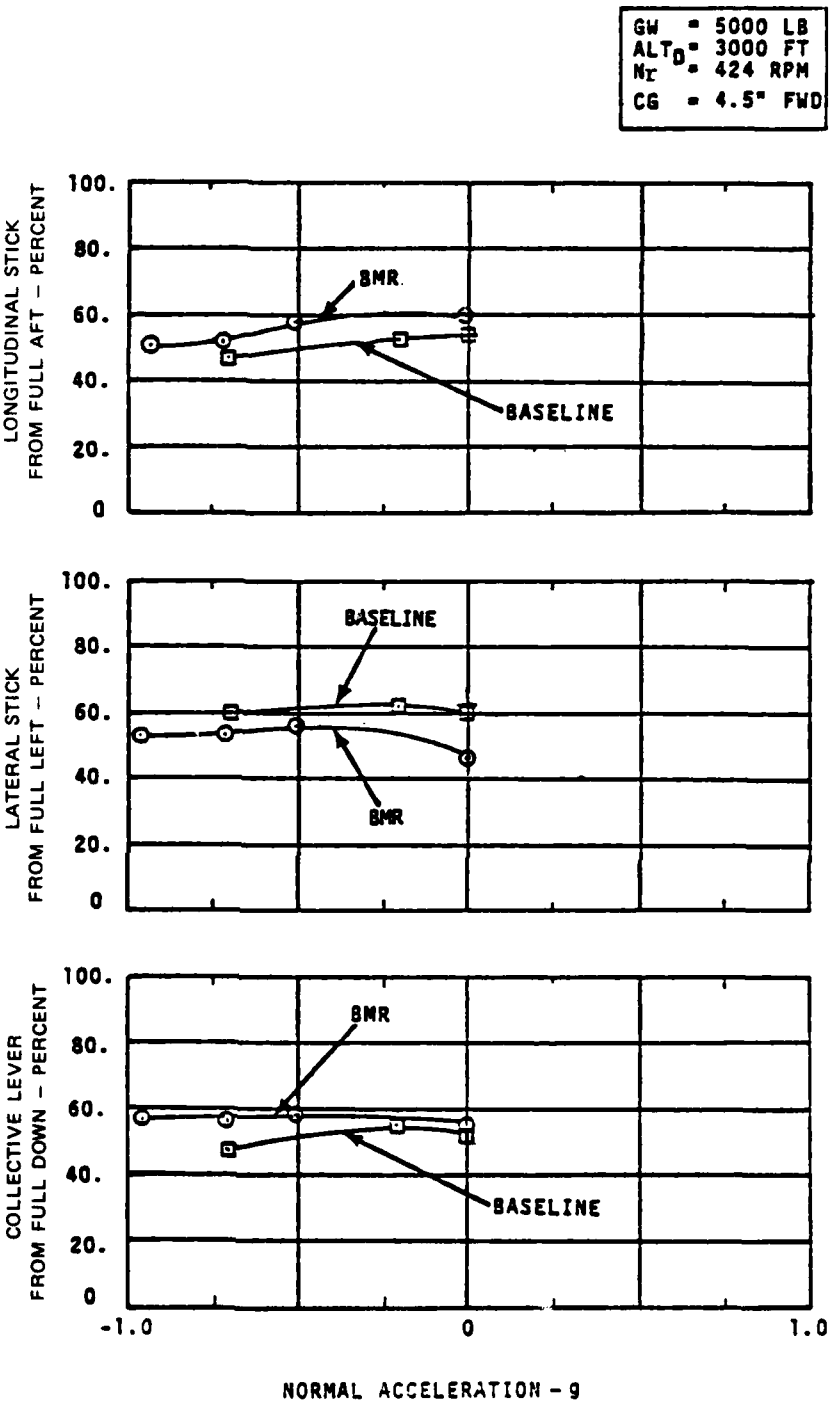

FIGURE 75. CONTROL POSITIONS AS A FUNCTION OF NORMAL ACCELERATION IN SYMMETRICAL PUSHOVERS, IAS = 100 Kn.

Probably the most interesting features of the BMR flying qualities were the much reduced blade pitch link load buildup during maneuvers as illustrated in Figure 76. Maximum pitch link loads on BMR maneuvers were less than one-half those of the baseline.

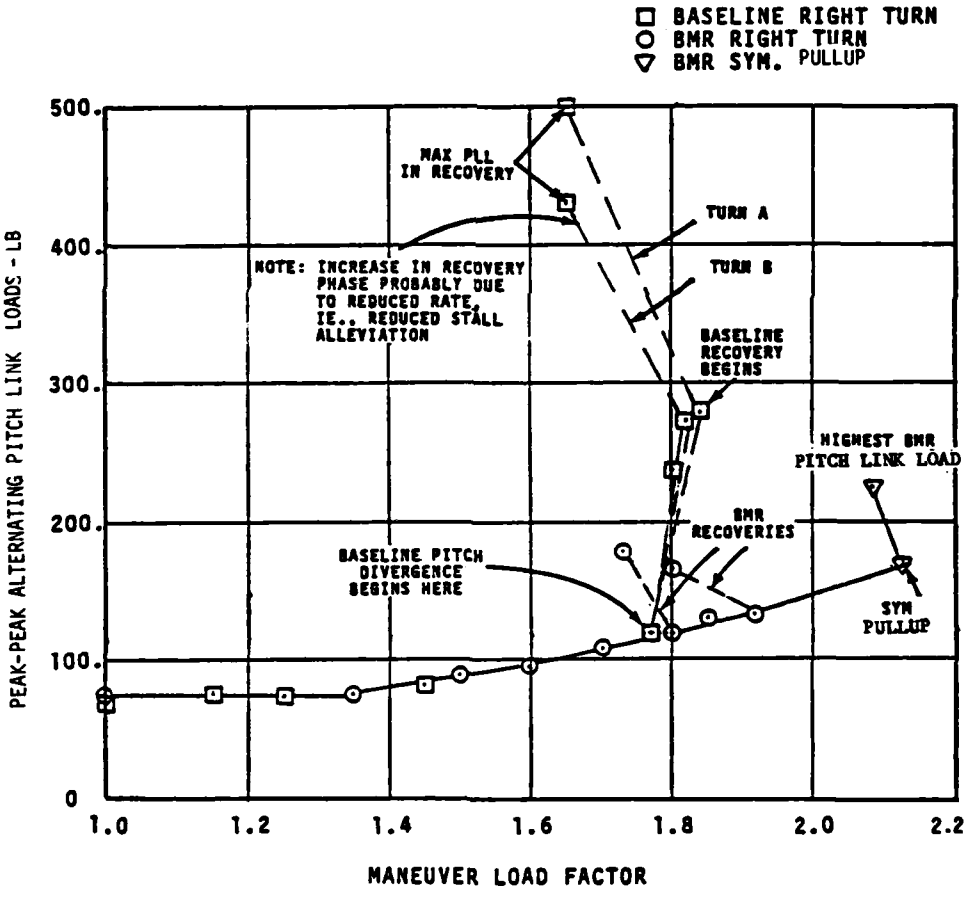

FIGURE 76. COMPARISON OF PITCH LINK LOADS DEVELOPED IN MANEUVERING FLIGHT WITH MANEUVER LOAD FACTOR, IAS = 95-100 KN, H_d = 3000 FT.

Another significant characteristic was the total absence of an aircraft pitch divergence, which was encountered on baseline flights at lead factors greater than 1. The flying qualities boundaries for the baseline aircraft are presented in Figure 77. The possibility of a relationship between divergence improvement and the greater control system flexibility (discussed later) of the BMR system should be considered in future analyses.

Pilot comment on improved dynamic stability and maneuver stability at cruise speeds are probably related to the improvement in pitch divergence.

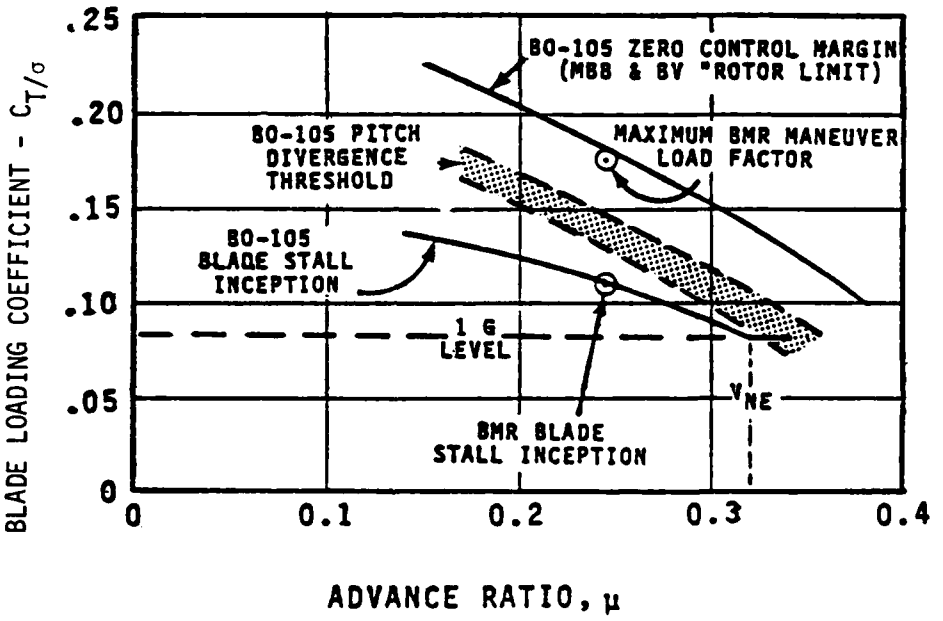

FIGURE 77. FLYING QUALITIES BOUNDARIES.

No other factor is evident in the comparative analyses of step and pulse time histories in level flight. Steps and pulses were not applied in accelerated flight conditions.

Effect of Control System Stiffness

Application of control system deflection test data (of which a typical example is shown in Figures 78 and 79) to the estimation of blade torsional deflections indicates that changes in control positions, compared to the baseline, are less than 2 percent of stop-to-stop travel over the flight test envelope due to the greater

torsional flexibility of the BMR control system. The deflection tests showed more nonlinearity, wider hysteresis, and greater closure error (Figure 80) for the BMR flight test program helicopter equipped with the 8-bar control linkage associated with the nonoperational improved rotor isolation system (IRIS) than for the production type two-bar control system (Figure 81). This explains the pilot report of greater workload with the BMR configuration, which exhibited to him a higher sensitivity and/or control response deadband as compared to his experience with a standard production BO-105 helicopter.

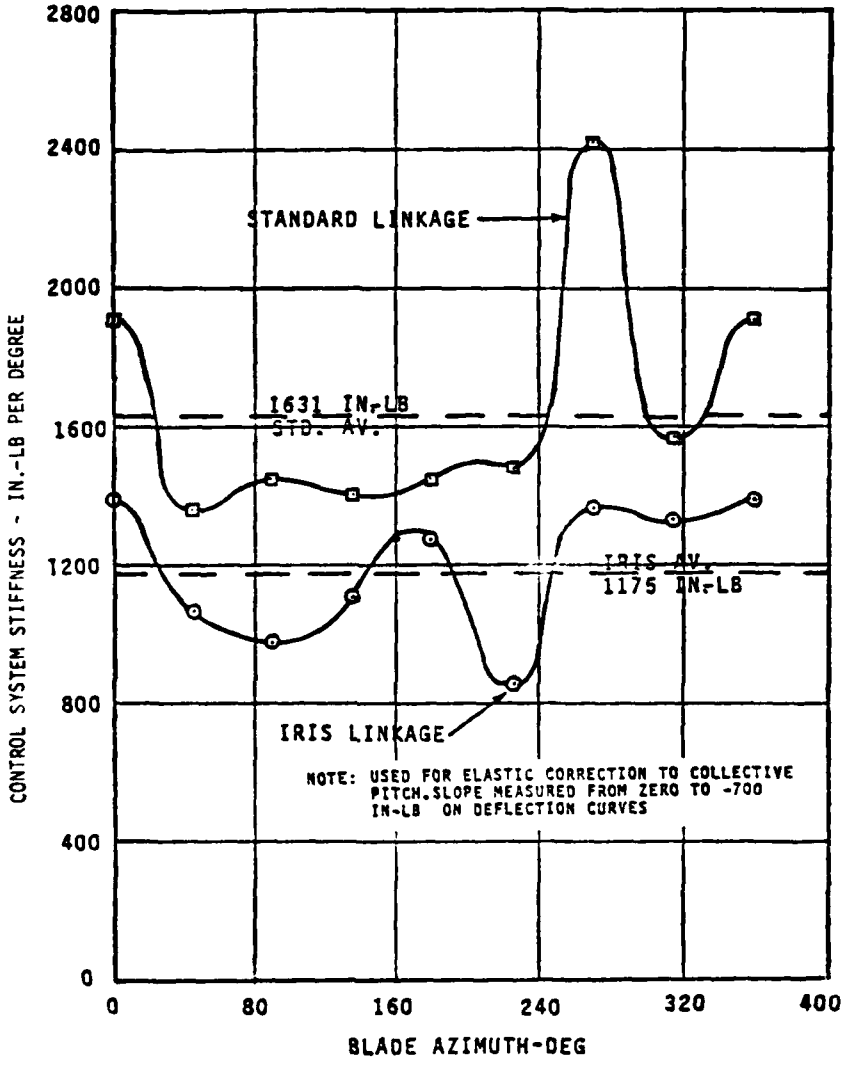

FIGURE 78. COLLECTIVE CONTROL SYSTEM STIFFNESS AS A FUNCTION OF BLADE AZIMUTH ANGLE, STANDARD AND IRIS LOWER LINKAGE.

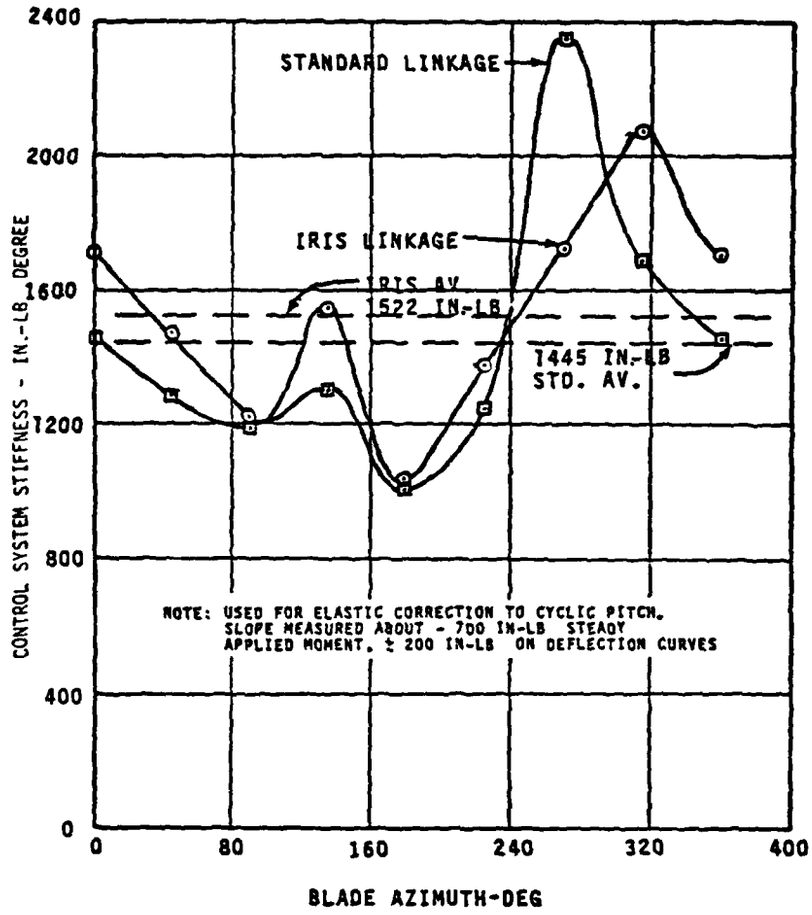

FIGURE 79. CYCLIC CONTROL SYSTEM STIFFNESS AS A FUNCTION OF BLADE AZIMUTH ANGLE, STANDARD AND IRIS LOWER LINKAGE.

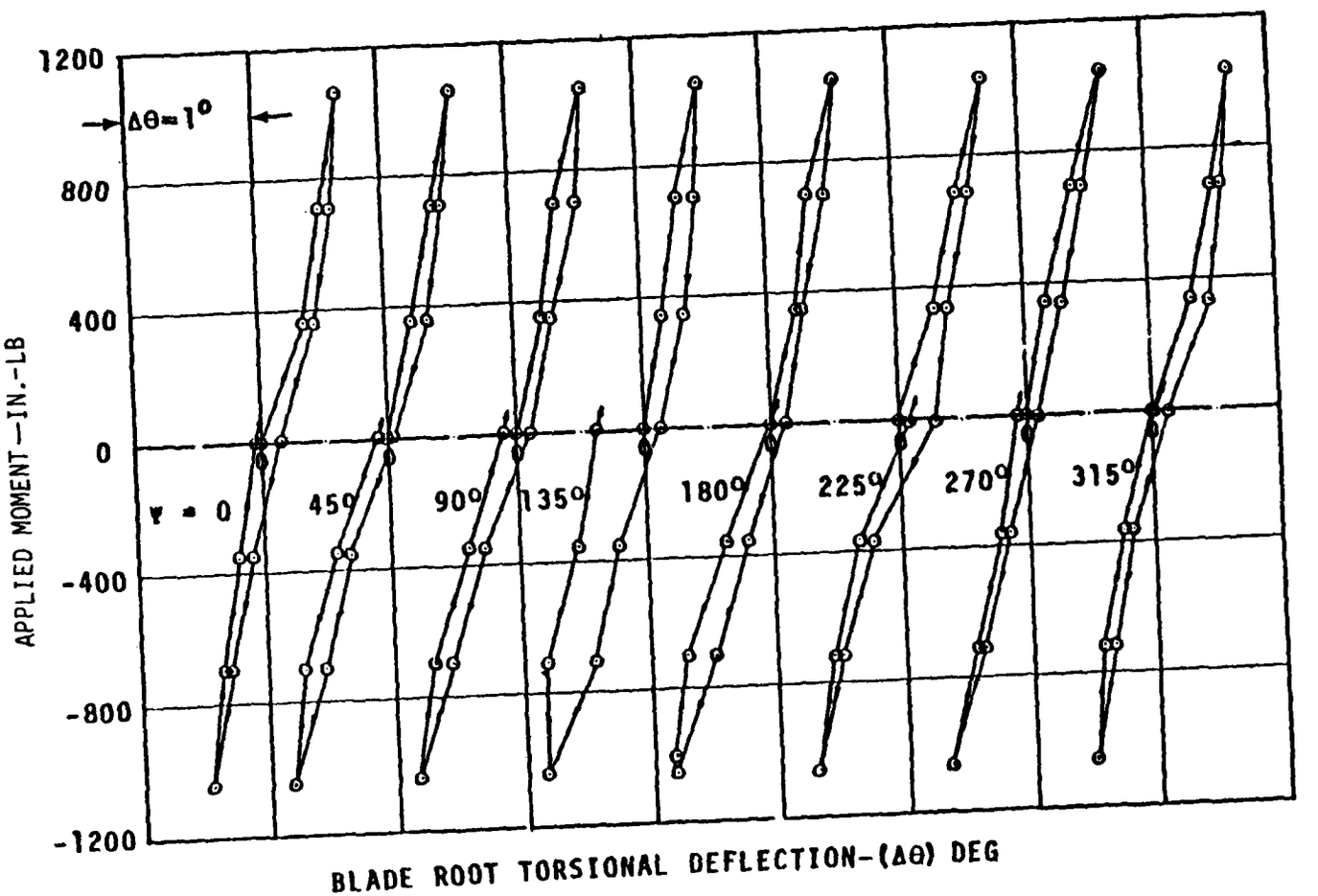

FIGURE 80. CONTROL SYSTEM DEFLECTION TEST - IRIS LOWER LINKAGE.

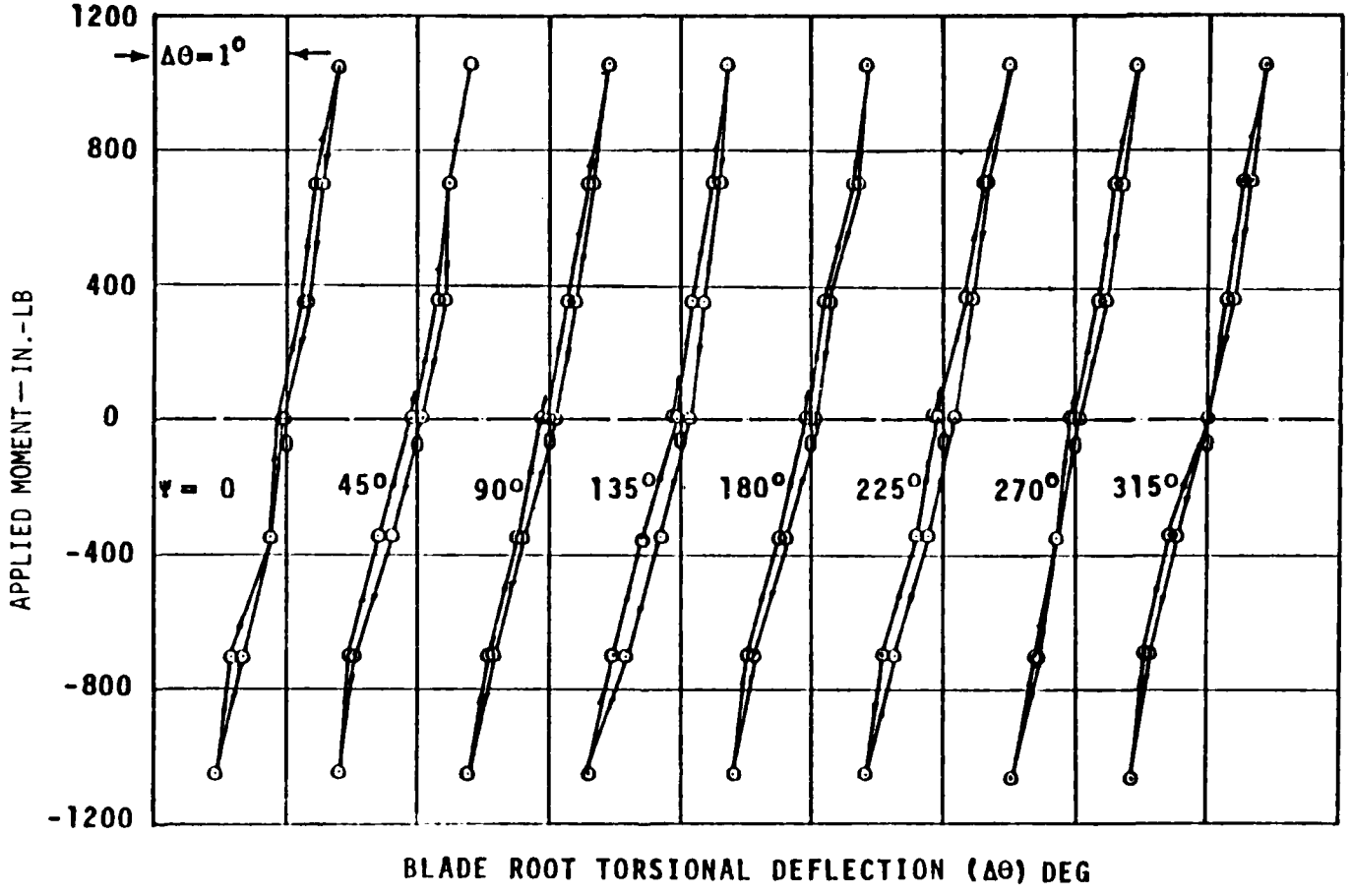

FIGURE 81. CONTROL SYSTEM DEFLECTION TEST - STANDARD LOWER LINKAGE (USED ON FLIGHT 230 ONLY).

VIBRATION

As stated previously in the Loads section, a characteristic of both the BMR and baseline BO-105 is the rise in vibration level between 20 and 30 knots forward speed in level flight and the slight worsening with low rates of descent at that speed. Experience with BO-105 indicates that the predominant vibration occurs at the blade passage frequency of 4/revolution and its second harmonic at 8/revolution. The data presented herein are restricted to these two frequencies.

A comparison of the baseline BO-105 and the BMR in level flight is presented in Figures 82 and 83, which show the variation in cockpit vibration level with forward speed. The 4/revolution level is generally higher for the BMR in the vertical and lateral modes; however, the baseline clearly has a higher vibration in the longitudinal mode. This modal vibration difference is also apparent for the 8/revolution frequency but both configurations suffer the same vibration level in the vertical and lateral modes. Additional data can be found in Reference 9.

The most severe vibration experienced with the baseline is known to be at low forward speeds and rates of descent. Figures 84 and 85 show how the level increases for the BMR configuration. Trends with change in rotor speed are also shown. The BMR and baseline test vehicle were equipped with the multi-linkage control system associated with the rotor isolation devices (IRIS) which were locked out for this test program. Flight 230 was conducted on the BMR-configured aircraft with the standard production control linkage installed. Figures 86 and 87 show that the control system has little effect on vibration level.

The comparison between the production version (without IRIS) and the BMR/BO-105 is presented in Figure 88, which shows that the BMR rotor system has done nothing to reduce the overall vibration level of the BO-105 aircraft.

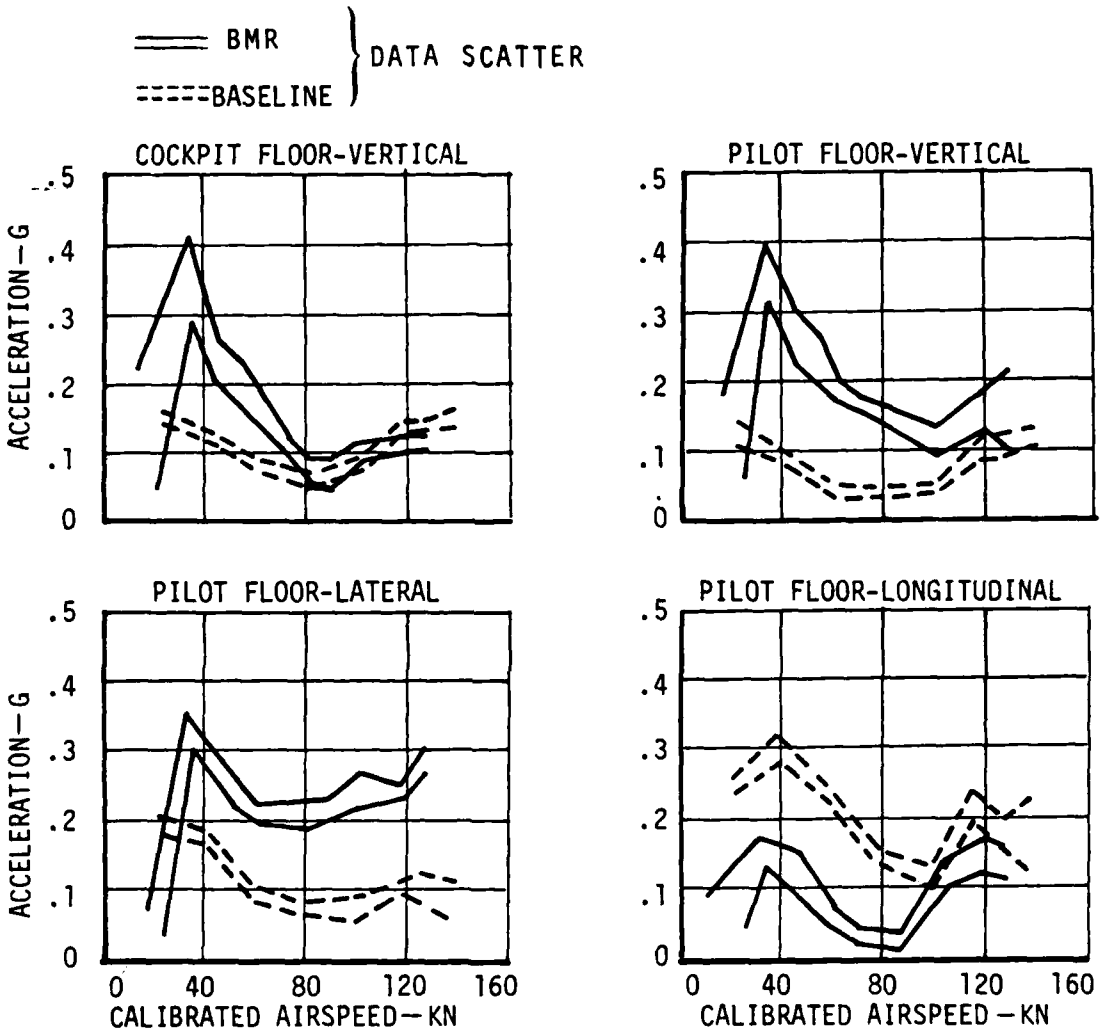

FIGURE 82. COCKPIT 4/REV VIBRATION, AIRSPEED SWEEP AT 425 RPM, BMR VERSUS BASELINE.

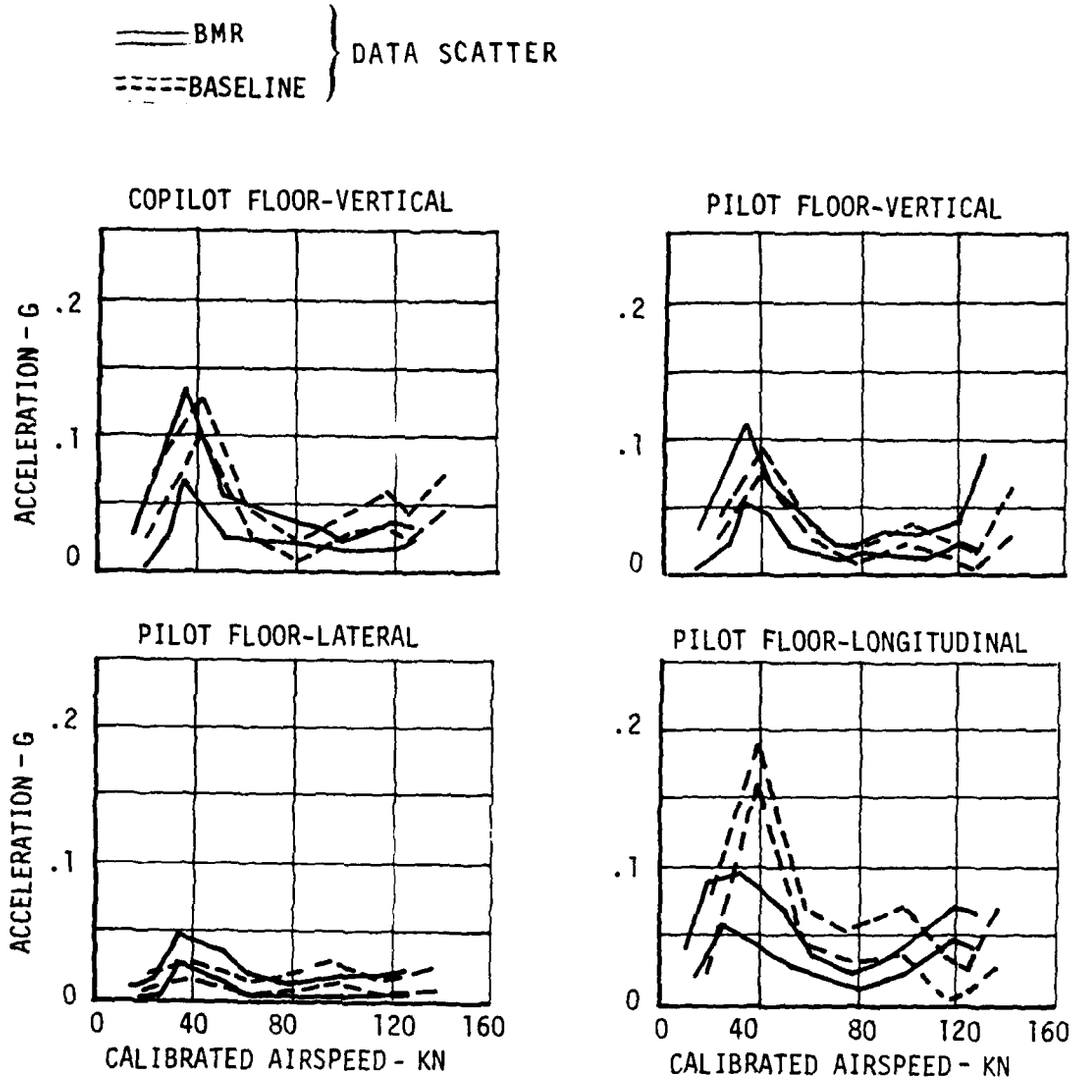

FIGURE 83. COCKPIT 8/REV VIBRATION, AIRSPEED SWEEP AT 425 RPM, BMR VERSUS BASELINE.

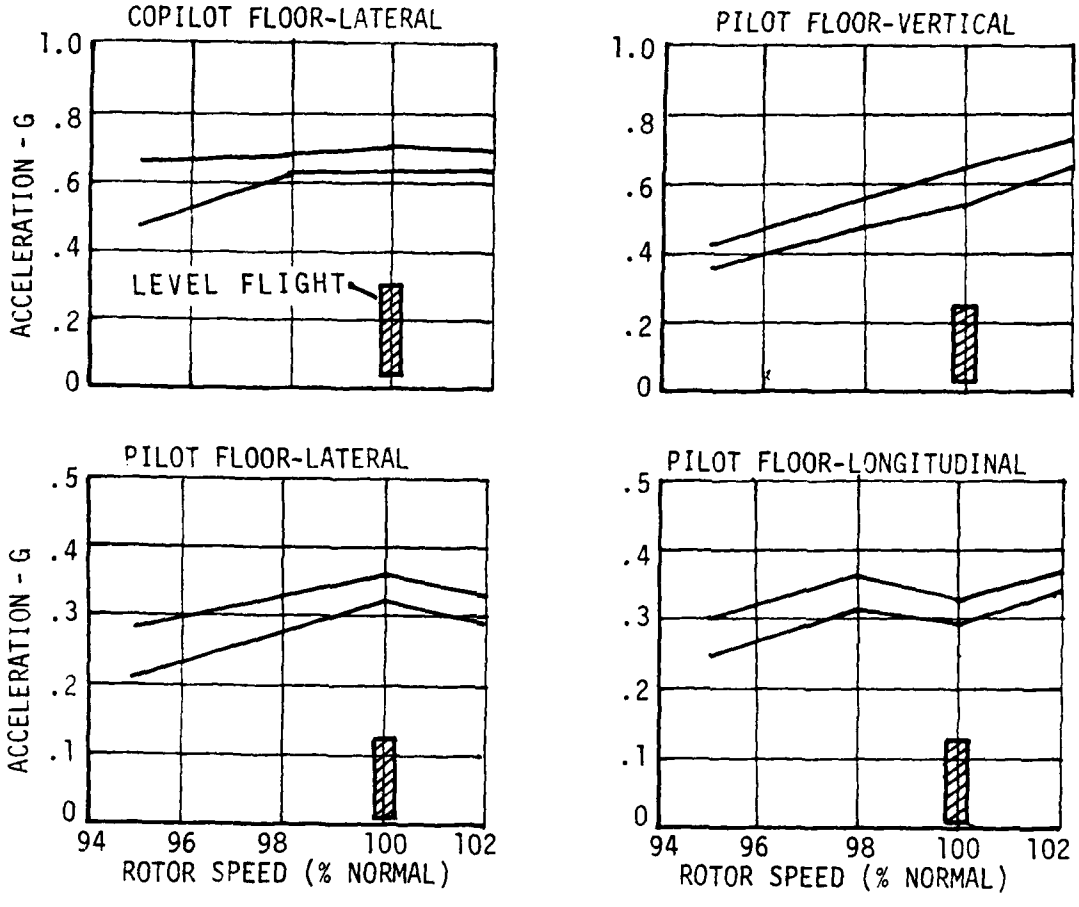

FIGURE 84. COCKPIT 4/REV VIBRATION, RPM SWEEP AT 20 KNOTS IN 500 FPM DESCENT. BMR CONFIGURATION.

NOTE: ENVELOPE OF DATA SCATTER SHOWN

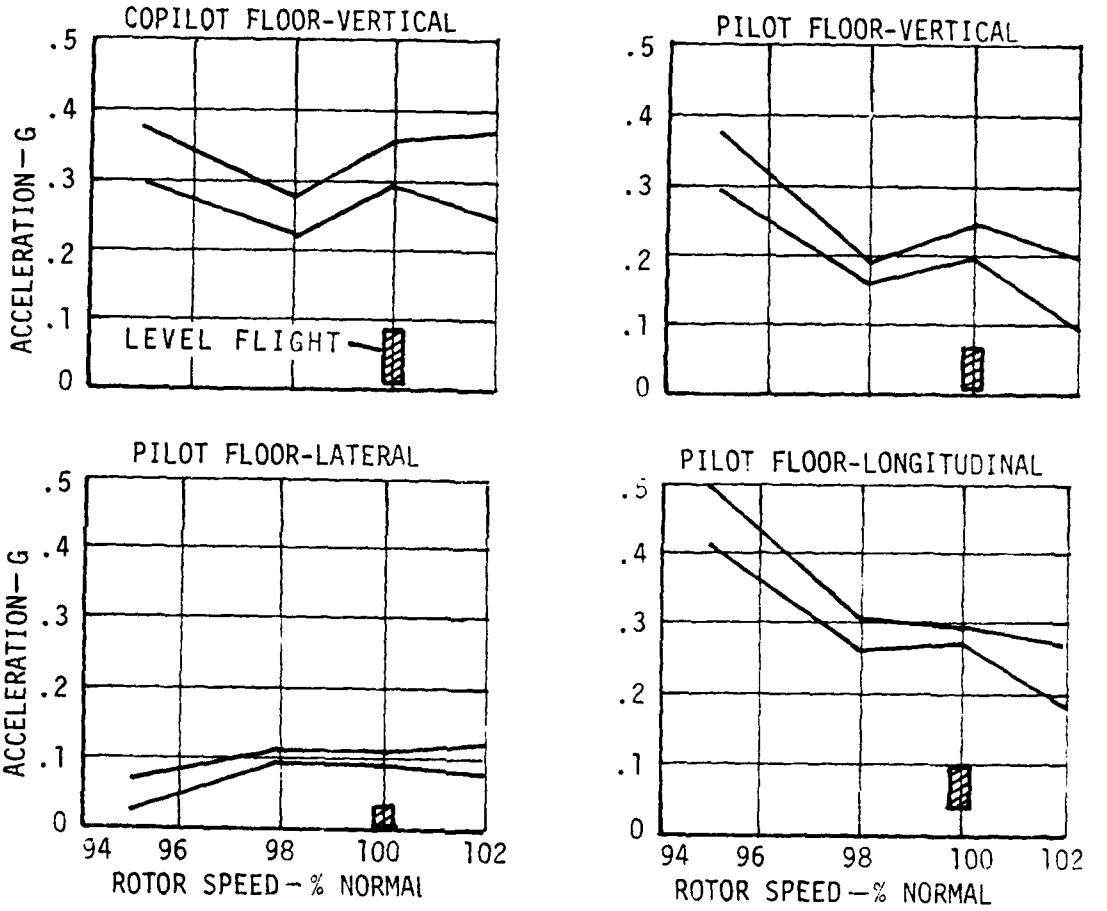

FIGURE 85. COCKPIT 8/REV VIBRATION, RPM SWEEP AT 20 KNOTS IN 500 FPM DESCENT. BMR CONFIGURATION.

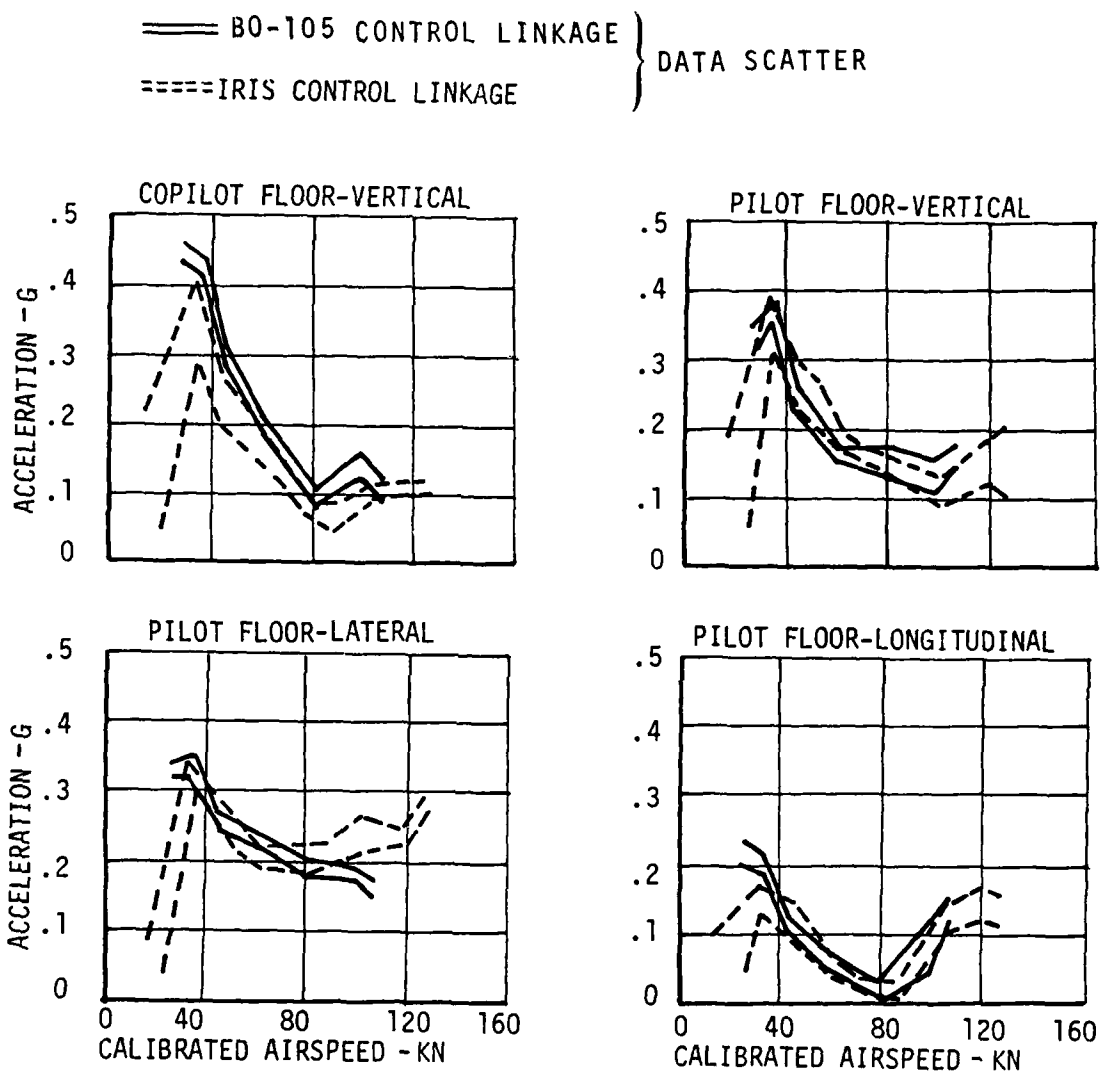

FIGURE 86. COCKPIT 4/REV VIBRATION, AIRSPEED SWEEP AT 425 RPM, BO-105 VERSUS IRIS CONTROL LINKAGE.

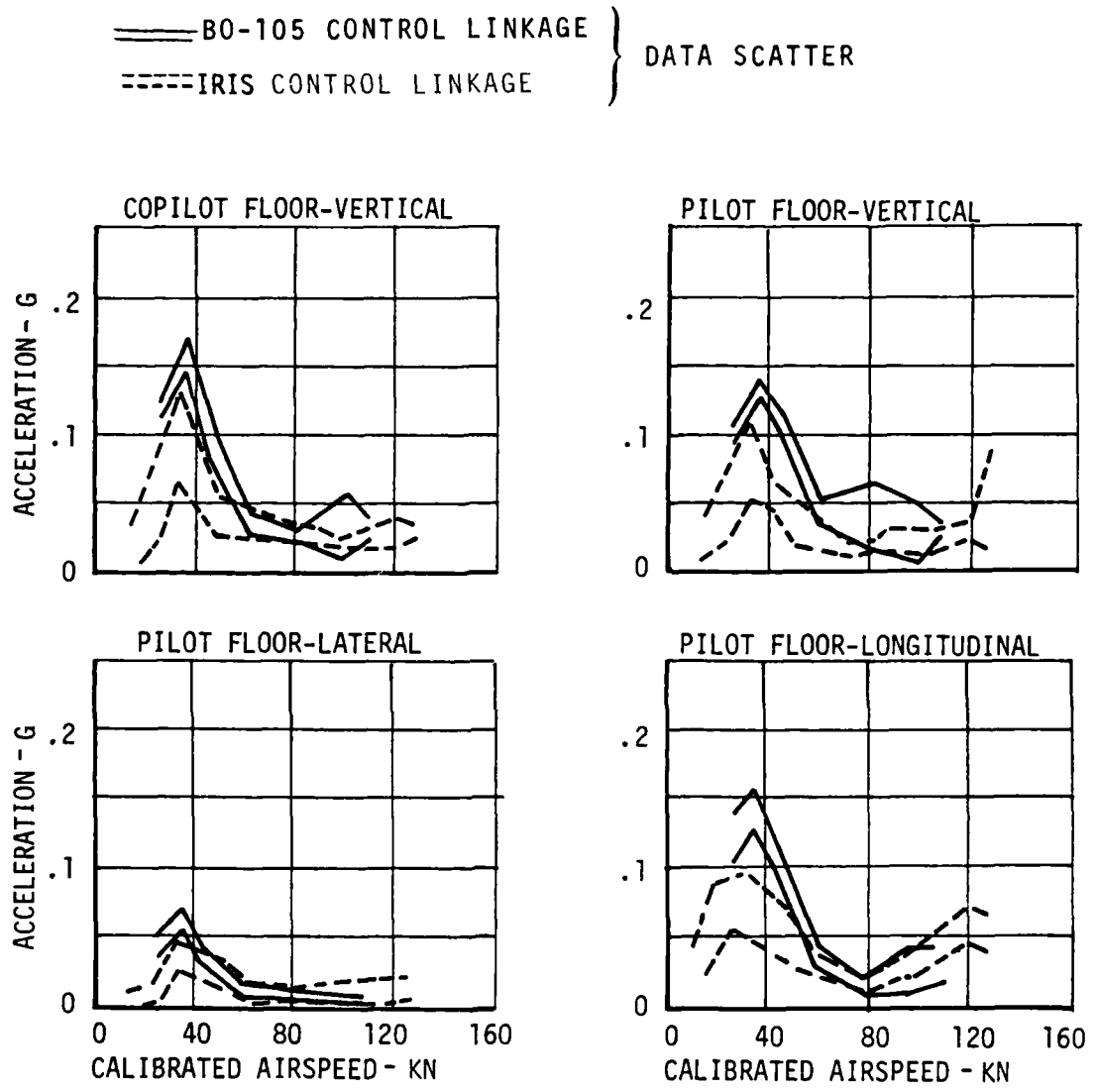

FIGURE 87. COCKPIT 8/REV VIBRATION, AIRSPEED SWEEP AT 425 RPM, BO-105 VERSUS IRIS CONTROL LINKAGE.

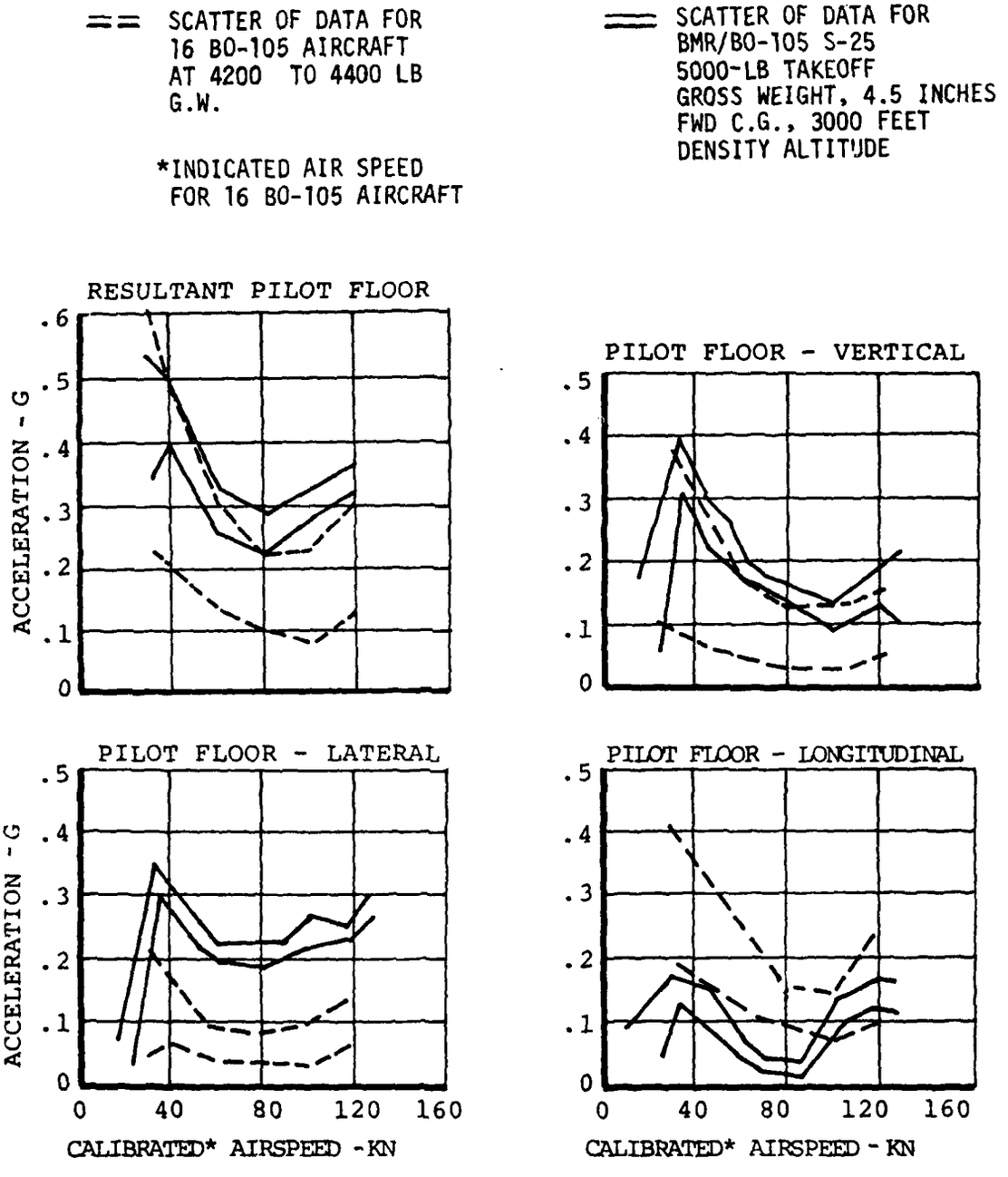

FIGURE 88. COCKPIT 4/REV VIBRATION, AIRSPEED SWEEP AT 425 RPM, BMR VERSUS SCATTER FOR 16 PRODUCTION BO-105 AIRCRAFT.

DISCUSSION OF RESULTS

In this section, the results of the BMR program are compared with analytical predictions and the achieved program objectives are discussed. An assessment of the potential of this BMR concept is made and specific technical problems and potential solutions are defined. A reassessment of a redefined bearingless main rotor system is then provided, based on the inclusion of those potential solutions.

RESULTS COMPARED TO PREDICTIONS

Stability

The level of ground stability of the BMR/BO-105 aircraft, equipped with the basic unmodified landing gear, proved disappointing in the preliminary tests. Potential instabilities were encountered that were not present in the qualitative assessment of the baseline aircraft, nor in the analytical predictions in which the BMR rotor system was modeled to include all known characteristics. Analytically, it was assumed that the landing gear would achieve four-point contact with the ground immediately on touchdown and that the respective four landing gear spring systems were fully effective. A much more accurate analytical representation is required to model the true sequence of landing events, which are not consistent. However, a typical sequence may be right rear skid, left rear skid, right front skid and, lastly, left front skid, which is suggested by recordings from landing gear stiffening brace tension instrumentation together with external and pilot observation. Initial predictions also regard pitch as the primary mode, but ground shake tests reported in Reference 9 identified strong coupling with a longitudinal translational mode.

Further attempts at a more accurate representation of the landing gear characteristics using the elastomeric torsion spring gear/fuselage supports, shown in Figure 18, were made with moderate success. Damping levels were predicted to be higher than measured (Figure 89) even after stiffening of the landing gear to raise the critical resonant frequency.

Figure 89 compares the ground resonance stability test data with analytical predictions. Reasonable agreement at zero collective pitch is obtained over the rotor speed range; however, the analysis fails to predict the marked decrease in stability over a narrow range of intermediate collectives where the landing gear may not have full four-point contact with the ground. This "bucket" is charac-

teristic for all rotor speeds tested and is more severe for the unstiffened landing gear and softer turf surface where it occurs at a lower collective range, thus resulting in lower damping and in some cases, potential instability.

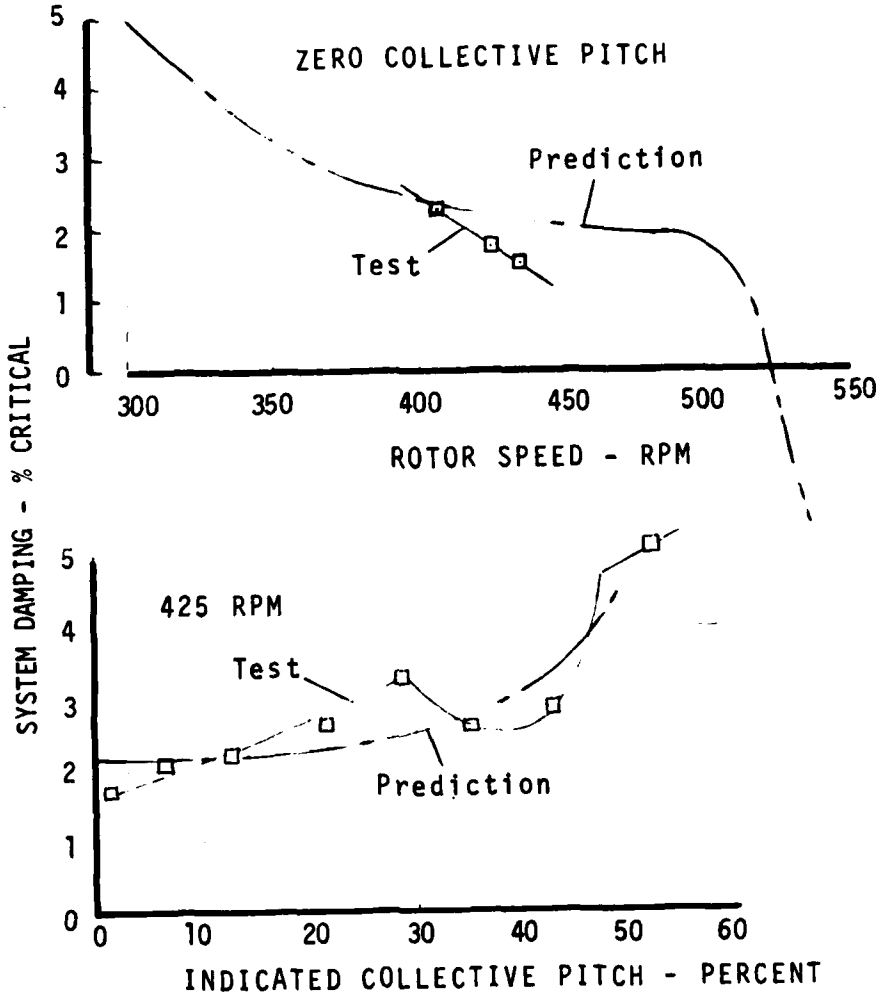

FIGURE 89. DAMPING VERSUS INDICATED COLLECTIVE PITCH AND ROTOR SPEED COMPARISON WITH ANALYTICAL PREDICTIONS. CONCRETE SURFACE AND GROUND RESONANCE MODE.

Hover air resonance predictions are more straightforward. Figure 90 presents those comparisons that show good agreement.

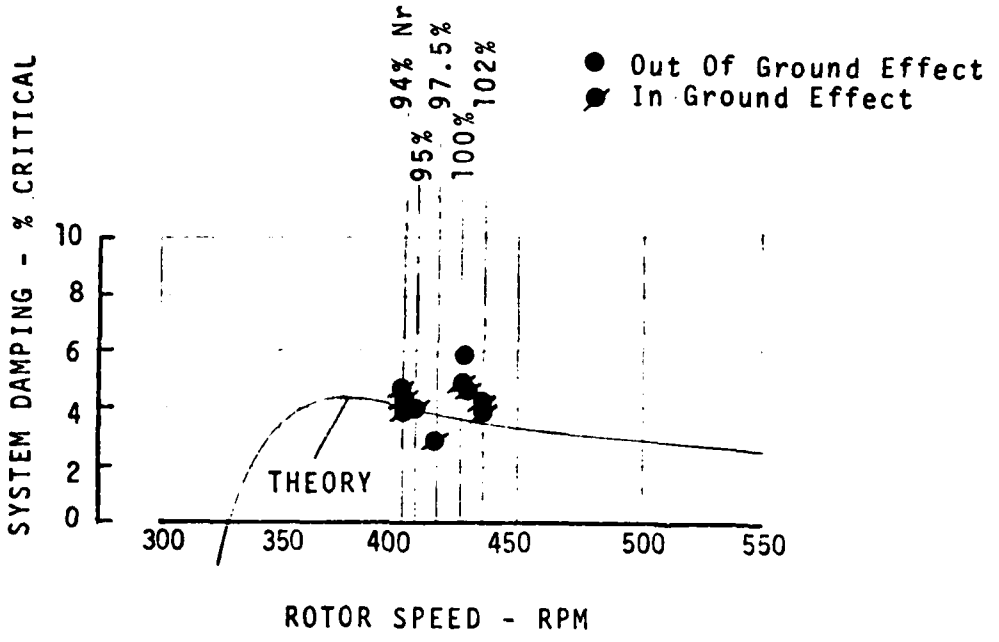

FIGURE 90. DAMPING VS. ROTOR SPEED. COMPARISON BETWEEN TEST AND ANALYTICAL PREDICTION FOR AIR RESONANCE IN HOVER.

The available analytical tools were unable to predict stability in forward flight regimes.

A design objective for the BMR was to make the physical characteristics of the system as close to the BO-105 as possible in order to result in like dynamic characteristics and retain some of the inherent stability of that system. It can be concluded, from the evidence presented in this report, that the overall stability level of the BMR is not as high as the baseline BO-105. Even with the configuration similarities, inescapable differences still remain.

1. By definition, the BMR does not have the inboard feathering bearings of the BO-105 and since the effective hinge for the BMR occurs outboard of the flap and lag equivalent hinges, the stabilizing coupling between the bending and feathering modes is somewhat different than the BO-105 with its pitch/flap/lag equivalent hinge sequence.

2. The coupling referred to above, for the BO-105, results from the relative displacement between the torsional axis of the deflected blade and the axis of the feathering hinge. This offset is maintained in the BMR through a pre-droop angle at the radial location of the torsion hinge at the junction of the blade and flexure, but blade deflections outboard of that station can add to or subtract from the built-in pre-droop effect, hence different stability characteristics.

Figure 91 compares the systems and shows how lag torsion coupling is reduced at low thrust due to reduction in blade-to-feathering-axis offset by the negative blade displacements. Conversely, for the BO-105, minimum lag/torsion coupling is expected to occur at 1 g thrust collective (minimum deflection) and to increase as thrust is increased or decreased. The difference in control system stiffness for the two configurations will also result in differences in the degree of this type of mechanical coupling.

3. The BO-105 rotor blade is retained in a root clamshell socket against chordwise bending. With axial strains in the root loop fibers, due to centrifugal force, the root composite material is known to shrink chordwise and the rigidity of the root chord bending restraint is reduced, which allows motion in the socket that results in chordwise friction damping. The two-pin retention systems used in the BMR preclude this motion and the resultant additional stability therefrom. Nonrotating/rotating equivalent viscous damping for the BO-105 and BMR have been estimated from bench and flight test data to be of the order of 3 percent/3 percent and 1 percent/ 0.75 percent, respectively.

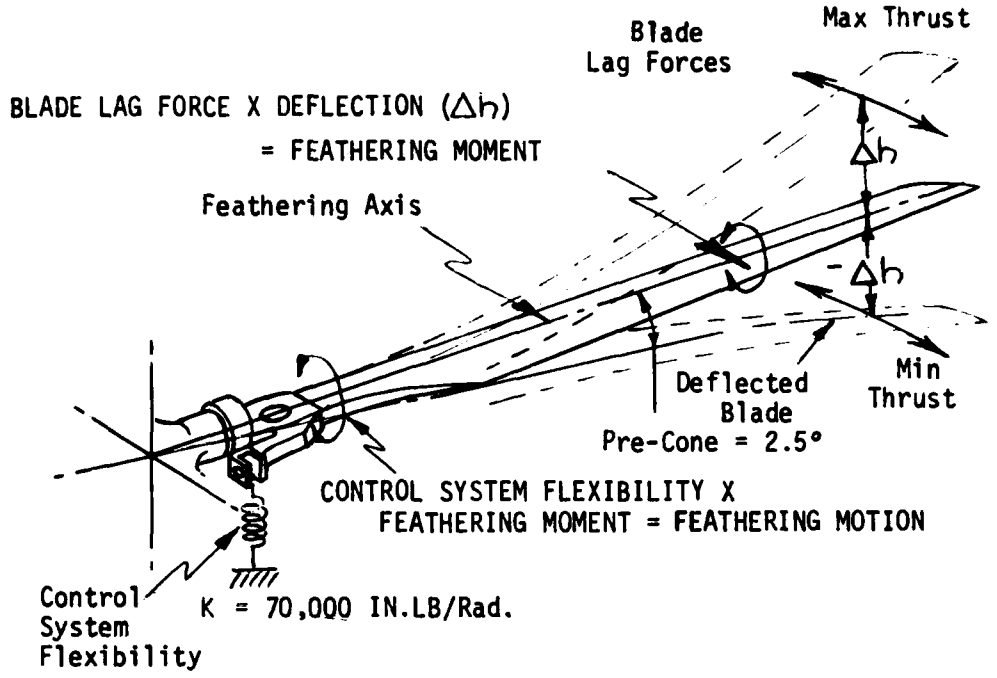

BO-105 ROTOR

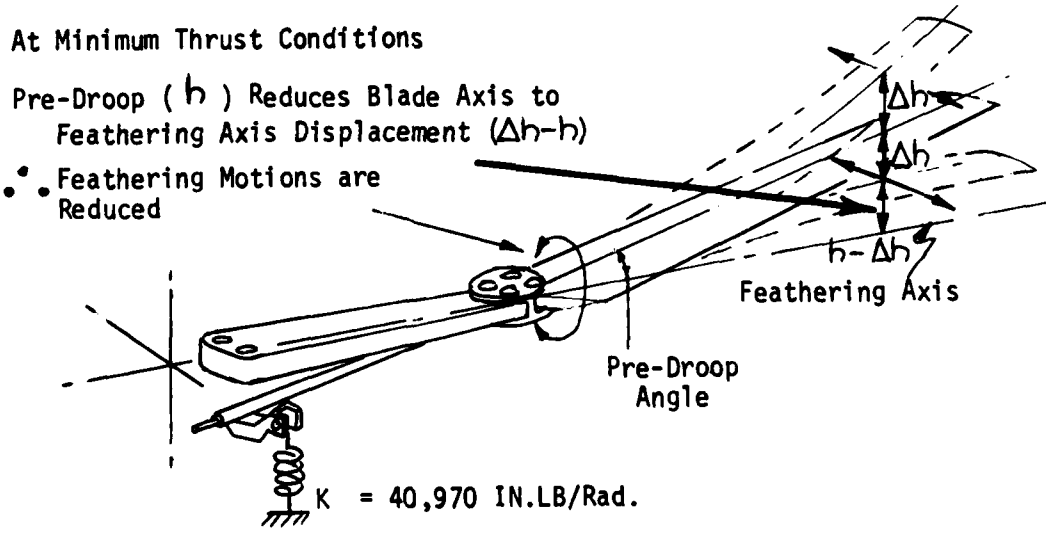

BMR ROTOR

FIGURE 91. LAG/TORSION COUPLING IN THE BO-105 AND BMR ROTOR SYSTEMS.

Structural Loads

As expected, measured shaft bending moments agree with BO-105 based predictions very well, as shown in Figure 92. Similar success is achieved with the flexure and blade flap bending moment distributions shown in Figure 93, for which the loads analysis was used.

Figure 94 presents analytical versus test data for chord bending moments. This shows how the steady bending moments are developed and that improvement is needed. One possible cause for the mismatch for flexure data is the calculation for neutral axis offset in each of the two beams, resulting in high steady local chord bending induced by centrifugal force loads. The local moments cause the beams to bend asymmetrically about the central radial axis of the flexure and thus the problem equation is nonlinear.

Fatigue data has been plotted irrespective of sign; therefore, reasonable agreement between test and theory is presented.

For the blade pitch control system, collective actuator loads have been shown to be predictable in Figure 59, which is also the case for pitch control torque tube flap bending, shown in Figure 95. However, torque tube chord bending was always unexpectedly above the predicted level as shown in Figure 96. Further understanding of the mechanics of the system is required, possibly through the use of much modified C-60 loads analysis or extensive NASTRAN modeling.

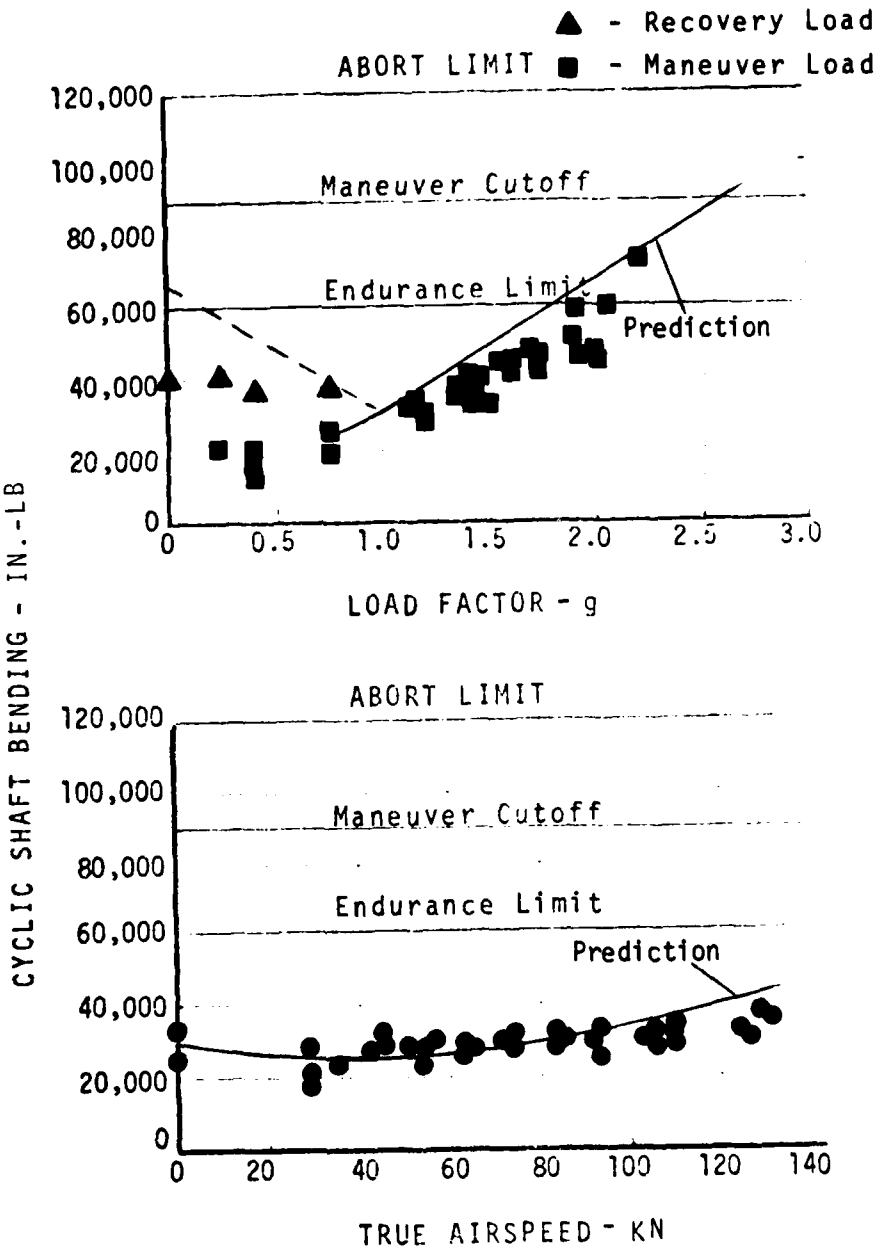

FIGURE 92. SHAFT BENDING MOMENTS VERSUS LOAD FACTOR AND TRUE AIRSPEED. THEORY AND TEST.

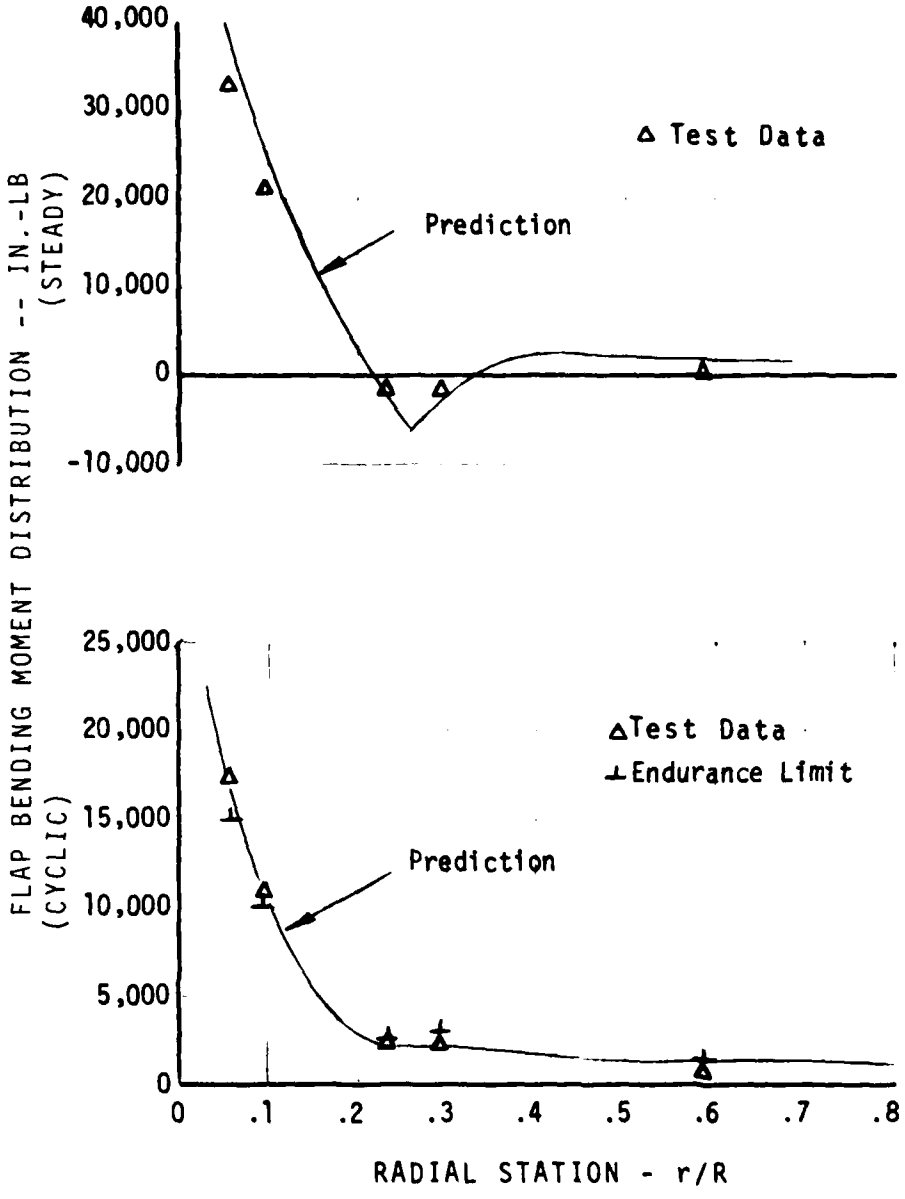

FIGURE 93. FLAP BENDING MOMENT DISTRIBUTION VERSUS RADIAL STATION FOR 2g STEADY TURN - THEORY AND TEST.

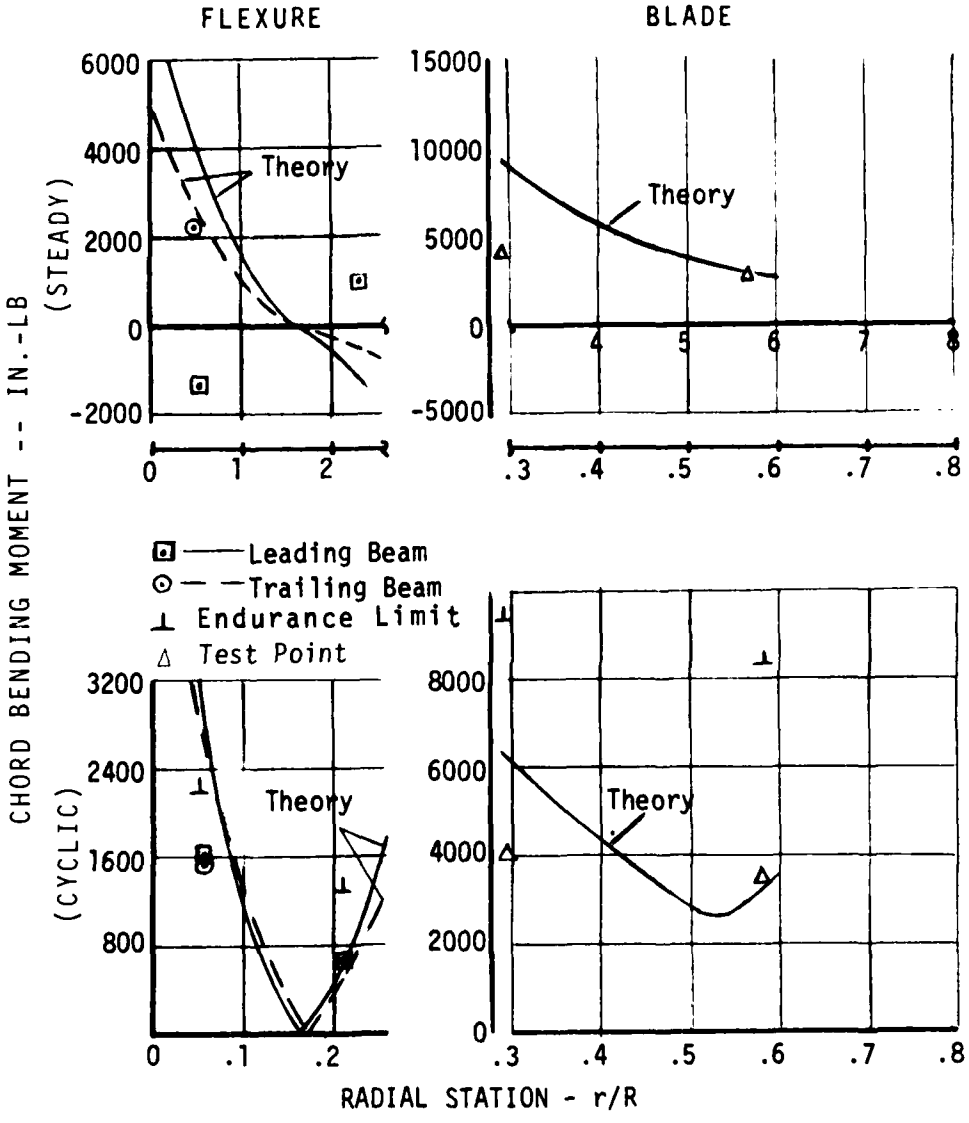

FIGURE 94. CHORD BENDING MOMENT DISTRIBUTION VERSUS RADIAL STATION FOR 2g STEADY TURN - THEORY AND TEST.

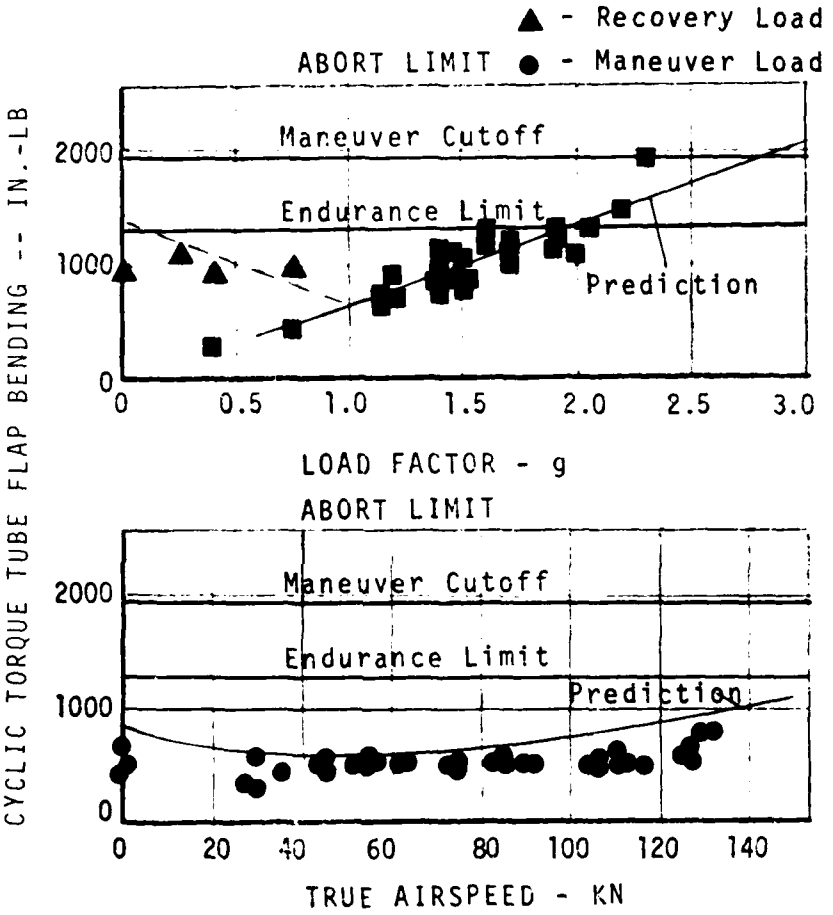

FIGURE 95. TORQUE TUBE FLAP BENDING VERSUS LOAD FACTOR AND TRUE AIRSPEED THEORY AND TEST.

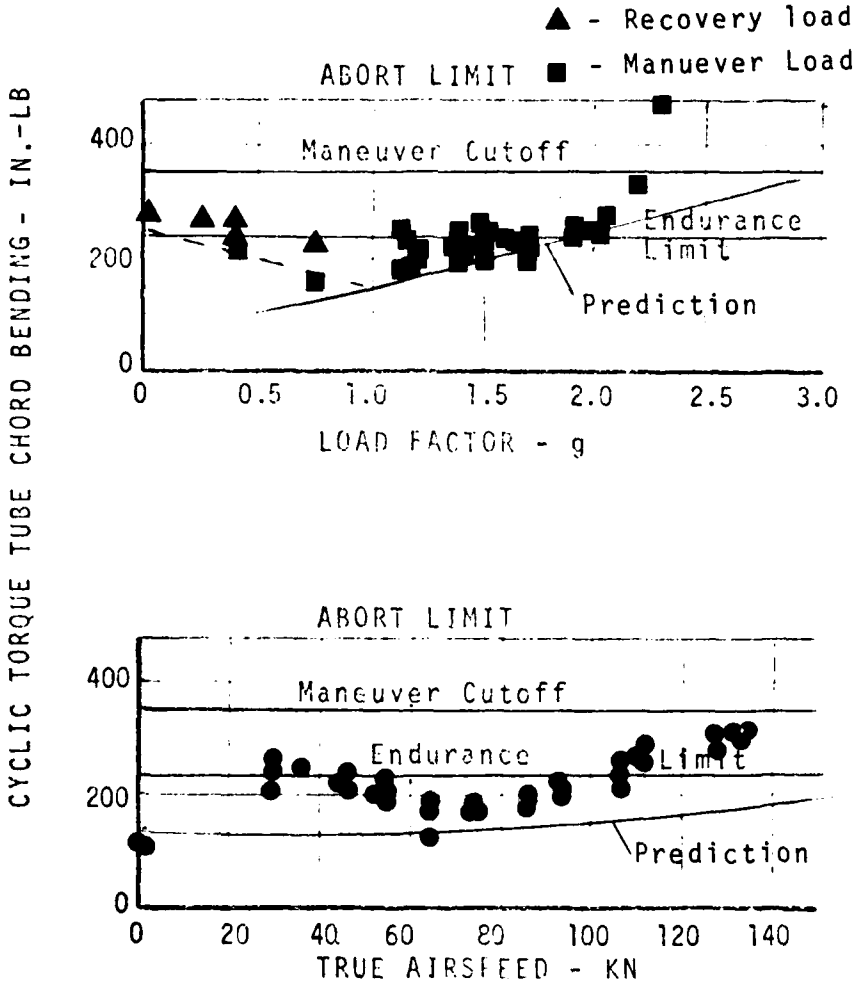

FIGURE 96. TORQUE TUBE CHORD BENDING VERSUS LOAD FACTOR AND TRUE AIRSPEED - THEORY AND TEST.

ASSESSMENT OF POTENTIAL

An assessment of the bearingless main rotor was conducted in September 1976 and is reported in Reference 3. The results of the flight test program have verified the findings of that assessment insomuch that the BMR is stable, not structurally limited for the flight envelope flown, and has vibration levels and flying qualities similar to the baseline BO-105; however, the ground resonance stability was not up to expectations. The following section discusses technical inadequacies of this configuration and proposed probable solutions, and reassesses the potential of the system with changes incorporated.

PROBLEMS AND SOLUTIONS

1. Analysis. Foremost of the technical inadequacies is the inability to accurately predict the stability of such a system on the ground, together with the inability to predict the degree of stability in forward flight, climb, and descent at this time. Major weaknesses in the analysis are the assumption of 1 percent critical structural damping, employing the virtual hinge analogy, and inadequate modeling of the landing gear. Therefore, continued development of the analysis for stability prediction in which the virtual hinge analogies have been replaced by the more fundamental model approach is needed. Sophisticated experimentation is required to determine the true structural damping within the system.

The dual beam configuration requires more sophisticated loads analysis to more accurately predict the steady chordwise moment distribution in each of the two beams together with that component of the blade root moment which is transmitted inboard down the two beams and the torque tube.

To assist in the development and to verify the isolated rotor stability predictions in hover and forward flight, whirl tower and/or full scale wind tunnel tests should be conducted on both the BMR and BO-105 rotor systems.

2. Vibration and Handling Qualities. In the interests of a successful program, the dynamic criteria for the BMR rotor design were those characteristic of the standard production BO-105 rotor system. The BMR, therefore, has contributed nothing to improving the handling or vibration qualities of the BO-105 configuration. The inherent characteristics are due to the retention of the flapwise mode characteristics such as frequency and virtual hinge offset.

Understanding what is required to improve the handling and vibration qualities of the BO-105 is vital to achieving a successful BMR design.

The aircraft handling and vibration characteristics could be improved by designing and structurally substantiating modified blade root beam flexures with a virtual flap hinge offset less than 10 percent of rotor radius. The effects on stability should be demonstrated through scaled model wind tunnel tests, full scale whirl and wind tunnel tests, and finally through flight testing. The effect of the changes on flying qualities and vibrations should be demonstrated through full-scale flight tests.

3. Stability. Analysis, whirl tests, and flight testing have all shown that stability is affected by structural damping augmented by the aeroelastic damping produced by the lag/flap and lag/torsion coupling. The latter is most significant and results from the inclination of the blade axis (Figure 91) relative to the feathering axis. However, as thrust is decreased to zero, the centrifugal forces on the blade/flexure assembly reduce the flexure-to-blade precone. The consequent lag/torsion coupling reduction results in a decrease in stability. This phenomenon is demonstrated by the reduction in rotor stability with decrease in collective (thrust) in both the whirl tower and ground resonance testing (Figures 29 and 54).

Lag/flap coupling is affected by the inclination of the principal axes of flap and chordwise bending (Figure 97). The BMR flexure at the 1 g cruise collective setting is untwisted but is preinclined nose up at 12-1/2° to the horizontal plane. Asymmetric bending of this flexure causes flap motions from chord to lag motions. With decrease in collective, the beam flexure becomes twisted nose down resulting in a decrease in the inclination of the principal axes of bending. Thus, coupling and stability decrease with decrease in collective as evidenced by flight test data at 1 g thrust (but low collective) in steady autorotational descent (Figure 56).

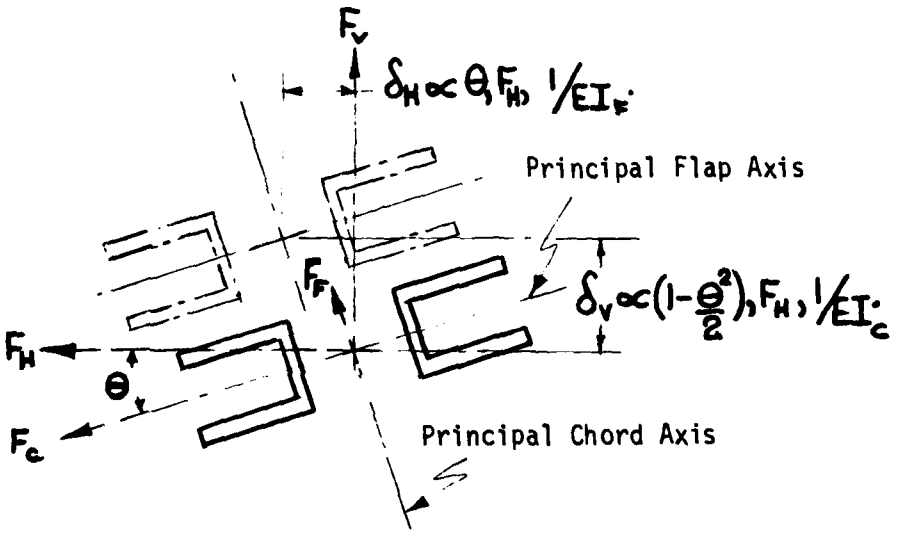

TYPICAL BEAM FLEXURE
CROSS SECTION

FIGURE 97. LAG/FLAP COUPLING PRODUCED BY INCLINATION OF THE PRINCIPAL AXES OF BENDING.

It should be noted that the lag/torsion coupling is not decreased since the 1 g precone between the blade and feathering (flexure) axis is maintained by the 1 g thrust. These minimum damping levels in ground run-up in flat pitch and autorotational descent can be supplemented by an increase in structural damping and/or geometric changes to the rotor system so that lag/torsion coupling is retained at zero thrust and/or lag/flap coupling is retained at low collectives. Using a reduction in pretwist, the resultant nose-down inclination of the principal axes of bending in the flexure will affect lag/flap coupling at zero collective in autorotation at 1 g thrust to augment that effect from the retained lag/torsion coupling.

In ground run-up, lag/torsion coupling could be achieved through an idea conceived subsequent to this program, where the inboard shear bearing is offset and the torque tube is stiff in both bending and in the tube-to-blade attachment, such that the lag shear loads transmitted from the blade down the stiff tube are reacted at the offset shear bearing and thus effect a torsional moment to the blade attachment. This produces lag/torsional coupling, which is independent of changes in blade-to-beam flexure precone. It could be noted that the stiff torque tube would relieve the beam flexure of some load, allowing the flexure dimensions to be reduced. Furthermore, it could encompass the beam and provide aerodynamic fairing (See Figure 98). Structural and stability improvements through a concept change of this nature require demonstration through analysis, by structural test, in the wind tunnel, and on the whirl tower. Drag reduction should be determined through flight or wind tunnel testing.

Nonrotating structural damping tests have produced encouraging results from an elastomeric layer bonded to the inside of the flexure flanges. Further development and the effects of such a simple system should be demonstrated.

4. Weight. The prime objective of the program was to demonstrate a stable rotor. To divert technical effort to this aim, the system was structurally overdesigned and consequently is overweight. Table 5 shows the comparison between the weight breakdowns of the BMR and BO-105. Furthermore, to reduce costs in manufacture of the experimental article and to permit geometric variations in the blade/flexure joint, a simple but heavy attachment clevis was used. Modifications to the design to remove the structural excess and attachment clevis would result in a substantial decrease in weight.

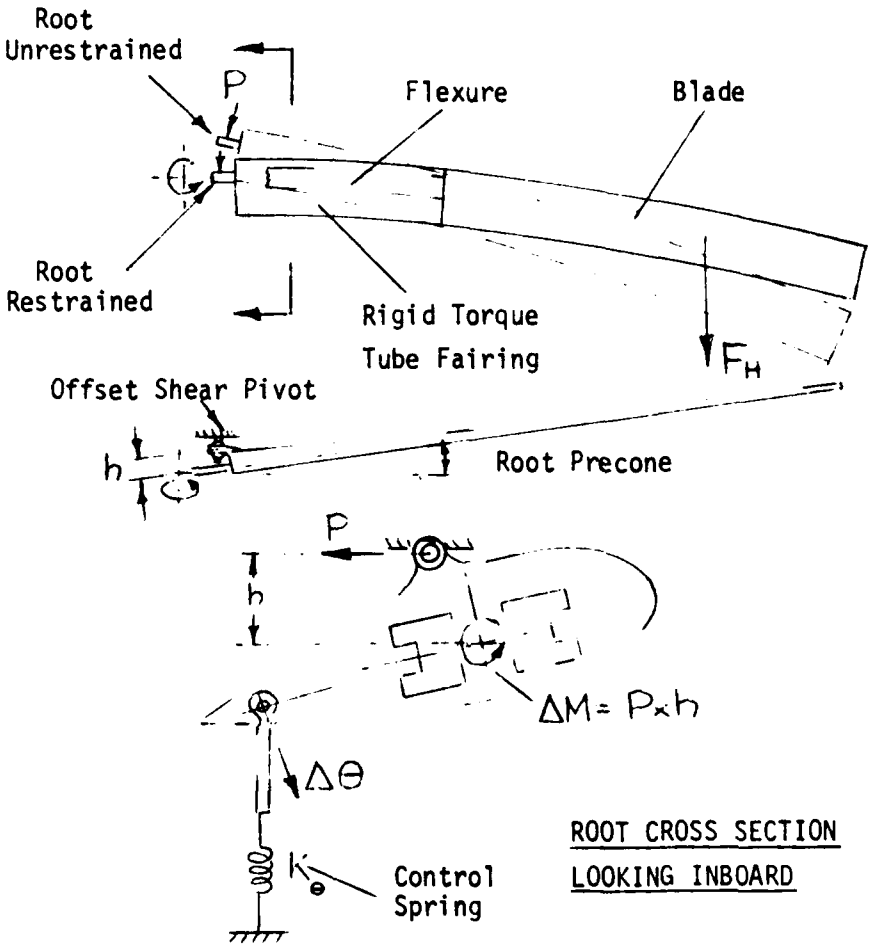

FIGURE 98. LAG/TORSION COUPLING INDEPENDENT OF PRECONE.

As suggested above, if lag/torsion coupling is achieved through a stiff torque tube, the 1 g precone at the flexure/blade attachment could be replaced by conventional precone at the rotor shaft. The resultant decrease in steady flap shear loads would result in a smaller blade/shaft attachment and thus less weight.

TABLE 5. WEIGHT BREAKDOWN

ITEM	QTY	RESEARCH BMR (LB)	BO-105 (LB)	EST FOR PRODUCTION BMR (LB)
Center Hub	1	185.0	193	100
Beams	4	89.8	-	55
Torque Tube Assy.	4	41.7	-	27
Clevis Assemblies	4	81.4	-	--
Blades	4	191.6	275	190
Oil	-	-	4	-
	TOTAL	589.5 LB	472 LB	372 LB

5. Drag. V_H was limited by available power to overcome the drag of the rotor system, hub and instrumentation package, boom, landing gear modifications, and pitch attitude of the aircraft necessary to sustain this speed. An estimated drag breakdown is presented in Table 6. Incorporating the suggestions from paragraphs 3 and 4, the dimensions of the beam flexure could be reduced and the attachment clevises eliminated. Incorporating the enshrouding stiff torque tube suggested above could result in an aerodynamic fairing. However, such a fairing would have to be removable to provide inspectability of the flexures.

TABLE 6. BMR DRAG BREAKDOWN (Increase Above BO-105)

ITEM	DRAG AREA (FT^2)	AFFECT ON V_{H*} (Kn)
Center Hub Beams Torque Tube Assemblies Clevis Assemblies Blades	2	-4
Boom	1	-4
Landing Gear Cables	1	-2
Instrumentation Package	1	-2
Trim Attitude	0.6	-1.2
TOTAL	5.6 FT^2	-11.2 KN

* Based on 2 KN/FT^2 at 120 KN TAS.

V_H of BO-105 = 127 Knots. TAS at 5070 lb G.W.

V_H of Test BMR = 111 Knots. TAS at 5070 lb G.W.

6. Performance. Rotor performance was limited by drag and airfoil characteristics of the BO-105 blades. Reduction in drag as suggested in paragraph 5, together with more advanced airfoils, would result in a substantial increase in performance.

7. Blade Folding. Rotor system folding was not a requirement of this program; however, introduction of this characteristic could result in diluting the potential of bearingless rotor systems. Any future design effort should include a study into the application of folding methods and their effect on virtual hinge offset, rotor dynamics, weight, and drag.

8. Producibility. By elimination of the blade-to-beam flexure joint, the number of parts will be substantially reduced. However, this will be offset by the additional complexity in replacing the metal-to-metal outboard torque tube connection with a metal-to-composite or composite-to-composite joint. The twin beam flexures could be inboard extensions of two blade spars. Minimal effort on producibility has been expended to date, but the suggestions given are within the current state of the art.

CONCLUSIONS AND RECOMMENDATIONS

The aeroelastic stability and loads together with vibration and flying qualities characteristics have been successfully demonstrated on this bearingless main rotor configuration. The concept has been proven feasible in strength and stability and can be designed to provide a one-for-one replacement for the BO-105 hingeless rotor system. However, it was shown that the stiffness characteristics of the standard BO-105 landing gear were incompatible with the BMR and that the air resonance stability characteristics of this system are different from those of the baseline rotor.

Understanding of these differences and their source is incomplete, so analysis of the results of this program requires further effort. However, lessons have been learned which have led to the probable improvements recommended herein.

ANALYSIS

Prediction of the ground resonance characteristics would be greatly simplified if the skid landing gear was replaced by the oleo strut and wheel suspension suggested below. Hover air resonance analysis methodology can be considered acceptable but the lack of a forward flight analysis is a severe deficiency in the complement of mathematical tools required to design bearingless and even hingeless systems.

Rotor flexure, blade loads, and control loads are predictable with the exception of the chordwise bending moment distribution. This twin beam flexure configuration reported herein is too complex a system for analysis using state of the art methods. The simplicity of a single beam flexure solves the structural analysis problem, using proven solutions. This simplification would be negated to some extent due to the possible requirement for a torque-tube-to-blade attachment flexure if a single element flexure were adapted.

Another alternative is to devise more complex computer programs to predict the correct loads distribution.

LANDING GEAR

As has been demonstrated on Vertol's design of the YUH-61A (UTTAS) prototype helicopter, the ground resonance problem for hingeless rotor aircraft may be eliminated through the use of soft landing gear oleos; these would make the BMR/ BO-105 ground resonance body mode frequencies approach those of the air resonance body modes which

have been demonstrated to be stable. Stiffening the landing gear may improve the ground resonance stability under certain landing surface conditions only.

CONFIGURATION

The stabilizing lag/torsion coupling has been improved for this configuration by the addition of pre-droop between the blade and the feathering axis or axis of the horizontal beam flexures. If precone only between the flexure and the shaft attachment were used and this stabilizing coupling could be achieved by other kinematic geometries, the beam flexure could be reduced in strength and, therefore, size and torsional stiffness and weight would be reduced. Means of providing lag/torsion coupling require conception and assessment. The stabilizing lag/flap coupling has been enhanced by the flexure pre-twist of 12-1/2° at the shaft attachment. This inclination increases hub drag, which degrades the performance of the helicopter system. The magnitude of the stability gained from this pre-twist needs further study since its elimination would greatly enhance the simplicity and performance of this BMR concept.

The torque tube is inclined below the flexure axis of symmetry and, therefore, is a source of additional drag. A torque sleeve/fairing as suggested above may be advantageous and requires further study.

The blade attachment hardware weight and drag is excessive in the interests of schedule and economy. Further stability analysis may result in the optimum blade/flexure attachment angle, which could be fixed and the beams integrated with the rotor blade, eliminating the offending hardware.

Advanced airfoils and tip shapes are always being developed and incorporation of those with proven characteristics would greatly enhance the performance characteristics of the BMR system.

The BMR has not improved the vibration characteristics of the BO-105 due to features such as the 14-percent radius flap hinge offset. Offset reduction would reduce the rotor induced vibration and gust sensitivity. The previously mentioned addition of precone would allow reduction in flexure cross section and consequent reduction in flap hinge offset.

A further reduction in flap hinge offset would be permissible if the additional material wrapped around the flexure root attachment pins to accommodate the resultant stress concentrations was not required. If the root configuration shown in Figure 5 was used, the retention

pins would not be required. Through some ingenuity the blade-to-flexure attachment could be made through a composite-to-composite joint and thus eliminate the attachment hardware.

REFERENCES

1. PROPOSAL FOR AN IMPROVED ROTOR HUB CONCEPT, Boeing Vertol Document D210-10860-1, October 1974.

2. Cardinale, S. V., SOFT IN-PLANE MATCHED-STIFFNESS/FLEXURE-ROOT-BLADE ROTOR SYSTEM SUMMARY REPORT, Lockheed-California Co.; USAAVLABS Technical Report 68-72, U. S. Army Aviation Materiel Laboratories, Fort Eustis, Virginia, August 1979, AD 863063.

3. INTERIM TECHNICAL REPORT FOR TASK I, PRELIMINARY DESIGN, Volumes A, B, and C, Boeing Vertol Document D210-11129-1, September 1976.

4. INTERIM TECHNICAL REPORT FOR TASK II, 1/5.86 FROUDE SCALED MODEL TEST RESULTS, Boeing Vertol Document D210-11245-1, June 1977.

5. STRUCTURAL ANALYSIS REPORT OF BMR/BO-105 (HELICOPTER), Boeing Vertol Document D210-11398-1, June 1978.

6. MODEL AND BENCH TEST EVALUATION OF THE PRELIMINARY DESIGN, Boeing Vertol Document D210-11245-2, November 1977.

7. BMR WHIRL TEST REPORT, Boeing Vertol Document D210-11428-1, September 1978.

8. INSTRUMENTATION DESIGN DOCUMENT, BMR FLIGHT TEST PROGRAM, Boeing Vertol Document D210-11299-1, 22 September 1977.

9. AEROELASTIC STABILTY AND VIBRATION CHARACTERISTICS OF A BEARINGLESS MAIN ROTOR, Boeing Vertol Document D210-11498-1, June 1979.

10. BO-105 BEARINGLESS MAIN ROTOR GROUND AND FLIGHT TEST PLAN, Boeing Vertol Document D210-11362-1, August 1978.

11. FLIGHT TEST SUMMARY, Boeing Vertol Document D210-11501-1, April 1979.

12. SAFETY OF FLIGHT DATA (3 Volumes), Boeing Vertol Document D210-11437-1, October 1978.

13. LOADS CHARACTERISTICS OF A BEARINGLESS MAIN ROTOR, Boeing Vertol Document D210-11417-1, August 1979.

REFERENCES (Continued)

14. FLYING QUALITIES CHARACTERISTICS OF A BEARINGLESS MAIN ROTOR, Boeing Vertol Document D210-11499-1, July 1979.

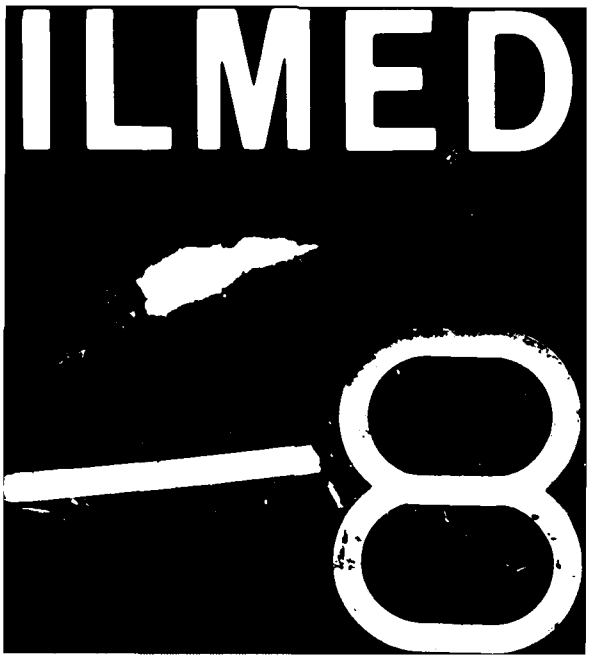
ILMED
8